THE ROLE OF THE *ESCHERICHIA COLI* RNA PYROPHOSPHOHYDROLASE (RPPH) IN RNA METABOLISM

by

KATHERINE ELAINE BOWDEN

(Under the Direction of Sidney R. Kushner)

ABSTRACT

RNA turnover in *Escherichia coli* was originally thought to initiate through the action of ribonucleases. It was not until the discovery of the "decapping" enzyme RNA pyrophosphohydrolase (RppH) in *Escherichia coli* that this hypothesis was called into question. Prior to the experiments described here, RppH had only been implicated in mRNA decay and hybrid jamming.

Here, we have analyzed the role of RppH in tRNA maturation and called into question the original idea that the catalytic activity of RppH was required to promote endonucleolytic cleavages by RNase E. We have shown that this is actually not the case for tRNA processing. In contrast, RppH activity is required for the 5'-maturation of certain tRNAs by RNase P. In addition, we saw that this effect was regulated by RNase PH, a 3'→5' exoribonuclease.

After analysis of tRNA maturation, we examined the role of RppH on regulation of the entire transcriptome. Previous microarray analysis has been limited by the use of probes for only open-reading frames (ORFs). Here, through

the use of a tiling microarray, which provides probes across the entire transcriptome, we have discovered that RppH is involved in regulation of the flagellar gene regulatory network. Based on these findings, we have shown that *E. coli* carrying a *rppHΔ754* mutation is hypermotile and restores motility to the nonmotile *ΔapaH* mutant strain.

This work has attempted to uncover processes that RppH has not been previously known to play a role. Although more insight has been gained, there still remains a question as to how RNase PH is involved in RppH-dependent regulation. In addition, it has become apparent that the activity of RppH is much more complex than originally thought.

INDEX WORDS: RNase P, RNase PH, tRNA maturation, *Escherichia coli*

THE ROLE OF THE *ESCHERICHIA COLI* RNAPYROPHOSPHOHYDROLASE RPPH IN RNA METABOLISM

by

KATHERINE ELAINE BOWDEN

BS, University of Georgia, 2006

A Dissertation Submitted to the Graduate Faculty of The University of Georgia in Partial Fulfillment of the Requirements for the Degree

DOCTOR OF PHILOSOPHY

ATHENS, GEORGIA

2012

THE ROLE OF THE *ESCHERICHIA COLI* RNA PYROPHOSPHOHYDROLASE RPPH IN RNA METABOLISM

by

KATHERINE ELAINE BOWDEN

Major Professor: Sidney R. Kushner

Committee: Richard B. Meagher
Anna C. Glasgow Karls
Mary A. Bedell
Janet Westpheling

Electronic Version Approved:

Maureen Grasso
Dean of the Graduate School
The University of Georgia
December 2012

DEDICATION

To my parents, brother, sister, and O’Malley.

ACKNOWLEDGEMENTS

I would first like to acknowledge my major professor Dr. Sidney R. Kushner, for without him, none of this would have been possible. He is the reason I entered into science research and the reason I became a scientist. I will forever be indebted to him for his guidance, advice, patience, expertise and unwavering support throughout this chapter of my life. I would also like to thank my advisory committee, Dr. Richard B. Meagher, Dr. Anna C. Glasgow-Karls, Dr. Mary A. Bedell, and Dr. Janet Westpheling, for their candid advice and leadership throughout this process.

I would also like to thank everyone who I have worked with in the Kushner lab, past and present. They all have provided an amazing environment for me to learn and grow in and they will always have a place in my heart and always be family to me. I would like to extend a special thank you to Dr. Bijoy Mohanty for teaching me the language of science and helping me grow as a scientist and a person on a daily basis. He has been extremely patient with me throughout this process and I would not be where I am today without him.

I want to thank my friends that have supported me throughout this entire process. Dr. Brunie Burgos, Veronica Burgos, Dr. Marly Richter-Roche, and Tiffany Pottinger-Sutton have all stood by my side through thick and thin, on good days and bad days, through laughter and tears. I would not have made it

without them. Lastly, thank you to my amazing parents who have supported me, tolerated me, loved me and provided for me since the day I was born. Also, to my brother and sister, who, although are both younger, have always protected me and loved me like the baby of the family. Love you and thank you, beyond words.

TABLE OF CONTENTS

Page

CHAPTER 1

INTRODUCTION AND LITERATURE REVIEW

Since the discovery of nucleic acids by Friedrich Miescher in 1868, researchers have spent their careers trying to understand how these essential molecules are constructed and function in the cell to support life. RNA, being the most ancient of nucleic acids, is known to function in both protein synthesis, with the use of transfer RNAs (tRNAs), ribosomal RNAs (rRNAs) and messenger RNAs (mRNAs), and gene expression via small RNAs (sRNAs).

A major component of the ability of these RNAs to function efficiently in each process resides in their processing, maturation, and degradation by means of ribonucleases. The activity of these enzymes is essential for controlling the half-lives of mRNAs thereby helping to regulate the ever-changing needs of protein synthesis, the correct stereochemistry of tRNAs and rRNAs to allow for their proper functioning during translation, and providing different forms of sRNAs to differentially regulate gene expression, particularly when cells encounters periods of stress.

For some time it was thought that the enzymatic activity of ribonucleases was the first step in all pathways of RNA metabolism. Other than the ability of

RNase E, an essential endoribonuclease, to regulate the stability of its own mRNA, no known post-transcriptional mechanisms that affected the catalytic activity of the ribonucleases in bacteria were apparent. The discovery of the "decapping" enzyme RNA pyrophosphohydrolase (RppH) in *Escherichia coli* led to the realization that RNA metabolism was far more complex than previously envisioned.

In bacteria, RNA polymerase initiates transcription *de novo*, such that all primary transcripts have a 5'-triphosphate. However, unlike in eukaryotes, the 5'-triphosphate is not further processed with the addition of a 5' methyl-G cap. Decapping of eukaryotic mRNAs by the primary decapping enzyme Dcp2 is a critical step in their decay. As it turns out Dcp2 is a Nudix protein. The Nudix motif, originally discovered in *E. coli*, is found in a large family of proteins that hydrolyze various types of nucleotide motifs [1]. In fact, of the thirteen distinct Nudix proteins in *E. coli*, the *rppH* gene encodes a RNA pyrophosphohydrolase [2] that converts 5'-triphosphorylated RNA substrates to 5'-monophosphorylated species.

This review summarizes what is currently known about RppH, including information on the protein family, enzymatic characteristics, and its major functions in *E. coli* and other bacteria.

NUDIX HYDROLASES

RppH belongs to the Nudix hydrolase protein family. Previously called the MutT family [1], these proteins can be found across 250 species, including

eukaryotes, bacteria, viruses, and archaea. These Mg^{2+}-requiring enzymes hydrolyze a *nu*cleoside *di*phosphate linked to another moiety (*x*) (hence the name "nudix") and have been shown to be involved in various regulatory, signaling, and protective roles in metabolism [1, 3]. With substrates widely ranging from organic polyphosphates, nucleotide sugars, coenzymes, and RNA caps, these enzymes function to control metabolite pools and regulate DNA replication, RNA decay, transcription, and translation. Interestingly, several Nudix proteins, specifically RppH, have been implicated in the control of cell division, the ability of bacteria to prevent injury during oxidative stress and heat shock, and the ability of pathogenic bacteria to invade human cells [4-7].

Nudix motif

Nudix proteins are small proteins (16-21 kDa) that contain a highly conserved 23-amino acid (aa) sequence motif known as the Nudix motif or Nudix box [1, 3, 8-11] (Fig. 1). This Nudix motif has been shown to be essential for the pyrophosphatase activity of these enzymes [10, 11]. Based on sequence analysis of the eukaryotic Dcp2 protein, a Nudix protein that is involved in mammalian mRNA decapping and has high sequence similarity to RppH, the 23-aa Nudix motif ($GX_5EX_7REUXEEXGU$, where X is any aa and U is an aliphatic hydrophonic aa) consensus sequence is within a 109-aa Nudix fold [8, 9] (Fig. 1). The Nudix motif, which forms a loop-α helix-loop structure, contains two glutamic acid residues that are critical for metal coordination and pyrophosphatase activity [12-16] (Fig. 1). Within the motif, there is significant variation in the location of the nucleophilic attack on the substrate, the position of the catalytic base, and the

number of divalent ions involved [17]. The Nudix fold that encompasses the Nudix motif consists of two β-sheets sandwiched between two α-helices, providing additional side chains and motifs that confer substrate specificity and mechanistic diversity for individual enzymes [13].

Nudix protein diversity in bacteria and *E. coli*

Seeing that Nudix hydrolases are known to provide the cell with a mechanism to remove potentially harmful metabolites and modulate the amount of intermediates that build up during various biochemical processes, one could predict a link between the number of Nudix genes and the complexity of the metabolic pathways and adaptability of a particular organism [1, 18]. With this thought in mind, there seems to be a linear correlation between genome size and the number of Nudix genes an organism possesses, with only a few exceptions [18]. Organisms with multiple pathways that synthesize metabolites tend to have a greater number of Nudix genes, while organisms like parasites and symbionts have a reduced number or no Nudix genes at all [18]. Interestingly, in the case of certain bacteria that live in extreme environments, genome size fails to correlate with the number of Nudix genes. For example, the radiation resistant *Deinococcus radiodurans* has a 3.3 Mbp genome and encodes 26 Nudix genes, the highest number per Mbp of any bacteria [18-20]. On the other hand, large numbers of Nudix genes could also imply the occurrence of gene duplication events, as in the case with *Bacillus halodurans* which has 10 Nudix genes, while its close relatives *B. cereus*, *B. anthracis*, and *B. thuringiensis* have close to 30 Nudix genes [21].

There are 13 known Nudix proteins in *E. coli*. The first Nudix protein to be studied was MutT (NudA), with the original name of the Nudix protein family being the MutT family [1, 22]. MutT is known to convert the mutagenic, oxidized nucleotide 8-OH-dGTP to 8-OH-dGMP and PPi, which has been shown to prevent incorporation of *syn*-8-OH-dG into DNA. Misincorporation of this modified base leads to ~1000-fold increase in spontaneous mutations due to AT:CG transversions [23-25]. Misincorporation of this modified base has also been linked to tumors in mice [26]. Seeing that it also degrades 8-OH-GTP, MutT has also been linked to preventing transcription errors and the ability to suppress mutations induced by this metabolite *in vivo* [27, 28].

NudG, originally called YnjG and another Nudix protein in *E. coli* shown to have activity towards dNTPs, has been implicated in preventing H_2O_2-induced mutations by reducing the amount of 2-OH-dATP, which leads to GC:AT transitions and GC:TA transversions [29]. NudB (formally NtpA or YebD), the most abundant Nudix protein in *E. coli*, is the only Nudix protein that has been shown to be essential for aerobic growth in rich medium [30, 31]. Its substrates include dATP, 8-OH-dATP, and 8-OH-dADP [32, 33]. NudF (formally AspP or TrgB) is known as an ADP-ribose pyrophosphohydrolase and has been implicated in the elimination of ADP-ribose, a toxic byproduct of NAD catabolism [34]. The gene encoding NudF is part of the *cre* regulon and has been shown to be up-regulated by the CreBC regulatory system during growth on minimal medium in response to changes in the carbon supply [35, 36]. Downstream of the CreBC regulatory system, NudF has also been suggested to regulate

glycogenesis due to high levels of glycogen in the *nudF*⁻ mutant and loss of glycogen with its overexpression [35].

NudD (WcaH) is limited to enterobacteria and *Vibrio* species and is known to hydrolyze GDP-α-D-mannose and GDP-α-D-glucose to GDP and the subsequent β-sugar [17, 37, 38]. Interestingly, the NudD enzymatic mechanism differs from other Nudix proteins due to a lack of two of the Mg^{2+}-binding Glu residues, a change in the catalytic base due to a six-residue deletion, and the nucleophilic substitution at the sugar C1 rather than at phosphorus [17, 37-39]. The gene encoding NudD is located in a gene cluster that is required for the production of colanic acid, an extracellular polysaccharide [40].

NudC (YjaD) is a NADH pyrophosphohydrolase that contains a conserved sequence (SQPWPFPQS) ten residues downstream of the Nudix box that is found in all NADH hydrolases and possibly confers pyridine nucleotide specificity [34, 41]. Based on evidence that NudC may regulate intracellular NAD^+/NADH ratios, it has also been shown to be involved in the survival of *Haemophilus influenza* in an animal host [41, 42]. The remaining five Nudix proteins found in *E. coli* are poorly characterized regarding their activities and substrate specificities. YeaB has a sequence motif upstream of the Nudix box that is found in proteins that are active on coenzyme A, so it is assumed to be a CoA pyrophosphohydrolase [43-46]. YmfB is a nucleoside triphosphatase that hydrolyzes nucleoside triphosphates in a stepwise manner to yield P_i rather than PP_i and has also been shown to confer resistance to bacimethrin, a toxic thiamine analogue [47, 48]. YfaO is unique to *E. coli*, *Shigella flexneri*, and

Salmonella enterica and shows a preference for pyrimidine deoxynucleoside triphosphates dUTP, dTTP, and dCTP [18, 48]. Seeing that NudB, MutT, and NudG prefer dATP, dGTP, and dCTP, respectively, YfaO is the final enzyme to encompass the Nudix proteins in *E. coli* that act on the four canonical deoxynucleoside triphosphates, which are hydrolyzed into a nucleoside monophosphate and inorganic pyrophosphate [48]. Based on conserved sequence similarities, YffH was originally thought to be an ADP-ribose pyrophosphatase. However, upon further analysis it was determined to utilize GDP-mannose as a better substrate [34, 48]. YffH has also been implicated in biofilm formation by the remodeling of extracellular polysaccharides [49]. Lastly, YfcD has no reported information to date.

SUBSTRATE SPECIFICITY AND CATALYTIC MECHANISM OF RppH

Technically, RppH proteins are asymmetrically cleaving diadenosine tetraphosphate hydrolases. The first RppH homolog was discovered in embryonic cysts of *Artemia franciscana* [50]. This class of enzymes is known to catalyze the hydrolysis of an Np_4N' to a nucleoside triphosphate (NTP or pppN) and an NMP (N'MP or pN').

Protein structure

E. coli RppH is a 20-kDa protein that is monomeric in solution and is inhibited by fluoride ions [51]. Like most Nudix hydrolases it has an alkaline pH optimum between 8.5 and 9.0 with a specific activity of ~3.3 units mg^{-1} protein [51]. According to the crystal structure of *Bdellovibrio bacteriovorus* RppH

(BdRppH), the only known bacterial RNA pyrophosphohydrolase for which a crystal structure has been determined, the protein actually forms a dimer with the two monomers composed of the Nudix domain, which extends from residue Gly54 to Ile77 and folds into the characteristic b-strand-loop-a-helix-loop motif [13, 52]. The interface of the two monomers, which are arranged in a head-to-head orientation, is made up of hydrophobic interactions and hydrogen bonds between 20 residues of each monomer [52]. This arrangement of monomers is similar to the *E. coli* GDP-mannose hydrolase dimer [39, 52].

Role of divalent cations

E. coli RppH shows a requirement of divalent cations and is most active at 10 mM Mg^{2+} [51]. Zn^{2+} and Mn^{2+} are also required but at lower concentrations [51]. Analysis of the divalent cation binding data showed that diadenosine tetraphosphate pyrophosphatases require three cations, two bound to the enzyme and one bound to the substrate, which is usually the highly negatively charged leaving group ATP^{4-} [17]. This observation is similar to the crystal structure of X29, the Nudix decapping enzyme in *Xenopus laevis*, when complexed with m^7GpppA, the eukaryotic 5'-cap [52]. Interestingly, seeing that the eukaryotic 5'-cap contains a methylated guanine, only 3 cations are present in the BdRppH while 4 cations are seen in X29 of *X. laevis* [52].

Substrate specificity

Assymetrical Np_4N hydrolases have several potential substrates which include Np_4N's containing various nucleosides, mainly N^1,N^6-ethenoAp$_4$As and

mRNA 5'-cap analogues; chain length homologues of Ap_4A or Gp_4G; nucleoside 5'-tetra- and –pentaphosphates (p_4N and p_5N); methylene and halomethylene analogues of Ap_4A; adenylayed derivatives of methanetriphosphonate; and 2'-(deoxy)adenylated Ap_4As [53]. Relative specificity assays showed that *E. coli* RppH prefered Ap_5A (100% hydrolysis), followed by Ap_6A and Ap_4A with 92% and 14% hydrolysis, respectively [54]. The typical hydrolysis products resulting from this reaction are ATP and ADP [51, 55]. *E. coli* RppH showed little or no activity on Ap_3A, and other nucleoside diphosphate derivatives such as ADP-ribose, NADH, and UDP-glucose, which are typical substrates of the Nudix proteins [51]. With hydrolysis of Ap_5A, ATP and ADP were formed; Ap_4A hydrolysis led to the formation of ATP and AMP, while hydrolysis of Ap_6A resulted in the formation of a 2 mol of ATP [51]. These data indicated that nucleophilic attack was occurring at the gamma or delta phosphorus [51].

Catalytic mechanism

There is still some debate as to what residue acts as the catalytic base in the active site of RppH. A number of possible catalysis mechanisms exist for Nudix hydrolases, all suggesting different catalytic bases. The catalytic base is either the second glutamate of the Nudix motif, or a glutamate or histidine in the loop equivalent to L6 in BdRppH [17, 52]. In GDPMH and ADPRase, the catalytic base that deprotonates the water molecule and one of the ligands to the catalytic metal are within the loop that is equivalent to L6 [13, 39]. In *E. coli* MutT and Ap_4A pyrophosphatase, the second glutamic acid of the Nudix motif acts as both the catalytic base and the ligand of the catalytic metal [17] (Fig. 1). In BdRppH, a

glutamic acid (Glu70) is present in the location equivalent to the MutT protein and has shown complementation of the MutT phenotype in *E. coli* [52, 56] (Fig. 1). Interestingly, this residue in BdRppH is not likely to be the catalytic base seeing that it coordinates two divalent cations [52]. Furthermore, the residues in loop L6 are not in a position to activate a water molecule for hydrolysis [52].

Using kinetic assays of various mutants, Messing *et al.* [52] showed that Glu70 of BdRppH may in fact act as one of the metal ligands. Additionally, they demonstrated that His115 played a role in substrate binding but not catalysis, while the loop L6 showed weak mutational effects, indicating the flexibility of different residues functioning as catalytic bases in this region [52].

RppH DIVERGENCE ACROSS BACTERIA

It is known that the *E. coli* RppH has known homologues in both Gram-positive and Gram-negative bacteria. In Gram-positive bacteria, BsRppH (originally called YtkD in *Bacillus subtilis*) is known to initiate the 5'-exonucleolytic degradation of mRNAs by RNase J through removal of a pyrophosphate from the 5'-termini of transcripts, much like *E. coli* RppH [57]. In Gram-negative bacteria, RppH homologs have been linked to the ability of the pathogenic bacteria to invade hosts, regulate Ap_nA levels in the cell, and decapping of RNA transcripts much like Gram-positive bacteria and eukaryotes.

Gram-positive Bacteria

There is limited data available concerning RppH homologs in Gram-positive bacteria. Aside from *Bacillus subtilis*, *Staphylococcus aureus* and *Listeria monocytogenes* are the only other Gram-positive bacteria that have been identified to have a protein with sequence homology to *E. coli* RppH [58]. *B. subtilis* has 6 known proteins that contain a canonical or near-canonical Nudix motif, while *Bacillus cereus* and *Bacillus anthracis* have 26 and 30 known Nudix proteins, respectively [57, 59].

B. subtilis mRNA processing is quite different than that of *E. coli*, specifically due to the fact that *B. subtilis* has no RNase E homolog [60]. Unlike *E. coli*, *B. subtilis* contains RNase Y, a membrane-associated endonuclease, and RNase J, an enzyme made up of the J1 and J2 subunits and that has both endonuclease and 5' exonuclease activity [60-66]. Richards *et al.* [57] showed that BsRppH exhibited RNA pyrophosphohydrolase activity *in vitro* and that BsRppH converts the triphosphorylated transcripts to monophosphorylated RNA by releasing the γ and β phosphates as separate orthophosphate ions, unlike *E. coli* RppH which releases a pyrophosphate 85% of the time [2]. Catalytic activity was inhibited when the 5' end of the RNA substrate was paired and directly affected the decay rate of the downstream mRNA [57]. Interestingly, the group determined that RNase J1 was the 5' monophosphate-dependent ribonuclease that degraded their mRNA substrate, while RNase Y showed no activity [57]. Both RNase J1 and the RNase J1-J2 complex degraded transcripts primarily by exonucleolytically (5'→3'), which occurred at a higher rate when the transcript was monophosphorylated. In contrast, endonucleolytic cleavages occurred as a

slower secondary mechanism, irrespective of the status of the 5' terminus [57]. This mechanism of RNA degradation is reminiscent of what is observed in eukaryotes where decapping leads to 5'→3' exonucleolytic degradation of mRNAs.

BsRppH has also been shown to degrade 8-oxo-(d)GTP, a reactive oxygen species that can be incorporated into mRNAs and cause transcriptional errors and mutagenesis [25, 27]. Ramírez *et al.* [67] have shown that BsRppH is produced during vegetative growth and sporulation, with its mRNA being transcribed by the sequential activity of RNA polymerases containing the main sigma factor of vegetatively growing *B. subtilis*, σ^A, and the spore-specific sigma factor, σ^F. It was also determined that the BsRppH transcript was not induced by oxidative stress, SOS, or σ^B general stress responses, which would indicate a role in managing oxidative stress solely during sporulation [67].

Gram-negative Bacteria

Bartonella bacilliformis is a Gram-negative bacterium that is known to transmit Oroya fever in humans via sand flies by invading human erythrocytes and endothelial cells [5, 55]. Currently, *B. bacilliformis* is the only known bacterium to invade human blood cells and leads to severe hemolytic anemia [55]. Initially studies were conducted in order to find genes associated with the ability of this bacterium to invade human erythrocytes. In their search, a two gene locus, *ialA* and *ialB*, was identified [5]. Upon conducting protein sequence alignments with other bacterial species, IalA, a Nudix hydrolase, showed high sequence homology to RppH in *E. coli* and demonstrated high catalytic activity

on the same substrates (Ap_4A being the highest, followed by Ap_5A, Ap_6A, Gp_4G, and Gp_5G) [55]. Unlike RppH, IalA prefers Ap_4A as a substrate and produces ATP and AMP as the product of its hydrolysis [55].

Using this same approach to find genes that led to *E. coli* K12 invasiveness in human brain microvascular endothelial cells (BMEC), the primary cause of neonatal bacterial meningitis, researchers found RppH to be a likely candidate [4, 51]. These studies demonstrated that transcript levels of *rppH* were increased under growth conditions that induced BMEC *E. coli* K12 invasion, while transcript levels decreased when the strain was grown under non-inducing conditions [4]. Subsequently, the orthologous correlation between *rppH* in *E. coli* and the gene *ialA* in *B. bacilliformis* was confirmed, due to their high sequence homology. These findings led other groups to find additional Gram-negative bacteria in which the genome encoded genes homologous to *rppH* and to determine the effects it had on virulence, invasiveness, and other major biological functions that support survival of these pathogens.

NudA, in *Legionella pneumophila*, the most common cause of a type of pneumonia called Legionnaires' disease, was found to be a Nudix hydrolase that prefers Ap_nA's as a substrates, which corresponded to the catalytic activity of RppH in *E. coli*. NudA was shown to be a virulence factor in *L. pneumophila* in that the *ΔnudA* mutant strain was incapable of invading guinea pig alveolar macrophages [68]. The study also showed that the *ΔnudA* mutant strain exhibited delayed growth at 25°C, 37°C, and 42°C, auxotrophy and salt

resistance [68]. Interestingly, this mutant did not show a decrease in motility as reported for other Nudix hydrolase mutants [68].

Richettsia prowazekii, the Gram-negative bacterium responsible for epidemic typhus, contains an invasion gene, *invA*, that has 37-44% homology to RppH in *E. coli* and countless other putative bacterial invasion proteins and pyrophosphatases [54]. InvA is a dinucleoside oligophosphate pyrophosphatase and a Nudix protein that preferentially degrades Ap_5A and exhibits no activity on dinucleoside oligophosphates ($n \geq 4$), while demonstrating a decrease in catalytic activity with decreasing phosphate chain length [54]. InvA, along with RppH, produced ATP and ADP from Ap_5A hydrolysis [54]. Although Mn^{2+} is required for catalytic activity of RppH in *E. coli* and IalA in *B. bacilliformis*, it does not support hydrolytic activity of InvA [54].

Two unrelated dinucleoside polyphosphate hydrolases, YgdP (RppH) and ApaH, were found in *Salmonella enterica* servar Typhimurium and were implicated in the ability of the bacterium to adhere to and invade human epithelial cells [69]. With evidence that both enzymes hydrolyzed the same substrates (Ap_4A, Ap_5A, and Ap_6A), ApaH always produced ADP as a product while YgdP always produced ATP as a product, having a preference for Ap_5A similar to the *E. coli* and *R. prowazekii* enzymes [69]. Deletion of both YdpP and ApaH, singly or in combination, led to an increase in the intracellular Ap_nN levels, indicating both enzymes played a role in controlling the Ap_nN pool in *S. typhimurium* [69]. Deletion of *ygdP* decreased invasion of HEp-2 epithelial cells by 9-fold compared to wild type control, while deletion of *apaH* reduced invasion by 250-fold.

Furthermore, the double mutant produced a 3000-fold reduction [69]. These results indicated that ApaH and RppH were distinct in their phenotypes, although acting on the same substrates and both regulating the Ap_nN pool. Interestingly, an *ΔapaH* mutant strain exhibited filamentous growth, which was also seen in *E. coli* [69, 70]. In combination with the previously mentioned studies, researchers began to hypothesize that RppH, along with its homologs in other Gram-negative bacteria, was in some way regulating these stress-induced dinucleoside oligophosphate levels during host cell invasion to allow for a better chance at intracellular survival [1, 4, 5, 51, 53-55, 68, 69, 71, 72].

Bdellovibrio bacteriovorus is the only Gram-negative bacteria other than *E. coli* in which RppH has been identified to be both a GTPase and have decapping activity [52]. It is also the first of bacterial RNA pyrophosphohydrolases for which the structure has been determined [52]. The protein structure of BdRppH indicated the presence of a dimer formed by two monomers arranged in a head-to-head fashion, resembling the dimer of the *E. coli* GDP-mannose hydrolase (GDPMH) [39, 52]. Interestingly, these enzymes have entirely different activities: BdRppH hydrolyzes a diphosphate bond, while GDPMH cleaves at a carbon instead of phosphorus [39, 52]. Like the *E. coli* RppH, BdRppH prefers Mg^{2+}, but shows no activity with Mn^{2+} [52]. The arrangement and localization of residues around the Nudix box are similar to those observed in the nuclear decapping enzyme X29 of *Xenopus laevis* [52, 73]. The coordination and arrangement of the metal ions with the substrate resemble that of the *E. coli* ADPRase when magnesium and the substrate are in complex together [13, 52]. The glutamic acid

(Glu70) of BdRppH correlates with the *E. coli* MutT catalytic base and can complement the MutT phenotype in *E. coli*. However, it does not act as a catalytic base in BdRppH, but only as a metal ligand [52, 56]. Through *in vitro* analysis of BdRppH pyrophosphohydrolase activity, Messing *et al.* [52] were able to show concentration-dependent catalytic activity resembling that of the *E. coli* RppH, along with complementation of an RppH deficient strain of *E. coli* when analyzing half-lives of an RppH-dependent transcript.

FUNCTIONS OF RppH IN *E. coli*

Regulation of Ap_4A, Ap_5A, and Ap_6A levels in the cell

Seeing that RppH acts on Ap_4A, Ap_5A, and Ap_6A, it is of interest to understand the roles of these diadenosine polyphosphates in the cell when they accumulate. These polyphosphates are a byproduct of aminoacyl-tRNA synthetases and since their discovery, many groups have found their presence in many different cell types and their involvement in numerous cell processes [74]. These processes include inhibition of ATP-sensitive K^+ channels, activation of purinoceptors, regulation of cell differentiation and apoptosis, pain transduction, and cell division [7, 75-80]. One important aspect of these phosphates is their ability to act as signals in stress responses, specifically in heat shock and oxidative stress, in which they are termed “alarmones” and their concentrations increase more than 100-fold [81, 82]. It is thought that RppH, along with IalA in *B. bacilliformis*, help regulate the levels of these alarmones during the invasion process [51, 55, 71].

In an attempt to understand how this process actually occurs in *E. coli*, several groups have set out to determine what these signal molecules are interacting with, if they are not degraded by RppH and other Nudix hydrolases. Farr *et al.* [70] showed that through the construction of a *ΔapaH* mutant strain in *E. coli*, Ap_4A accumulated and showed drastic effects on cell motility and catabolic repression. It should be noted that ApaH is also a hydrolase, though not a Nudix hydrolase, that is known to degrade Ap_4A into two ADP moieties, unlike RppH which degrades Ap_4A into AMP and ATP [70]. *ΔapaH* mutants were nonmotile and showed a decrease in transcription of flagellar genes and all CAP-cAMP-controlled genes [70].

To understand how the loss of ApaH was inducing such a dramatic response, Johnstone and Farr [6] set out to test what types of proteins can actually bind to Ap_4A when its intracellular levels increased. Using crosslinking experiments, they showed that in unstressed, wild type cells, the concentration of Ap_4A was ~1-3 µM, but increased to ~160 µM during heat shock [6]. 2D-PAGE gels and expression of several heat shock and oxidative stress proteins on high-copy plasmids showed that Ap_4A strongly binds to E89 and GroEL, two heat shock proteins [6]. These results also showed Ap_4A binds to DnaK, but this binding may be facilitated by another protein [6]. Seeing that Ap_4A bound to several heat shock and oxidative stress proteins, they also were able to show that *ΔapaH* mutants were in fact temperature sensitive, and that Ap_4A binding to these specific proteins inhibited their ability to protect cells against heat shock injury [6].

Another interesting aspect of Ap_4A is its ability to control the timing of cell division. Nishimura *et al.* [7, 80] demonstrated that the cfcA11 mutant in *E. coli* showed uncoupling of DNA replication and cell division along with a high frequency of cell division and high intracellular levels of Ap_4A. This specific phenotype was the cause of early cell division in cells that completed cell division at a smaller size than that of wild type control cells. It is still unclear what causes this phenomenon. Several laboratories have speculated that Ap_4A is synthesized as a result of stalled replication forks and in turn slows down replication to allow for DNA repair [83-85].

As for Ap_5A and Ap_6A, little is known about their intracellular role. Ap_5A is known to inhibit adenylate kinase, which is involved in the maintenance of cellular energy charge and myocardial bioenergetics [86, 87]. Like Ap_3A and Ap_4A, high levels of Ap_5A and Ap_6A inhibit the opening of K_{ATP} channels, specifically in cardiac myocytes and pancreatic β-cells where these channels are abundant [75, 76, 88-90].

Hybrid Jamming

In *E. coli*, the general secretory pathway (Sec) is a post-transcriptional process that allows for a majority of proteins to be exported to extracytoplamic locations via the inner membrane translocation complex SecYEG [91]. The production of one protein in particular, the LamB-LacZ hybrid protein Hyb42-1, leads to maltose sensitivity and blocks the translocation complex, resulting in the inability of the cell to export envelope proteins and cause hybrid jamming, a lethal secretion defect [91, 92]. Through mutational analysis, Hand and Silhavy [91]

identified *E. coli ΔrppH* as a suppressor of this hybrid jamming, and that it shared similar phenotypes to another hybrid jamming suppressor that inactivates the Lon protease, *ΔprlF1*. These phenotypes included cold sensitivity and suppression of the temperature sensitivity of *ΔdegP*, a mutation in a periplasmic protease that degrades the hybrid protein in the periplasm [91]. Hand and Silhavy [91] hypothesized that the *ΔrppH* mutation may in some way be increasing an innate property of the SecYEG pore, allowing Hyb42-1 to be released into the periplasm. Their results suggested that RppH mediates an alarmone response that affects protein secretion, which would in turn allow the cell to release the alarmones initially causing the stress response [91]. They also hypothesized that the higher levels of alarmone stemming from *ΔrppH* may positively regulate the activity of a protease, as seen in the *ΔapaH* background in the absence of Lon, a cytoplasmic protease [91, 93].

Decapping

As previously mentioned, endonucleolytic cleavages of messenger RNAs (mRNAs) have been thought to be the initiating step of mRNA decay in prokaryotes for some time [94]. In contrast, it has been shown that removal of the 5’-methyl-G cap from eukaryotic RNA transcripts by a decapping enzyme was required to initiate the decay of these transcripts [95]. While prokaryotic transcripts do not contain a 5’-methyl-G cap, there is a 5’-triphosphate on each primary transcript. Since most prokaryotic mRNAs are decayed

endonucleolytically, since *E. coli* lacks a 5'→3' exoribonuclease, it was assumed for a long time that removal of the 5'-triphosphate was not essential for mRNA decay. More recently, however, RppH has been shown to remove a 5'-pyrophosphate from mRNAs, which stimulates cleavage by the endoribonuclease RNase E [2]. RppH is a Nudix protein, a family of proteins that also includes the eukaryotic decapping enzyme Dcp2 [2, 12, 18]. In the absence of RppH, the half-lives of many mRNA transcripts increased, presumably due to inefficient decay initiation in the presence of a 5'-triphosphate [2]. The biochemical evidence for this conclusion was derived from earlier experiments showing that RNase E is a 5' end-dependent endonuclease that is inhibited by a 5'-triphosphate [96, 97].

Based on the idea that mRNA decay proceeds in a net 5'-3' direction, Mackie [96] determined that RNase E is a 5'-end-dependent endonuclease that targets single-stranded substrates containing unpaired 5' ends. The fact that RNA polymerase initiates transcription such that the 5' terminus contains a 5'-triphosphate led researchers to examine what 5' structure RNase E was capable of recognizing. Several groups established that RNase E, along with its homolog RNase G, was catalytically activated by a 5'-monophospate [96, 98]. However, due to some flexibility within the 5' sensor pocket of RNase E, 5'-triphosphorylated and 5'-hydroxylated transcripts were recognized but were processed at much slower rates [98]. It was subsequently determined that the removal of a 5' pyrophosphate stimulated the initiation of the RNase E-dependent processing of several mRNAs [99].

Additionally several studies have suggested that RNase P, the essential enzyme involved in generating the mature 5’ termini of all tRNAs, also has preference for certain nucleotides and leader lengths (the region upstream of +1 nucleotide of the mature tRNA sequence) at the 5’ termini of RNA substrates, it was important to assess if decapping by RppH also stimulated RNase P cleavages during the of maturation of the 5’ termini of tRNA precursors [100-108].

Evidence has shown that the RNase P holoenzyme directly interacts with the 5’-leader of precursor tRNAs and this subsequent binding affinity is maintained in a leader-length dependent manner up to 4-6 nucleotides [101, 102, 105, 108]. Binding affinity is then maintained in a leader-length independent manner due to structural dynamics of the longer 5’ leader regions [101]. Cleavage assays have also show that as the leader length increases, the ability of RNase P to properly cleave at +1 nucleotide of the precursor tRNA decreases [104]. These two studies demonstrated a very intricate relationship between the status of the 5’-leader of the precursor tRNA and the ability of RNase P to properly bind and cleave the precursor tRNA.

My dissertation research has provided a more extensive examination of the role of RppH in *E. coli*. Thus far, mRNA decay and hybrid jamming are the only major processes that RppH has been identified to play a role. RNase E and RNase J1 are the only ribonucleases that have been shown to require the enzymatic activity of RppH for catalytic activation. Along with these results, the current microarray data assessing the effects RppH has on the entire

transcriptome has been limited to only open reading frames (ORFs) [2]. This dissertation provides a broader look at RppH's effect on the entire transcriptome, thereby encompassing non-coding RNAs and major regulatory pathways. As described in Chapter 2, our data suggest that RNase P requires the removal of 5'-pyrophosphate from the 5'-termini of certain precursor tRNAs to efficiently endonucleolytically remove the 5'-leader that results in a mature 5'-terminus of these tRNAs. With the use of high-density tiling arrays, Chapter 3 demonstrates the role of RppH in regulating the stability of the *flhD flhC* transcript, the master regulator of flageller transcription. These data show that in the *ΔrppH* mutant background, *flhD flhC* is stabilized, which results in the downstream up-regulation of all flagellar operons. This in turn leads to increased motility and shows complementation to the motility defect seen in the *ΔapaH* mutant background.

REFERENCES

1. Bessman, M.J., D.N. Frick, and S.F. O'Handley, *The MutT proteins of "Nudix" hydrolases, a family of versatile, widely distributed "housecleaning enzymes.* J. Biological Chemistry, 1996. **271**: p. 25059-25062.
2. Deana, A., H. Celesnik, and J.G. Belasco, *The bacterial enzyme RppH triggers messenger RNA degradation by 5' pyrophosphate removal.* Nature Biotechnology, 2008. **451**: p. 355-8.
3. Zheng, Q.C., et al., *Homology modeling and substrate binding study of Nudix hydrolase Ndx1 from Thermos thermophilus HB8.* Biochem Biophys Res Commun, 2005. **333**: p. 881-7.

4. Badger, J.L., C.A. Wass, and K.S. Kim, *Identification of Escherichia coli K1 genes contributing to human brain microvascular endothelial cell invasion by differential fluorescence induction.* Mol Microbiol, 2000. **36**: p. 174-82.

5. Mitchell, S.J. and M.F. Minnick, *Characterization of a two-gene locus from Bartonella bacilliformis associated with the ability to invade human erythrocytes.* Infect Immun, 1995. **63**: p. 1552-62.

6. Johnstone, D.B. and S.B. Farr, *ApppppA binds to several proteins in Escherichia coli, including the heat shock and oxidative stress proteins DnaK, GroEL, E89, C45 and C40.* EMBO J, 1991. **10**: p. 3897-904.

7. Nishimura, A., *The timing of cell division: Ap4A as a signal.* Trends Biochem Sci, 1998. **23**: p. 157-9.

8. Piccirillo, C., R. Khanna, and M. Kiledjian, *Functional characterization of the mammalian mRNA decapping enzyme hDcp2.* RNA, 2003. **9**: p. 1138-47.

9. Wang, Z., et al., *The hDcpr protein is a mammalian mRNA decapping enzyme.* Proceedings of the National Academy of Sciences of the United States of America, 2002`. **99**: p. 12663-12668.

10. Mejean, V., et al., *Characterization of the mutX gene of Streptococcus pneumoniae as a homologue of Escherichia coli mutT, and tentative definition of a catalytic domain of the dGTP pyrophosphohydrolases.* Mol Microbiol, 1994. **11**: p. 323-30.

11. Koonin, E.V., *A highly conserved sequence motif defining the family of MutT-related proteins from eubacteria, eukaryotes and viruses.* Nucleic Acids Res, 1993. **21**: p. 4847.

12. Dunckley, T. and R. Parker, *The DCP2 protein is required for mRNA decapping in Saccharomyces cerevisiae and contains a function MutT motif.* EMBO J, 1999. **18**: p. 5411-5422.

13. Gabelli, S.B., et al., *The structure of ADP-ribose pyrophosphatase reveals the structural basis for the versatility of the Nudix family.* Nat Struct Biol, 2001. **8**: p. 467-72.

14. Abeygunawardana, C., et al., *Solution structure of the MutT enzyme, a nucleoside triphosphate pyrophosphohydrolase.* Biochemistry, 1995. **34**: p. 14997-5005.

15. Lin, J., et al., *The role of Glu 57 in the mechanism of the Escherichia coli MutT enzyme by mutagenesis and heteronuclear NMR.* Biochemistry, 1996. **35**: p. 6715-26.

16. Safrany, S.T., et al., *A novel context for the 'MutT' module, a guardian of cell integrity, in a diphosphoinositol polyphosphate phosphohydrolase.* EMBO J, 1998. **17**: p. 6599-607.

17. Mildvan, A.S., et al., *Structures and mechanisms of Nudix hydrolases.* Arch Biochem Biophys, 2005. **433**: p. 129-43.

18. McLennan, A.G., *The Nudix hydrolase superfamily.* Cell Mol Life Sci, 2006. **63**: p. 123-43.

19. Makarova, K.S., et al., *Specific expansion of protein families in the radioresistant bacterium Deinococcus radiodurans.* Genetica, 2000. **108**: p. 25-34.

20. Xu, W., et al., *The Nudix hydrolases of Deinococcus radiodurans.* Mol Microbiol, 2001. **39**: p. 286-90.

21. Xu, D. and J.C. Cote, *Phylogenetic relationships between Bacillus species and related genera inferred from comparison of 3' end 16S rDNA and 5' end 16S-23S ITS nucleotide sequences.* Int J Syst Evol Microbiol, 2003. **53**: p. 695-704.

22. McLennan, A.G., *The MutT motif family of nucleotide phosphohydrolases in man and human pathogens (review).* Int J Mol Med, 1999. **4**: p. 79-89.

23. Yanofsky, C., E.C. Cox, and V. Horn, *The unusual mutagenic specificity of an E. Coli mutator gene.* Proc Natl Acad Sci U S A, 1966. **55**: p. 274-81.

24. Fowler, R.G., et al., *Interactions among the Escherichia coli mutT, mutM, and mutY damage prevention pathways.* DNA Repair (Amst), 2003. **2**: p. 159-73.

25. Maki, H. and M. Sekiguchi, *MutT protein specifically hydrolyses a potent mutagenic substrate for DNA synthesis.* Nature, 1992. **355**: p. 273-5.

26. Tsuzuki, T., et al., *Spontaneous tumorigenesis in mice defective in the MTH1 gene encoding 8-oxo-dGTPase.* Proc Natl Acad Sci USA, 2001. **98**: p. 11456-61.

27. Taddei, F., et al., *Counteraction by MutT protein of transcriptional errors caused by oxidative damage.* Science, 1997. **278**: p. 128-30.

28. Kamiya, H., C. Ishiguro, and H. Harashima, *Increased A:T-->C:G mutations in the mutT strain upon 8-hydroxy-dGTP treatment: direct evidence for MutT involvement in the prevention of mutations by oxidized dGTP.* J Biochem, 2004. **136**: p. 359-62.

29. Kamiya, H., et al., *Suppression of spontaneous and hydrogen peroxide-induced mutations by a MutT-type nucleotide pool sanitization enzyme, the Escherichia coli Orf135 protein.* Genes Cells, 2003. **8**: p. 941-50.

30. Corbin, R.W., et al., *Toward a protein profile of Escherichia coli: comparison to its transcription profile.* Proc Natl Acad Sci U S A, 2003. **100**: p. 9232-7.

31. Gerdes, S.Y., et al., *Experimental determination and system level analysis of essential genes in Escherichia coli MG1655.* J Bacteriol, 2003. **185**: p. 5673-84.

32. O'Handley, S.F., et al., *Escherichia coli orf17 codes for a nucleoside triphosphate pyrophosphohydrolase member of the MutT family of proteins.* J. Biological Chemistry, 1996. **271**: p. 24649-24654.

33. Hori, M., et al., *Dual hydrolysis of diphosphate and triphosphate derivatives of oxidized deoxyadenosine by Orf17 (NtpA), a MutT-type enzyme.* DNA Repair (Amst), 2005. **4**: p. 33-9.

34. Dunn, C.A., et al., *Studies on the ADP-ribose pyrophosphatase subfamily of the nudix hydrolases and tentative identification of trgB, a gene associated with tellurite resistance.* J Biol Chem, 1999. **274**: p. 32318-24.

35. Moreno-Bruna, B., et al., *Adenosine diphosphate sugar pyrophosphatase prevents glycogen biosynthesis in Escherichia coli.* Proc Natl Acad Sci U S A, 2001. **98**: p. 8128-32.

36. Avison, M.B., et al., *Escherichia coli CreBC is a global regulator of gene expression that responds to growth in minimal media.* J Biol Chem, 2001. **276**: p. 26955-61.

37. Frick, D.N., B.D. Townsend, and M.J. Bessman, *A novel GDP-mannose mannosyl hydrolase shares homology with the MutT family of enzymes.* J Biol Chem, 1995. **270**: p. 24086-91.

38. Legler, P.M., et al., *GDP-mannose mannosyl hydrolase catalyzes nucleophilic substitution at carbon, unlike all other Nudix hydrolases.* Biochemistry, 2000. **39**: p. 8603-8.

39. Gabelli, S.B., et al., *Structure and mechanism of GDP-mannose glycosyl hydrolase, a Nudix enzyme that cleaves at carbon instead of phosphorus.* Structure, 2004. **12**: p. 927-35.

40. Stevenson, G., et al., *Organization of the Escherichia coli K-12 gene cluster responsible for production of the extracellular polysaccharide colanic acid.* J Bacteriol, 1996. **178**: p. 4885-93.

41. Frick, D.N. and M.J. Bessman, *Cloning, purification, and properties of a novel NADH pyrophosphatase. Evidence for a nucleotide pyrophosphatase catalytic domain in MutT-like enzymes.* J Biol Chem, 1995. **270**: p. 1529-34.

42. Herbert, M.A., et al., *Signature tagged mutagenesis of Haemophilus influenzae identifies genes required for in vivo survival.* Microb Pathog, 2002. **33**: p. 211-23.

43. Cartwright, J.L., et al., *The Saccharomyces cerevisiae PCD1 gene encodes a peroxisomal nudix hydrolase active toward coenzyme A and its derivatives.* J Biol Chem, 2000. **275**: p. 32925-30.

44. Gasmi, L. and A.G. McLennan, *The mouse Nudt7 gene encodes a peroxisomal nudix hydrolase specific for coenzyme A and its derivatives.* Biochem J, 2001. **357**: p. 33-8.

45. AbdelRaheim, S.R. and A.G. McLennan, *The Caenorhabditis elegans Y87G2A.14 Nudix hydrolase is a peroxisomal coenzyme A diphosphatase.* BMC Biochem, 2002. **3**: p. 5.

46. Kang, L.W., et al., *Structure of a coenzyme A pyrophosphatase from Deinococcus radiodurans: a member of the Nudix family.* J Bacteriol, 2003. **185**: p. 4110-8.

47. Lawhorn, B.G., S.Y. Gerdes, and T.P. Begley, *A genetic screen for the identification of thiamin metabolic genes.* J Biol Chem, 2004. **279**: p. 43555-9.

48. Xu, W., et al., *Three new Nudix hydrolases from Escherichia coli.* J Biol Chem, 2006. **281**: p. 22794-8.

49. Ferrieres, L. and D.J. Clarke, *The RcsC sensor kinase is required for normal biofilm formation in Escherichia coli K-12 and controls the*

expression of a regulon in response to growth on a solid surface. Mol Microbiol, 2003. **50**: p. 1665-82.

50. Warner, A.H. and F.J. Finamore, *Isolation, purification, and characterization of P1,P4-diguanosine 5'-tetraphosphate asymmetrical-pyrophosphohydrolase from brine shrimp eggs.* Biochemistry, 1965. **4**: p. 1568-75.

51. Bessman, M.J., et al., *The gene ygdP, associated with the invasiveness of Escherichia coli K1, designates a Nudix hydrolase, Orf176, active on adenosine (5')-pentaphospho-(5')-adenosine (Ap5A).* J Biol Chem, 2001. **276**: p. 37834-8.

52. Messing, S.A., et al., *Structure and biological function of the RNA pyrophosphohydrolase BdRppH from Bdellovibrio bacteriovorus.* Structure, 2009. **17**: p. 472-81.

53. Guranowski, A., *Specific and nonspecific enzymes involved in the catabolism of mononucleoside and dinucleoside polyphosphates.* Pharmacol Ther, 2000. **87**: p. 117-39.

54. Gaywee, J., et al., *The Rickettsia prowazekii invasion gene homolog (invA) encodes a Nudix hydrolase active on adenosine (5')-pentaphospho-(5')-adenosine.* Mol Cell Proteomics, 2002. **1**: p. 179-85.

55. Conyers, G.B. and M.J. Bessman, *The gene, ialA, associated with the invasion of human erythrocytes by Bartonella bacilliformis, designates a nudix hydrolase active on dinucleoside 5'-polyphosphates.* J Biol Chem, 1999. **274**: p. 1203-6.

56. Steyert, S.R., et al., *Identification of Bdellovibrio bacteriovorus HD100 Bd0714 as a Nudix dGTPase.* J Bacteriol, 2008. **190**: p. 8215-9.

57. Richards, J., et al., *An RNA pyrophosphohydrolase triggers 5'-exonucleolytic degradation of mRNA in Bacillus subtilis.* Mol Cell, 2011. **43**: p. 940-9.

58. Jester, B.C., P. Romby, and E. Lioliou, *When ribonucleases come into play in pathogens: a survey of gram-positive bacteria.* Int J Microbiol, 2012. **2012**: p. 592196.

59. Xu, W., et al., *The 26 Nudix hydrolases of Bacillus cereus, a close relative of Bacillus anthracis.* J Biol Chem, 2004. **279**: p. 24861-5.

60. Shahbabian, K., et al., *RNase Y, a novel endoribonuclease, initiates riboswitch turnover in Bacillus subtilis.* EMBO J, 2009. **28**: p. 3523-33.

61. Hunt, A., et al., *Functional analysis of 11 putative essential genes in Bacillus subtilis.* Microbiology, 2006. **152**: p. 2895-907.

62. Commichau, F.M., et al., *Novel activities of glycolytic enzymes in Bacillus subtilis: interactions with essential proteins involved in mRNA processing.* Mol Cell Proteomics, 2009. **8**: p. 1350-60.

63. Even, S., et al., *Ribonuclease Jq and J2: two novel endoribonucleases in B. subtilis with functional homology to E. coli RNase E.* Nucleic Acids Research, 2005. **33**: p. 2141-2152.

64. Mathy, N., et al., *5'-to-3' exoribonuclease activity in Bacteria: Role of RNase J1 in rRNA maturation and 5' stability of mRNA.* Cell, 2007. **129**: p. 681-692.

65. Li de la Sierra-Gallay, I., et al., *Structural insights into the dual activity of RNase J.* Nat Struct Mol Biol, 2008. **15**: p. 206-12.

66. Abadie, J., et al., *Directional Limits on Persistent Gravitational Waves Using LIGO S5 Science Data.* Phys Rev Lett, 2011. **107**: p. 271102.

67. Ramirez, M.I., et al., *The ytkD (mutTA) gene of Bacillus subtilis encodes a functional antimutator 8-Oxo-(dGTP/GTP)ase and is under dual control of sigma A and sigma F RNA polymerases.* J Bacteriol, 2004. **186**: p. 1050-9.

68. Edelstein, P.H., et al., *Legionella pneumophila NudA Is a Nudix hydrolase and virulence factor.* Infect Immun, 2005. **73**: p. 6567-76.

69. Ismail, T.M., C.A. Hart, and A.G. McLennan, *Regulation of dinucleoside polyphosphate pools by the YgdP and ApaH hydrolases is essential for the ability of Salmonella enterica serovar typhimurium to invade cultured mammalian cells.* J Biol Chem, 2003. **278**: p. 32602-7.

70. Farr, S.B., et al., *An apaH mutation causes AppppA to accumulate and affects motility and catabolite repression in Escherichia coli.* Proc Natl Acad Sci U S A, 1989. **86**: p. 5010-4.

71. Cartwright, J.L., et al., *The IalA invasion gene of Bartonella bacilliformis encodes a (de)nucleoside polyphosphate hydrolase of the MutT motif family and has homologs in other invasive bacteria.* Biochem Biophys Res Commun, 1999. **256**: p. 474-9.

72. McLennan, A.G., *Dinucleoside polyphosphates-friend or foe?* Pharmacol Ther, 2000. **87**: p. 73-89.

73. Scarsdale, J.N., B.A. Peculis, and H.T. Wright, *Crystal structures of U8 snoRNA decapping nudix hydrolase, X29, and its metal and cap complexes.* Structure, 2006. **14**: p. 331-43.

74. Zamecnik, P.C., et al., *Enzymatic synthesis of diadenosine tetraphosphate and diadenosine triphosphate with a purified lysyl-sRNA synthetase.* Biochem Biophys Res Commun, 1966. **24**: p. 91-7.

75. Jovanovic, A. and A. Terzic, *Diadenosine tetraphosphate-induced inhibition of ATP-sensitive K+ channels in patches excised from ventricular myocytes.* Br J Pharmacol, 1996. **117**: p. 233-5.

76. Jovanovic, A., A.E. Alekseev, and A. Terzic, *Cardiac ATP-sensitive K+ channel: a target for diadenosine 5',5''-P1,P5-pentaphosphate.* Naunyn Schmiedebergs Arch Pharmacol, 1996. **353**: p. 241-4.

77. Pintor, J., et al., *Diadenosine polyphosphate receptors. from rat and guinea-pig brain to human nervous system.* Pharmacol Ther, 2000. **87**: p. 103-15.

78. Vartanian, A., et al., *Opposite effects of cell differentiation and apoptosis on Ap3A/Ap4A ratio in human cell cultures.* FEBS Lett, 1997. **415**: p. 160-2.

79. Burgstahler, R. and P. Grafe, *Diadenosine pentaphosphate is more potent than ATP at P2X receptors in isolated rat vagus nerve.* Neuroreport, 2001. **12**: p. 679-82.

80. Nishimura, A., et al., *Diadenosine 5',5'''-P1,P4-tetraphosphate (Ap4A) controls the timing of cell division in Escherichia coli.* Genes Cells, 1997. **2**: p. 401-13.

81. Lee, P.C., B.R. Bochner, and B.N. Ames, *AppppA, heat-shock stress, and cell oxidation.* Proc Natl Acad Sci U S A, 1983. **80**: p. 7496-500.

82. Bochner, B.R., et al., *AppppA and related adenylylated nucleotides are synthesized as a consequence of oxidation stress.* Cell, 1984. **37**: p. 225-32.

83. Varshavsky, A., *Do stalled replication forks synthesize a specific alarmone?* J Theor Biol, 1983. **105**: p. 707-14.

84. Varshavsky, A., *Diadenosine 5', 5'''-P1, P4-tetraphosphate: a pleiotropically acting alarmone?* Cell, 1983. **34**: p. 711-2.

85. Baker, J.C., et al., *Inhibition of simian virus 40 DNA replication in vitro by poly(ADP-ribosyl)ated diadenosine tetraphosphate.* J Biol Chem, 1987. **262**: p. 14855-8.

86. Lienhard, G.E. and Secemski, II, *P 1 ,P 5 -Di(adenosine-5')pentaphosphate, a potent multisubstrate inhibitor of adenylate kinase.* J Biol Chem, 1973. **248**: p. 1121-3.

87. Dzeja, P.P., et al., *Adenylate kinase-catalyzed phosphotransfer in the myocardium : increased contribution in heart failure.* Circ Res, 1999. **84**: p. 1137-43.

88. Jovanovic, A. and A. Terzic, *Diadenosine-hexaphosphate is an inhibitory ligand of myocardial ATP-sensitive K+ channels.* Eur J Pharmacol, 1995. **286**: p. R1-2.

89. Ripoll, C., et al., *Diadenosine polyphosphates. A novel class of glucose-induced intracellular messengers in the pancreatic beta-cell.* Diabetes, 1996. **45**: p. 1431-4.

90. Jovanovic, A., A.E. Alekseev, and A. Terzic, *Intracellular diadenosine polyphosphates: a novel family of inhibitory ligands of the ATP-sensitive K+ channel.* Biochem Pharmacol, 1997. **54**: p. 219-25.

91. Hand, N.J. and T.J. Silhavy, *Null mutations in a Nudix gene, ygdP, implicate an alarmone response in a novel suppression of hybrid jamming.* J Bacteriol, 2003. **185**: p. 6530-9.

92. Snyder, W.B. and T.J. Silhavy, *Beta-galactosidase is inactivated by intermolecular disulfide bonds and is toxic when secreted to the periplasm of Escherichia coli.* J Bacteriol, 1995. **177**: p. 953-63.

93. Fuge, E.K. and S.B. Farr, *AppppA-binding protein E89 is the Escherichia coli heat shock protein ClpB.* J Bacteriol, 1993. **175**: p. 2321-6.

94. Carpousis, A.J., B.F. Luisi, and K.J. McDowall, *Endonucleolytic initiation of mRNA decay in Escherichia coli.* Prog Mol Biol Transl Sci, 2009. **85**: p. 91-135.

95. Coller, J. and R. Parker, *Eukaryotic mRNA decapping.* Ann. Rev. Biochem., 2004. **73**: p. 861-890.

96. Mackie, G.A., *Ribonuclease E is a 5'-end-dependent endonuclease.* NAture, 1998. **395**: p. 720-723.

97. Mackie, G.A., *Stabilization of circular rpsT mRNA demonstrates the 5'-end dependence of RNase E action in vivo.* J. Biological Chemistry, 2000. **275**: p. 25069-25072.

98. Jiang, X. and J.G. Belasco, *Catalytic activation of multimeric RNase E and RNase G by 5'-monophosphorylated RNA.* Proceedings of the National Academy of Sciences of the United States of America, 2004. **101**: p. 9211-9216.

99. Celesnik, H., A. Deana, and J.G. Belasco, *Initiation of RNA decay in Escherichia coli by 5' pyrophosphate removal.* Molecular Cell, 2007. **27**: p. 79-90.

100. Kazantsev, A.V., A.A. Krivenko, and N.R. Pace, *Mapping metal-binding sites in the catalytic domain of bacterial RNase P RNA.* RNA, 2009. **15**: p. 266-76.

101. Rueda, D., et al., *The 5' leader of precursor tRNAAsp bound to the Bacillus subtilis RNase P holoenzyme has an extended conformation.* Biochemistry, 2005. **44**: p. 16130-9.

102. Niranjanakumari, S., et al., *Protein component of the ribozyme ribonuclease P alters substrate recognition by directly contacting precursor tRNA.* Proc Natl Acad Sci U S A, 1998. **95**: p. 15212-7.

103. Guerrier-Takada, C. and S. Altman, *A physical assay for and kinetic analysis of the interactions between M1 RNA and tRNA precursor substrates.* Biochemistry, 1993. **32**: p. 7152-61.

104. Brannvall, M., et al., *RNase P RNA structure and cleavage reflect the primary structure of tRNA genes.* J Mol Biol, 1998. **283**: p. 771-83.

105. McClain, W.H., L.B. Lai, and V. Gopalan, *Trials, travails and triumphs: an account of RNA catalysis in RNase P.* J Mol Biol, 2010. **397**: p. 627-46.

106. Li, H., *Complexes of tRNA and maturation enzymes: shaping up for translation.* Curr Opin Struct Biol, 2007. **17**: p. 293-301.

107. Hartmann, R.K., et al., *The making of tRNAs and more - RNase P and tRNase Z.* Prog Mol Biol Transl Sci, 2009. **85**: p. 319-68.

108. Koutmou, K.S., et al., *Protein-precursor tRNA contact leads to sequence-specific recognition of 5' leaders by bacterial ribonuclease P.* J Mol Biol, 2010. **396**: p. 195-208.

Fig. 1 Nudix motif of RppH from *Bdellovibrio bacteriovorus*

This image of the active site was taken from Messing *et al.* 2009. This image shows the residues in the Nudix motif. Yellow indicates carbon, blue for nitrogen, and red for oxygen; b strands are indicated in cyan, a helices in magenta, and loops in brown.

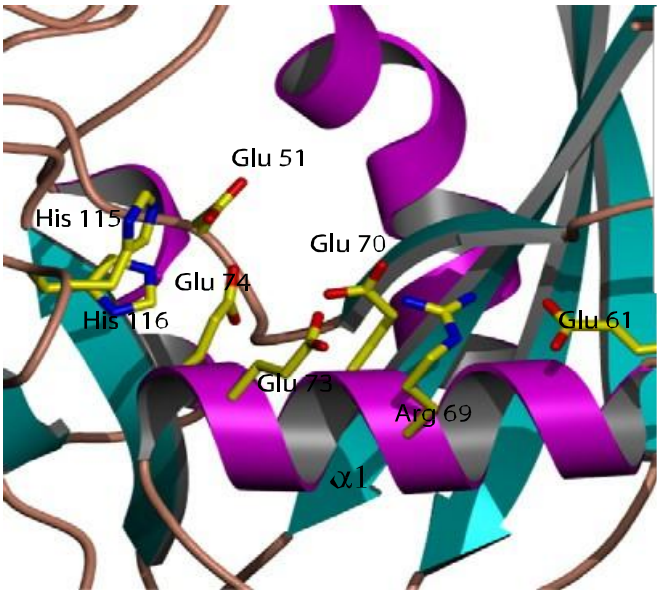
Glu 51
His 115
Glu 70
Glu 74
His 116
Glu 61
Glu 73
Arg 69
α1

CHAPTER 2

ANALYSIS OF THE ROLE OF RNA PYROPHOSPHOHYDROLASE (RPPH) IN TRNA PROCESSING IN *ESCHERICHIA COLI*[1]

---

[1]Bowden, Katherine E., Bijoy K. Mohanty, and Sidney R. Kushner. To be submitted to Nucleic Acids Research.

ABSTRACT

RNase E, a 5'-end dependent endoribonuclease in *Escherichia coli*, rapidly processes many mono- and polycistronic primary tRNA transcripts into pre-tRNAs that are further matured into functional tRNAs that can be aminoacylated. Since the ability of RNase E to interact with many RNA substrates is inhibited by the presence of a 5' triphosphate, it was predicted that inactivation of RNA pyrophosphohydrolase (encoded by *rppH*) would interfere with the processing of many tRNA species. Although an *rppHΔ754* mutant showed a small growth defect, RNase E mediated tRNA processing was unaffected. However, in the absence of RppH, the 5' end maturation of a subset of tRNAS (*pheU, pheV*, and *ilex*) by RNase P was significantly inhibited. Specifically, primary tRNA transcripts with 5' leaders < 5 nucleotides in length were not processed by RNase P in an *rppHΔ754 rph-1* (encodes the 3' → 5' exonuclease RNase PH). The inhibition was suppressed in a *rne-1 rppHΔ754 rph-* triple mutant. Surprisingly, the inhibition of 5' processing by RNase P disappeared in the presence of functional RNase PH.

INTRODUCTION

In all organisms, tRNAs are synthesized as precursors that are rapidly processed by a series of ribonucleases to generate functional forms that can be successfully charged with their corresponding amino acids. In the case of polycistronic tRNA transcripts in *E. coli*, endonucleolytic cleavages by either RNase E and/or RNase P separate the pre-tRNAs [1-4]. Subsequently, the mature 5' termini are generated by the action of RNase P [5], while exonucleolytic processing at the 3' termini by a combination of exoribonucleases, including RNase T, RNase PH, RNase D and RNase BN, leads to the exposure of the encoded CCA determinants [6, 7].

In the case of monocistronic tRNA transcripts, Rho-independent transcription terminators are generally removed by a combination of RNase E, RNase G, RNase P or PNPase [4, 8], while Rho-dependent transcripts have their 3' extensions processed initially by a combination of RNase II and PNPase [3]. As is the case with pre-tRNAs generated from polycistronic transcripts, the final maturation of all 3' termini is thought to be carried out by some combination of RNase T, RNase PH, RNase D and RNase BN [9]. Previous studies have also shown that the ability of RNase P to effectively generate a mature 5’ terminus is partially dependent on prior 3’ processing of the pre-tRNA by RNase E [1].

A potential complication in the processing of primary tRNA transcripts arises from the fact that RNase E, the endonuclease involved in separating many

polycistronic tRNA transcripts [1, 2], has been shown to be inhibited by the presence of a 5’ triphosphate [10-12]. Recently it was shown that 5'-triphosphorylated RNA substrates can be converted to a 5'-monophosphorylated form by the *rppH* encoded RNA pyrophosphohydrolase and that this so-called “decapping” can stimulate the further processing of certain mRNA species by RNase E [10, 12-14]. Based on these observations, it seemed likely that the phosphorylation status of the 5' terminus relative to RNase E activity might play a role in the processing of primary tRNA transcripts.

Furthermore, several studies have presented evidence that RNase P also has preference for certain nucleotides and leader lengths (the region upstream of +1 nucleotide of the mature tRNA sequence) at the 5' termini of RNA substrates [15-22]. Other experiments have shown that the RNase P holoenzyme directly interacts with the 5’-leader of precursor tRNAs and the subsequent binding affinity is maintained in a leader-length dependent manner up to 4-6 nucleotides [16, 17, 20, 23]. With longer leader regions, binding affinity is then maintained in a leader-length independent manner due to structural dynamics [16]. *In vitro c*leavage assays have also shown that as the leader length increases, the ability of RNase P to properly cleave at +1 nucleotide of the precursor tRNA decreases [19]. These two studies demonstrated a very intricate relationship between the status of the 5'-leader of the precursor tRNA and the ability of RNase P to properly bind and cleave the precursor tRNA. Taken together, it appears 5' end decapping by RppH could play a role in the ability of both RNase E and RNase P to properly process tRNA precursors.

Here we show, surprisingly, that the presence of a 5' triphosphate on primary tRNA transcripts (either polycistronic or monocistronic) does not affect the ability of RNase E to initiate their processing. In contrast, the 5' triphosphate on short 5' leaders significantly inhibits RNase P activity, particularly if the 3' terminus has already been processed by RNase E. For example, the *pheU* and *pheV* tRNAs are monocistronic transcripts that contain Rho-independent transcription terminators and 5' leaders of 3-4 nt. Inactivation of RppH significantly inhibited the ability of RNase P to generate mature 5' termini. However, the inhibition of RNase P activity was not observed if the 3' Rho-independent transcription terminator was not removed from the primary transcript. Longer 5' leader regions (> 5 nt) were not affected by the presence of a 5' terminal triphosphate. Furthermore, the presence of a 5' triphosphate does not inhibit the ability of RNase P to separate polycistronic transcripts such as *valV valW* and *leuQ leuP leuV*. However, in the inhibition of RNase P processing was not observed if functional RNase PH was present in the cell.

MATERIALS AND METHODS

Bacterial Strains

The *E. coli* strains used in this study were all derived from MG1693 (*rph-1 thyA715*) (*E. coli* Genetic Stock Center, Yale University) and are listed in Table 1. MG1693 contains no RNase PH activity and shows reduced expression of *pyrE* due to the single nucleotide frameshift in the *rph* gene [24]. An rph^+ derivative (SK10153) was constructed as previously described [7]. The *rne-1* and *rnpA49*

alleles encode temperature-sensitive RNase E and RNase P proteins, respectively, which are unable to support cell viability at 44°C [25-27]. The construction of SK2525 [1], SK2534 [1], and SK5665 [25] have been previously described. SK3564 [*rneΔ1018::bla thyA715 rph-1 recA56 srlD::*Tn*10*/ pDHK30(*rng219* Sm^r/Sp^r)/ pWSK219(Km^r)] is an RNase E deletion strain that contains a mutant RNase G (*rng-219*) protein synthesized from a single copy plasmid to support cell viability [28]. The *rng::cat* allele is an insertion/deletion of a chloramphenicol resistance cassette into the gene encoding RNase G [29]. The construction of SK2541 has been previously described [30]. The construction of SK5704 has been previously described [31]. For this study, a P1 lysate grown on JW2798 (Keio Collection, Japan) was used to transduce MG1693, SK2525 (*rnpA49*), SK5665 (*rne-1*), and SK2534 (*rne-1 rnpA49*) to construct SK4390 (*ΔrppH::kan*), SK4395 (*ΔrppH::kan rnpA49*), SK4394 (*ΔrppH::kan rne-1*), and SK4397 (*ΔrppH::kan rne-1 rnpA49*), respectively.

Growth Curves

Cultures were grown with shaking in Luria broth containing thymine (50 µg/mL) and kanamycin (25 µg/mL) (when *ΔrppH754::kan* was present) at 37°C until they reached 20 Klett units above background (No. 42 green filter). Subsequently, the cultures were shifted to 44°C to inactivate the temperature sensitive RNase E and RNase P proteins. Cell densities were recorded every 30 min and the cultures were maintained in mid exponential phase (80 Klett units) by diluting with fresh prewarmed medium. The Klett values (Fig. 1) were adjusted to reflect the appropriate dilution factors. The growth curves for MG1693 (*rph-1*) and

SK10153 (wild type) were carried out at 37°C and the cultures were maintained at 80 Klett units above by diluting with fresh prewarmed medium.

Growth of bacterial strains and isolation of total RNA

Bacterial strains were grown with shaking in at 37°C in Luria broth supplemented with thymine (50 µg/mL) and kanamycin (25 µg/mL) (when *rppHΔ754::kan* was present) until a cell density of 20 Klett units above background (~5.0 x 10^7 cells/ml). Cultures were then shifted to 44°C for two hours and maintained at 80 Klett units above background by diluting, if necessary, with fresh prewarmed medium. Unless otherwise noted, RNA was extracted using the method described by Stead *et al.* [32]. RNA was quantified on a NanoDrop™ 2000c (Thermo Scientific) apparatus. Five hundred ng of each RNA sample were run on a 1% Agarose-Tris-acetate-EDTA gel and visualized with ethidium bromide to ensure satisfactory quality for further analysis. RNA to be used in primer extensions, RT-PCR cloning, and sequencing experiments was further treated with the DNA-free kit™ (Ambion) to remove any contaminating DNA. Subsequently, the treated samples were quantified with the NanoDrop™ 2000c machine. In some cases the RNA used in the initial RT-PCR cloning experiments were isolated using the Trizol® Reagent (Invitrogen) as described by the manufacturer. Subsequently, RNA isolated by both methods was directly compared in a series of Northern analyses and PCR cloning and sequencing experiments that demonstrated the comparability of both methods (data not shown).

Northern analysis

Northern analysis was performed as previously described in O'Hara *et al.* [31]. Five µg of total RNA was run on either 6% or 8% polyacrylamide-8.3 M urea gels and transferred to a positively charged nylon membrane (Nytran® SPC, Whatman®) for 2.5 hours at 20 volts followed 45 minutes at 40 volts. Northern blots were probed with ^{32}P-5'-end-labeled oligonucleotides [33] specific to the mature sequence of each tRNA being tested. The probe sequences are available on request. The blot was then scanned with a PhosphorImager (Storm™ 840, GE Healthcare) and the data were quantified using ImageQuant TL software (GE Healthcare).

Primer extension

Primer extension analysis of the various tRNA transcripts was carried out as previously described [3]. The sequences were analyzed on a 6% PAGE containing 8 M urea.

RT-PCR cloning and sequencing of 5'-3' ligated transcripts

The 5' and 3'-ends of the *pheU, pheV* and *ileX* transcripts were identified by cloning and sequencing the RT-PCR products obtained from 5'→3' end-ligated circular RNAs following the methods previously described [4], with the following modifications. Prior to RNA ligation, total RNA was denatured at 65°C for 5 minutes. Subsequently, the RNA ligation step was carried out at 16°C overnight. The 5'-3' junctions of the cDNAs were amplified with pairs of gene-specific primers using GoTaq® Green Master Mix (Promega).

RESULTS

Inactivation of RppH leads to significant growth defects

In order to examine the phenotypic properties of strains defective in converting 5' terminal triphosphates into 5' phosphomonoesters, we constructed an isogenic set of strains in the MG1693 (*rph-1 thyA715*) genetic background using a complete deletion/insertion of the structural gene for RNA pyrophosphohydrolase (*rppH∆754::kan*) and temperature sensitive alleles for both RNase E (*rne-1* [34]) and RNase P (*rnpA49* [26]) as described in the Materials and Methods. Since both the RNase E and RNase P endoribonucleases have been shown to play a major role in the processing of primary tRNA transcripts [1, 3, 4, 8, 35, 36] and previous work by Deana *et al.* [14] showed that the conversion of the 5'-triphosphate to a 5'-monophosphoester by RppH stimulated RNase E-mediated mRNA decay, we expected to see a significant growth phenotype in an *rne-1 rppH∆754* double mutant at 44^{o}C.

In fact, there was a significant growth effect in the *rppH∆754* single mutant compared to the wild type control at 44^{o}C (Fig. 1). Furthermore, in the *rppH∆754 rne-1* and *rppH∆754 rnpA49* double mutants, the inactivation of RppH exacerbated the conditional lethality associated with the inactivation of either RNase E or RNase P (Fig. 1). Thus, as seen previously [25], the *rne-1* single mutant continued to grow for several hours after the shift to 44^{o}C as did the *rnpA49* single mutant, but both double mutants showed a more dramatic reduction in both their growth rates and final cell densities (Fig. 1). Interestingly, the most striking phenotype was observed in the *rne-1 rnpA49 rppH∆754* triple

mutant, where growth ceased within 30 min after the shift to the nonpermissive temperature.

Failure to remove the 5' terminal triphosphate does not inhibit RNase E processing of primary polycistronic tRNA transcripts

It has been shown previously that RNase E is responsible for separating a significant number of polycistronic transcripts into pre-tRNAs that can be further processed into mature species [1, 36]. tRNA precursors are processed very rapidly, with half-lives estimated to be <30 seconds [1]. Since it has been shown that RNase E is a 5' end-dependent endonuclease that is inhibited by a 5' triphosphate [10-14], we expected to see an inhibition of processing of the polycistronic *glyW cysT leuZ* and *argX hisR leuT proM* primary transcripts in the *rppHΔ754 rph-1* mutant, because both of these transcripts require RNase E for their initial processing [1, 36]. However, as shown in Fig. 2 (lane 4), inactivation of RppH did not affect the processing of the *argX hisR leuT proM* primary. In contrast, inactivation of RNase E led to the appearance of the primary transcript as well as a number of partially processed intermediates (Fig. 2B, 2C, lane 3). In addition, inactivation of RNase P led to the expected accumulation of pre-tRNAs that retained their 5' leader sequences as well as larger partially processed species (Fig. 2B, 2C, lane 2). The processing of the transcript in the *rne-1 rppHΔ754 rph-1* triple mutant was identical to what was observed in the *rne-1 rph-1* double mutant (Fig. 2C, lanes 3 and 5). Similar results were observed for the *glyW cysT leuZ* transcript (data not shown).

Inactivation of RppH does not affect the processing of polycistronic tRNA transcripts by RNase P

It has been recently shown that a number of primary polycistronic tRNA transcripts, including *valV valW* and *leuQ leuP leuV* are separated into pre-tRNAs exclusively by RNase P [3]. Accordingly, we tested to see if failure to remove the 5' terminal triphosphate might affect the processing of these transcripts by RNase P. As shown previously, the *valV valW* operon is rapidly processed in an RNase P-dependent fashion (Fig. 3, lane 2) that does not involve the active of RNase E (Fig. 3, lane 3). Significantly, inactivation of RppH did not affect the processing of the operon (Fig. 3, lane 4). The processing profile was also not changed in the *rppHΔ754 rnpA49* double mutant (Fig. 3, lane 5). Similar results were observed with the *leuQ leuP leuV* operon (data not shown).

RppH does not affect the maturation of monocistronic tRNA precursors with 5' leaders longer than 8-10 nucleotides

Since the conversion of the terminal triphosphate to a monophosphate by the RppH protein had no effect on the processing of polycistronic tRNA transcripts, we decided to examine the processing of a number of monocistronic tRNA transcripts. Initially we tested the *leuX* transcript, which has been shown to have a 22 nucleotide 5' leader that is removed RNase P, and a Rho-independent transcription terminator that is processed primarily by the 3' → 5' exonuclease polynucleotide phosphorylase (PNPase) [8]. As observed above with the various

polycistronic transcripts (Figs. 2, 3), inactivation of RppH did not affect the processing of the *leuX* primary transcript (Fig. 4, lane 2). In addition, the processing profile of the *rppHΔ754 rnpA49 rph-1* triple mutant was identical to what was observed with the *rnpA49 rph-1* double mutant (Fig. 4, lanes 4,5).

Next, we tested the processing of the four *asn* tRNA precursors (*asnT, asnU, asnV*, and *asnW*), which have been shown to have ~9-10 nucleotide 5' leaders that are removed by RNase P. Removal of the 3' Rho-independent transcription terminators is partially dependent on RNase E [1]. In the case of these four monocistronic transcripts, we expected to see precursors accumulate in the presence of a 5' triphosphate inhibited either RNase E or RNase P activity. However, as shown in Fig. 5 (lane 2), inactivation of RppH had no effect on *asn* tRNA processing. In contrast, inactivation of RNase P led to the accumulation of precursor species that retained their 5' leader sequences (Fig. 5, lane 4), while inactivation of RNase E led to the appearance of transcripts that retained their Rho-independent transcription terminators (Fig. 5, lane 3). The most significant change in the processing of the four *asn* tRNAs transcripts occurred in the *rppHΔ754 rne-1 rnpA49 rph-1* quadruple mutant (Fig. 5, lane 7).

Inactivation of RppH inhibits the 5' end maturation of the *pheU* and *pheV* primary transcripts

Based on the data presented in Figs. 2-5, it appeared that the presence of a 5' triphosphate on primary tRNA transcripts did not interfere with their processing by either RNase E or RNase P. However, as previously mentioned,

the RNase P holoenzyme interacts with the 5' leader and proper cleavage is dependent on its length [16, 17, 19, 23]. Accordingly, we speculated that primary tRNA transcripts with 5' leaders of less than five nucleotides might demonstrate an RppH effect. Accordingly, we focused on the *pheU* and *pheV* transcripts, which have predicted 5' leaders of less than five nucleotides [1]. Both are monocistronic transcripts that have the same mature tRNA sequence and use RNase P and RNase E to process their 5' and 3' termini, respectively [Fig. 6A, [1]]. Since the presence of a 5' triphosphate did not affect RNase E-dependent 3'-maturation of other monocistronic tRNA precursors (Fig. 4, 5), we were not surprised that this observation also held true for the *pheU* and *pheV* transcripts, where no full-length transcripts were observed in the absence of RppH (Fig. 6B, lane 2). These results contrasted with what was observed in the *rne-1 rph-1* strain, where we saw a small amount of full-length transcripts in addition to the mature species (Fig. 6B, lane 4), in agreement with previously published results [1].

However, in the absence of RppH we observed a processing intermediate that was several nucleotides longer than the mature species (Fig. 6B, lane 2) and appeared to be comparable to the species observed in an *rnpA49 rph-1* double mutant (Fig. 6B, lane 3). Surprisingly, in the *rppHΔ754 rne-1 rph-1* triple mutant, the processing intermediate disappeared (Fig. 6B, lane 5). Furthermore, while the combination of *rppHΔ754 rnpA49 rph-1* gave the same processing profile as the *rnpA49 rph-1* double mutant, the further inactivation of RNase E significantly changed the processing profile (Fig. 6B, lane 7).

The 5' leaders of the *pheU* and *pheV* transcripts are not processed in the absence of RppH

Since the longer intermediates observed in the absence of RppH could have arisen from a failure to process properly at either the 5' or 3' terminus, we carried out primer extension analysis using RNA isolated from wild type, *rppHΔ754 rph-1* and *rnpA49 rph-1* strains (Fig. 7). Although it has been reported that the transcript start sites of both *pheU* and *pheV* are only one nucleotide upstream of the mature 5' terminus [37], our data clearly demonstrated that transcription actually starts at two sites, either 3 or 4 nucleotides upstream of the mature 5' terminus (Fig. 7). As expected, in the absence of RNase P, almost all of the *pheU* and *pheV* tRNAs retained their 5' leaders and there appeared to be almost equal amounts of the two transcription products (Fig. 7). Although inactivation of RppH did not completely block 5' end maturation by RNase P, the majority of the *pheU* and *pheV* species retained their primary 5' sequences (Fig. 7). It should also be noted that in the wild type control strain, approximately 20% of the mature *pheU* and *pheV* tRNAs contained an extra nucleotide at the 5' terminus.

Analysis of the 5' and 3' termini of the *pheU* and *pheV* transcripts using RNA ligation and RT-PCR

We have previously used an RNA self-ligation procedure to map the 5' and 3' ends of specific tRNA transcripts in various genetic backgrounds [4, 7, 8]. In the case of the *pheU* and *pheV* transcripts, differences in the 3' downstream

sequences made it possible for us to distinguish between the two primary sequences (Fig. 8). Initially, we examined tRNAs isolated from MG1693 (*rph-1*). As shown in Fig. 8A-B, in MG1693 between 75-85% of the clones had mature 5' termini depending on whether the RNA was pretreated with tobacco acid phosphatase (TAP, converts 5' triphosphates to 5' monophosphates), prior to the self-ligation step. The other clones had anywhere from 1-4 extra nucleotides at the 5' terminus. Interestingly, only a small fraction of the clones had mature 3' termini, with many having 1-3 downstream nucleotides, supporting previous data suggesting that RNase E cleaves several nucleotides downstream of the mature CCA terminus [1]. A higher percentage of mature 3' termini were observed in SK10153 (wild type), indicating that RNase PH plays a significant role in the final maturation of the *pheU* and *pheV* transcripts (data not shown).

Since both the Northern analysis (Fig. 6) and primer extension data (Fig. 7) suggested that most of the *pheU* and *pheV* transcripts had immature 5' termini, we next examined RNA isolated from an *rnpA49 rph-1* mutant that had been shifted to 44^{o}C to inactivate RNase P. Of the 45 independent clones sequenced, only one had a mature 5' terminus (Fig. 8C). The remainder of the clones had 2-4 extra nucleotides at their 5' ends. One clone had 8 extra nucleotides (Fig. 8C). In addition, 42% of the clones had mature 3' termini compared to 10% in the *rph-1* single mutant.

When we analyzed the RNA isolated from the *rppHΔ754 rph-1* mutant, the data again confirmed the results shown in Figs. 6-7. Specifically, 54% of the clones had between 3-5 extra nucleotides at their 5' termini (Fig. 8E). However,

an unexpected surprise was the observation that a large number of clones derived from the RNA that had not been treated with TAP had extra nucleotides at their 5' termini (Fig. 8D). These results suggested the presence of a second activity in the cell that was capable of removing the 5' triphosphate, a required step for self-ligation to work. The data from the 3' terminus was comparable to what was seen with the *rnpA49 rph-1* double mutant. It should also be noted that a small fraction (between 8-14%) of the clones in the various genetic backgrounds had short poly(A) tails added to immature 3' termini, in agreement with previously reported results [7].

Inactivation of RNase E suppress the inhibition of RNase P activity on the *pheU* and *pheV* transcripts in the absence of RppH

As previously seen in the Northern analysis of the *pheU* and *pheV* transcripts, inactivation of RNase E appeared to suppress the effect of the *rppHΔ754* allele on the 5' end maturation of the transcripts (Fig. 6, lane 5). Of the 40 clones obtained from RNA isolate from an *rne-1 rph-1* strain, 70% had mature 5' termini (data not shown). In addition, as expected a few contained the entire 3' terminator sequence (data not shown). In the *rppHΔ754 rne-1 rph-1* triple mutant, 78% (22/30) of the clones hade mature 5' termini (data not shown) compared to 46% (18/41) in the *rppHΔ754 rph-1* double mutant.

Multiple endoribonucleases are responsible for removing the 3' Rho-independent transcription terminator sequences from the *pheU* and *pheV* transcripts

Although previous work had suggested that the *pheU* and *pheV* transcript were very dependent on RNase E for the removal of their 3' termini [1], with the development of an improved RNA isolation procedure that gives a more accurate representation of the total intracellular RNA levels [38], we carried out a direct comparison of the fraction of full-length versus mature transcripts in an *rne-1* mutant using RNA isolated by either the catrimide detergent method [33] or the new RNAsnap™ procedure [38]. With the catrimide isolated RNA, in an *rne-1* mutant, the fraction of full-length/mature *pheU/pheV* transcripts was 50%, supporting a major role for RNase E in their processing. However, the fraction of full-length transcripts dropped dramatically in the RNAsnap™ isolated RNA to between 3-5%, indicating that our previous work had significantly underestimated the amount of mature tRNA in the total RNA population (data not shown). Accordingly, we reexamined that removal of the terminator sequences in an *rne∆1018* deletion mutant as well as combinations of *rne-1*(RNase E), *rnpA49* (RNase P), *rng::cat* (RNase G), *∆rnz* (RNase Z, and *rnlA2* (RNase LS). Northern analysis demonstrated that RNase E only processed ~25% of the transcripts, while the other four enzymes processed the remainder of the transcripts with almost equal efficiency (data not shown). Based on the sequencing data presented in Fig. 8, all of the endonucleases appear to cleave 1-4 nucleotides downstream of the encoded CCA determinant.

RppH affects the processing of the monocistronic *ileX* transcript

Since inactivation of RppH inhibited the 5' end processing of the *pheU* and *pheV* primary transcripts (Fig. 6), we also examined the *ileX* transcript, which has

a predicted leader of a single nucleotide [37]. In fact, Northern analysis suggested the presence of a slightly longer *ileX* transcript in both the *rppHΔ754 rph-1* and *rnpA49 rph-1* strains (Fig. 9, lanes 2-4). Since the difference in the electrophoretic mobilities between the various species in the wild type, *rne-1 rph-1, rnpA49 rph-1* and *rppHΔ754 rph-1* strains was very small, we used the RNA self-ligation assay described above to determine the 5' and 3' termini of the *ileX* transcripts isolated from the various strains.

In the *rph-1* single mutant, the bulk of the clones had mature 5' termini, with only 12% of the clones having 1-2 extra nucleotides at the 5' terminus (Fig. 10A). Interestingly, a number of the clones retained the complete Rho-independent transcription terminator, suggesting that the *ileX* primary transcript was not as efficiently processed as some of the tRNA species. In contrast, in the absence of RppH, most of the clones (86%) had immature 5' termini that contained 1-4 extra nucleotides (Fig. 10B). Similar results were seen in the *rnpA49* mutant (Fig. 10C). Surprisingly, in both the *rppHΔ754 rph-1* and *rnpA49 rph-1* mutants, many of the clones had truncated 3' termini (Fig. 10B, C). These results were not observed for the *pheU* and *pheV* transcripts (Fig. 8) or with the previously published data from *leuX* [8].

Inhibition of RNase P activity on tRNA precursors in the absence of RppH requires the inactivation of RNase PH

For many years, the analysis of RNA metabolism in *E. coli* has used derivatives of MG1655 as their control “wild type” strain. However, in reality

MG1655 contains a single base pair deletion in the structural gene for RNase PH [24]. We have previously shown that the absence of RNase PH does not play a role in mRNA decay (data not shown). However, since the enzyme does play a role in the final 3' end maturation of a significant number of tRNA species [39], we decided to determine whether having functional RNase PH altered the results we saw with the *pheU* and *pheV* transcripts in the absence of RppH. As shown in Fig. 11, in the *rppH∆754* single mutant, RNase P processing proceeded normally, suggesting some type of interaction between RNase PH and RppH.

DISCUSSION

Although previous work has shown that RNase E is activated by the presence of a 5'-monophosphate, after removal of a pyrophosphate by RppH, which then initiates mRNA decay, we show here that this is not the case for tRNA processing [10, 12, 13, 40]. Furthermore, we have presented evidence that the 5'-triphosphate does not inhibit processing of polycistronic operons that are RNase E and RNase P-dependent, and monocistronic transcripts where the leader length is more than 10 nucleotides. We have also shown that leader removal by RNase P is inhibited by the 5'-triphosphate when the leader is less than 5 nucleotides, but only if there is no RNase PH in the cell. Additionally, in the case of *ileX,* the 3'-termini can be found within the mature tRNA sequence when the 5'-leader is not properly processed.

The evidence to support these claims was initially apparent in regards to the growth properties of the various mutant strains. We initially expected the *ΔrppH rne-1 rph-1* triple mutant to grow much slower than the *ΔrppH rnpA49 rph-1* triple mutant. However, this was not the case. In fact, the *ΔrppH rne-1 rph-1* triple mutant actually grew better than the *ΔrppH rnpA49 rph-1* triple mutant (Fig. 1). This result indicated that RNase P activation may be more important than originally thought. Although RppH is not essential in *E. coli*, its activity is essential in the proper processing of monocistronic tRNAs *pheU, pheV,* and *ileX* by RNase P.

In regards to tRNA maturation, we saw no evidence that RNase E activity was inhibited by the presence of a 5'-triphosphate. In the case of polycistronic operons, no full-length tRNA precursors were seen in the *ΔrppH* mutant (Figs. 2, 3). This result was also true for monocistronic tRNA precursors with Rho-independent terminators that were removed by RNase E (Fig. 7, 8). What was of interest was the trend that the *rne-1* mutation actually suppressed the *ΔrppH* mutation (data not shown). This could indicate that either the 5'-triphosphate provides a better substrate for RNase E-dependent cleavages for these specific tRNA precursors, or that RNase E cleaves through an internal entry mechanism when a 5'-triphosphate is present, which is more efficient than the 5'-dependent mechanism. Further analysis would need to be conducted to determine which scenario is accurate.

With *pheU* and *pheV*, we saw an intermediate effect when the *ΔrppH rph-1* species were compared to the *rnpA49 rph-1* mutant species (Figs. 6, 7, 8). This

indicated to us that when the 5’-triphosphate is present, RNase P either has poor binding affinity to the tRNA precursor or can still bind but not cleave in the proper location. Seeing that studies have only been conducted on binding affinities of RNase P with specific nucleotides within the 5’-leader and mature sequences [16-20], it would be of interest to conduct binding affinity assays with substrates that contain a 5’-triphosphate versus a 5’-monophosphate. Additionally it is important to ascertain what is actually determining the ability of RNAse P to cleave: the leader or the mature tRNA sequence.

With these findings, we propose a new model for maturation of tRNA precursors (Fig. 12). In the case of polycistronic tRNA operons and monocistronic precursors where the leader is longer than 5 nucleotides and polycistronic tRNA operons, RppH is not required for proper processing (Fig.12). Endonucleases can still separate the individual precursors within the operon and remove the 5’-leader and 3’-terminator from monocistronic precursors. However, when the leader is less than 5 nucleotides, RppH is required for proper leader removal by RNase P. However, perhaps the most interesting finding of these experiments is the apparent interaction between RppH and the 3’→5’ exoribonuclease RNase PH.

FUNDING

This work was supported in part by a grant from the National Institutes of Health (GM081544) to S.R.K.

REFERENCES

1. Ow, M.C. and S.R. Kushner, *Initiation of tRNA maturation by RNase E is essential for cell viability in E. coli.* Genes Dev, 2002. **16**: p. 1102-15.
2. Li, Z. and M.P. Deutscher, *RNase E plays an essential role in the maturation of Escherichia coli tRNA precursors.* RNA, 2002. **8**: p. 97-109.
3. Mohanty, B.K. and S.R. Kushner, *Ribonuclease P processes polycistronic tRNA transcripts in Escherichia coli independent of ribonuclease E.* Nucleic Acids Res, 2007. **35**: p. 7614-25.
4. Mohanty, B.K. and S.R. Kushner, *Rho-independent transcription terminators inhibit RNase P processing of the secG leuU and metT tRNA polycistronic transcripts in Escherichia coli.* Nucleic Acids Res, 2008. **36**: p. 364-75.
5. Lundberg, U. and S. Altman, *Processing of the precursor to the catalytic RNA subunit of RNase P from Escherichia coli.* RNA, 1995. **1**: p. 327-334.
6. Reuven, N.B. and M.P. Deutscher, *Multiple exoribonucleases are required for the 3' processing of Escherichia coli tRNA precursors in vivo.* FASEB J., 1993. **7**: p. 143-148.
7. Mohanty, B.K., V.F. Maples, and S.R. Kushner, *Polyadenylation helps regulate functional tRNA levels in Escherichia coli.* Nucleic Acids Res, 2012. **40**: p. 4589-4603.
8. Mohanty, B.K. and S.R. Kushner, *Processing of the Escherichia coli leuX tRNA transcript, encoding $tRNA^{leu5}$, requires either the 3'–5' exoribonuclease polynucleotide phosphorylase or RNase P to remove the*

Rho-independent transcription terminator. Nucleic Acids Res, 2010. **38**: p. 5306-5318.

9. Li, Z. and M.P. Deutscher, *Maturation pathways for E. coli tRNA precursors: a random multienzyme process in vivo.* Cell, 1996. **86**: p. 503-12.
10. Mackie, G.A., *Ribonuclease E is a 5'-end-dependent endonuclease.* NAture, 1998. **395**: p. 720-723.
11. Mackie, G.A., *Stabilization of circular rpsT mRNA demonstrates the 5'-end dependence of RNase E action in vivo.* J. Biological Chemistry, 2000. **275**: p. 25069-25072.
12. Jiang, X. and J.G. Belasco, *Catalytic activation of multimeric RNase E and RNase G by 5'-monophosphorylated RNA.* Proceedings of the National Academy of Sciences of the United States of America, 2004. **101**: p. 9211-9216.
13. Celesnik, H., A. Deana, and J.G. Belasco, *Initiation of RNA decay in Escherichia coli by 5' pyrophosphate removal.* Molecular Cell, 2007. **27**: p. 79-90.
14. Deana, A., H. Celesnik, and J.G. Belasco, *The bacterial enzyme RppH triggers messenger RNA degradation by 5' pyrophosphate removal.* Nature 2008. **451**: p. 355-358.
15. Kazantsev, A.V., A.A. Krivenko, and N.R. Pace, *Mapping metal-binding sites in the catalytic domain of bacterial RNase P RNA.* RNA, 2009. **15**: p. 266-76.

16. Rueda, D., et al., *The 5' leader of precursor tRNAAsp bound to the Bacillus subtilis RNase P holoenzyme has an extended conformation.* Biochemistry, 2005. **44**: p. 16130-9.

17. Niranjanakumari, S., et al., *Protein component of the ribozyme ribonuclease P alters substrate recognition by directly contacting precursor tRNA.* Proc Natl Acad Sci U S A, 1998. **95**: p. 15212-7.

18. Guerrier-Takada, C. and S. Altman, *A physical assay for and kinetic analysis of the interactions between M1 RNA and tRNA precursor substrates.* Biochemistry, 1993. **32**: p. 7152-61.

19. Brannvall, M., et al., *RNase P RNA structure and cleavage reflect the primary structure of tRNA genes.* J Mol Biol, 1998. **283**: p. 771-83.

20. McClain, W.H., L.B. Lai, and V. Gopalan, *Trials, travails and triumphs: an account of RNA catalysis in RNase P.* J Mol Biol, 2010. **397**: p. 627-46.

21. Li, H., *Complexes of tRNA and maturation enzymes: shaping up for translation.* Curr Opin Struct Biol, 2007. **17**: p. 293-301.

22. Hartmann, R.K., et al., *The making of tRNAs and more - RNase P and tRNase Z.* Prog Mol Biol Transl Sci, 2009. **85**: p. 319-68.

23. Koutmou, K.S., et al., *Protein-precursor tRNA contact leads to sequence-specific recognition of 5' leaders by bacterial ribonuclease P.* J Mol Biol, 2010. **396**: p. 195-208.

24. Jensen, K.G., *The Escherichia coli K-12 "wild types" W3110 and MG1655 have an rph frameshift mutation that leads to pyrimidine starvation due to low pyrE expression levels.* J. Bacteriol., 1993. **175**: p. 3401-3407.

25. Arraiano, C.M., S.D. Yancey, and S.R. Kushner, *Stabilization of discrete mRNA breakdown products in ams pnp rnb multiple mutants of Escherichia coli K-12.* J Bacteriol, 1988. **170**: p. 4625-33.

26. Schedl, P. and P. Primakoff, *Mutants of Escherichia coli thermosensitive for the synthesis of transfer RNA.* Proceedings of the National Academy of Sciences of the United States of America, 1973. **70**: p. 2091-2095.

27. Ono, M. and M. Kuwano, *A conditional lethal mutation in an Escherichia coli strain with a longer chemical lifetime of mRNA.* Journal of Molecular Biology, 1979. **129**: p. 343-357.

28. Chung, D.-H., et al., *Single amino acid changes in the predicted RNase H domain of E. coli RNase G lead to the complementation of RNase E mutants.* RNA, 2010. **16**: p. 1371-1385.

29. Wachi, M., G. Umitsuki, and K. Nagai, *Functional relationship between Escherichia coli RNase E and the CafA protein.* Mol. Gen. Genet., 1997. **253**: p. 515-519.

30. Ow, M.C., T. Perwez, and S.R. Kushner, *RNase G of Escherichia coli exhibits only limited functional overlap with its essential homologue, RNase E.* Molecular Microbiol, 2003. **49**: p. 607-22.

31. O'Hara, E.B., et al., *Polyadenylylation helps regulate mRNA decay in Escherichia coli.* Proc Natl Acad Sci U S A, 1995. **92**: p. 1807-11.

32. Stead, M.B., et al., *RNAsnap™ : A rapid, quantitative, and inexpensive, method for isolating total RNA from bacteria.* Nucleic Acids Res, 2012: p. submitted.

33. Mohanty, B.K., et al., *Analysis of RNA decay, processing, and polyadenylation in Escherichia coli and other prokaryotes.* Methods Enzymol, 2008. **447**: p. 3-29.

34. Babitzke, P. and S.R. Kushner, *The Ams (altered mRNA stability) protein and ribonuclease E are encoded by the same structural gene of Escherichia coli.* Proc Natl Acad Sci U S A, 1991. **88**: p. 1-5.

35. Ow, M.C. and S.R. Kushner, *Initiation of tRNA maturation by RNase E is essential for cell viability in Escherichia coli.* Genes and Development, 2002. **16**: p. 1102-1115.

36. Li, Z. and M.P. Deutscher, *RNase E plays an essential role in the maturation of Escherichia coli tRNA precursors.* RNA, 2002. **8**: p. 97-109.

37. Keseler, I.M., et al., *EcoCyc: a comprehensive database of Escherichia coli biology.* Nucleic Acids Res, 2011. **39**: p. D583-90.

38. Stead, M.B., et al., *RNAsnap: a rapid, quantitative and inexpensive, method for isolating total RNA from bacteria.* Nucleic Acids Res, 2012.

39. Mohanty, B.K. and S.R. Kushner, *Deregulation of poly(A) polymerase I in Escherichia coli inhibits protein synthesis and leads to cell death.* Nucleic Acids Res, 2012: p. in press.

40. Deana, A., H. Celesnik, and J.G. Belasco, *The bacterial enzyme RppH triggers messenger RNA degradation by 5' pyrophosphate removal.* Nature Biotechnology, 2008. **451**: p. 355-8.

Table 1. Bacterial strains used in this work.

Strains	Genotype	Reference/source
MG1693	*thyA715 rph-1*	*E. coli* Genetic Stock Center
SK2525	*rnpA49 thyA715 rph-1 rbsD296::*Tn*10* Tc^r	[1]
SK2534	*rne-1 rnpA49 thyA715 rph-1 rbsD296::*Tn*10* Tc^r	[1]
SK2541	*rne-1 rng::cat thyA715 rph-1* Km^r	[30]
SK3564	*rneΔ1018::bal thyA715 rph-1 recA56 srlD::*Tn*10*/pDHK30(*rng219* Sm^r/Sp^r)/ pWSK219(Km^r)	[28]
SK4390	*ΔrppH::kan thyA715 rph-1*	This study
SK4394	*ΔrppH::kan rne-1 thyA715 rph-1*	This study
SK4395	*ΔrppH::kan rnpA49 thyA715 rph-1 rbsD296::*Tn*10* Km^r/Tc^r	This study
SK4397	*ΔrppH::kan rne-1 rnpA49 thyA715 rph-1 rbsD296::*Tn*10* Km^r/Tc^r	This study
SK5665	*rne-1 thyA715 rph-1*	[25]
SK10153	*thyA715*	[7]

Fig.1. Growth curves of strains carrying the *rppHΔ754*, *rne-1*, and *rnpA49* alleles.

Growth curves were conducted as described in Materials and Methods.

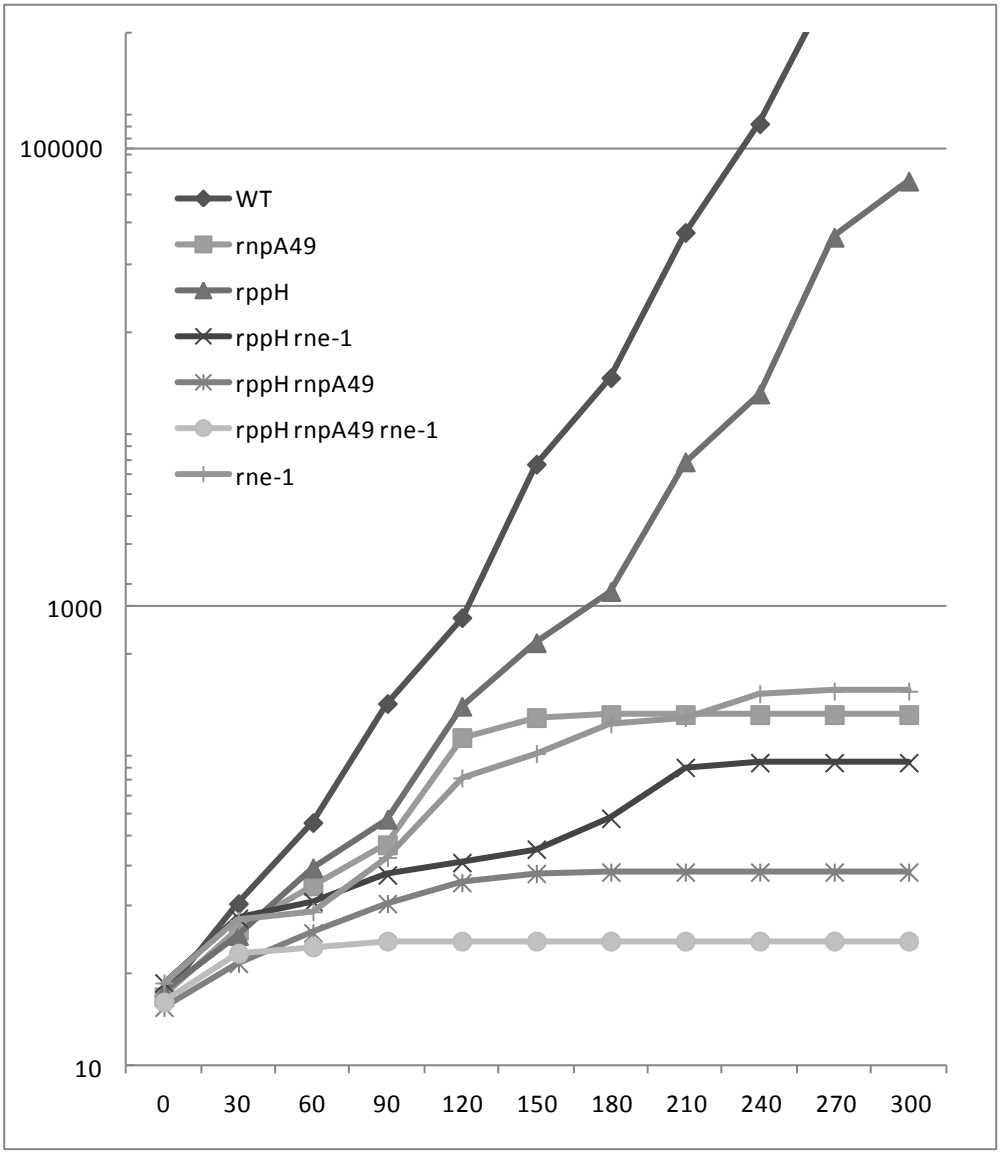
100000
1000
10
WT
rnpA49
rppH
rppH rne-1
rppH rnpA49
rppH rnpA49 rne-1
rne-1
0
30
60
90
120
150
180
210
240
270
300

Fig. 2. Processing of the *argX hisR leuT proM* polycistronic operon in the *rppHΔ754*, *rne-1*, and *rnpA49* mutant backgrounds.

Northern analysis was conducted as described in Materials and Methods. (A) Schematic of the *argX hisR leuT proM* transcript. Downward arrows labeled P indicate RNase P cleavage, while downward arrows labeled E indicate RNase E cleavage. Left-handed arrows indicate oligonucleotide probes. The diagram is not drawn to scale. (B) Northern analysis of *argX hisR leuT proM* transcript with the use of the *argX* oligonucleotide probe. Processing intermediates of the transcript are indicated on the right-hand side of the Northern blot. (C) Northern analysis of *argX hisR leuT proM* transcript with the use of the *hisR* oligonucleotide probe. Processing intermediates of the transcript are indicated on the right-hand side of the Northern blot.

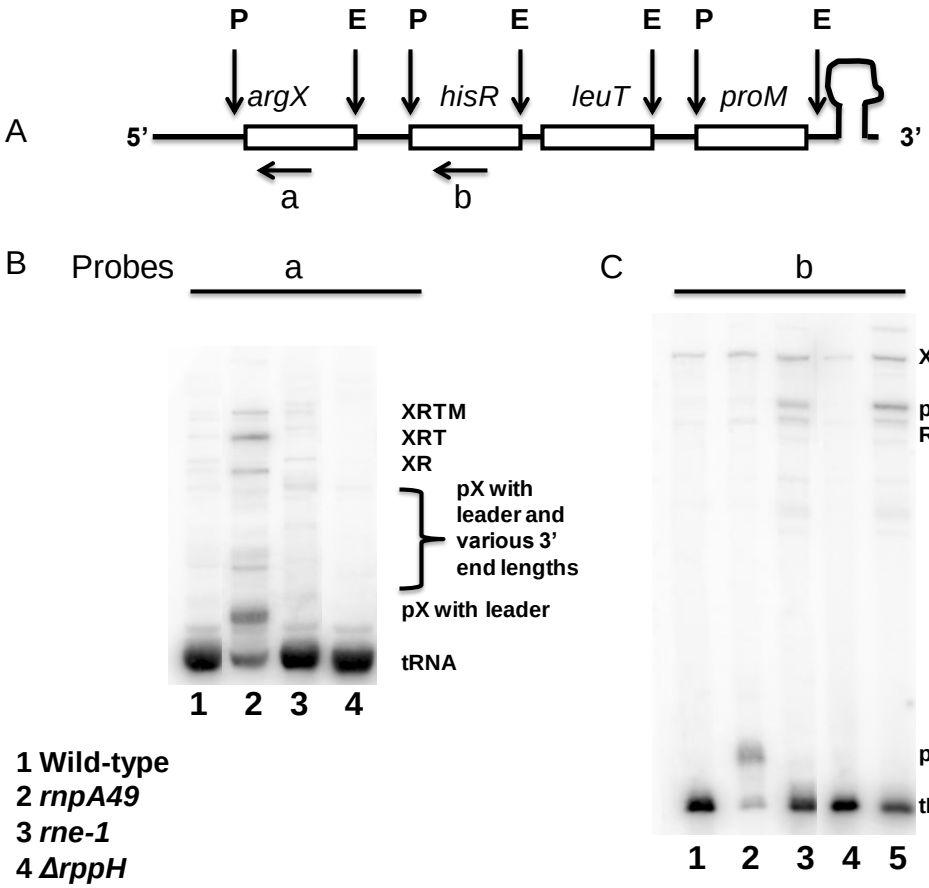
A
P
E
P
E
E
P
E
argX
hisR
leuT
proM
5'
3'
a
b
B
Probes
a
XRTM
XRT
XR
pX with leader and various 3' end lengths
pX with leader
tRNA
1 2 3 4
1 Wild-type
2 rnpA49
3 rne-1
4 ΔrppH
5 ΔrppH rne-1
C
b
XRTM
pRTM
RTM
pR
tRNA
1 2 3 4 5

Fig. 3. Processing of the *valV valW* polycistronic operon in the *rppHΔ754*, *rne-1*, and *rnpA49* mutant backgrounds.

Northern analysis was conducted as described in Materials and Methods. Schematic of the *valV valW* transcript indicates RNase P cleavage with downward arrows labeled with P. The diagram is not drawn to scale. Below the schematic, Northern analysis of the *valV valW* transcript with the use of the *valW* oligonucleotide probe that hybridizes to both mature sequences of valV and valW. Processing intermediates of the transcript are indicated on the left-hand side of the Northern blot.

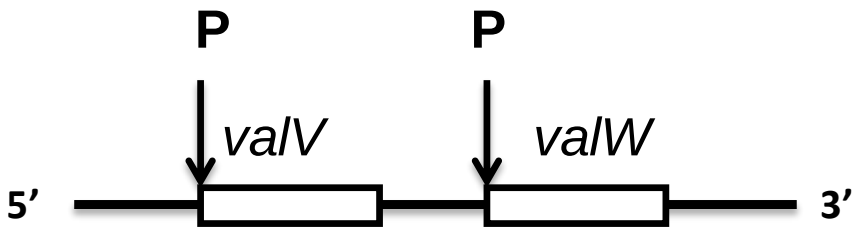
P
P
valV
valW
5’
3’

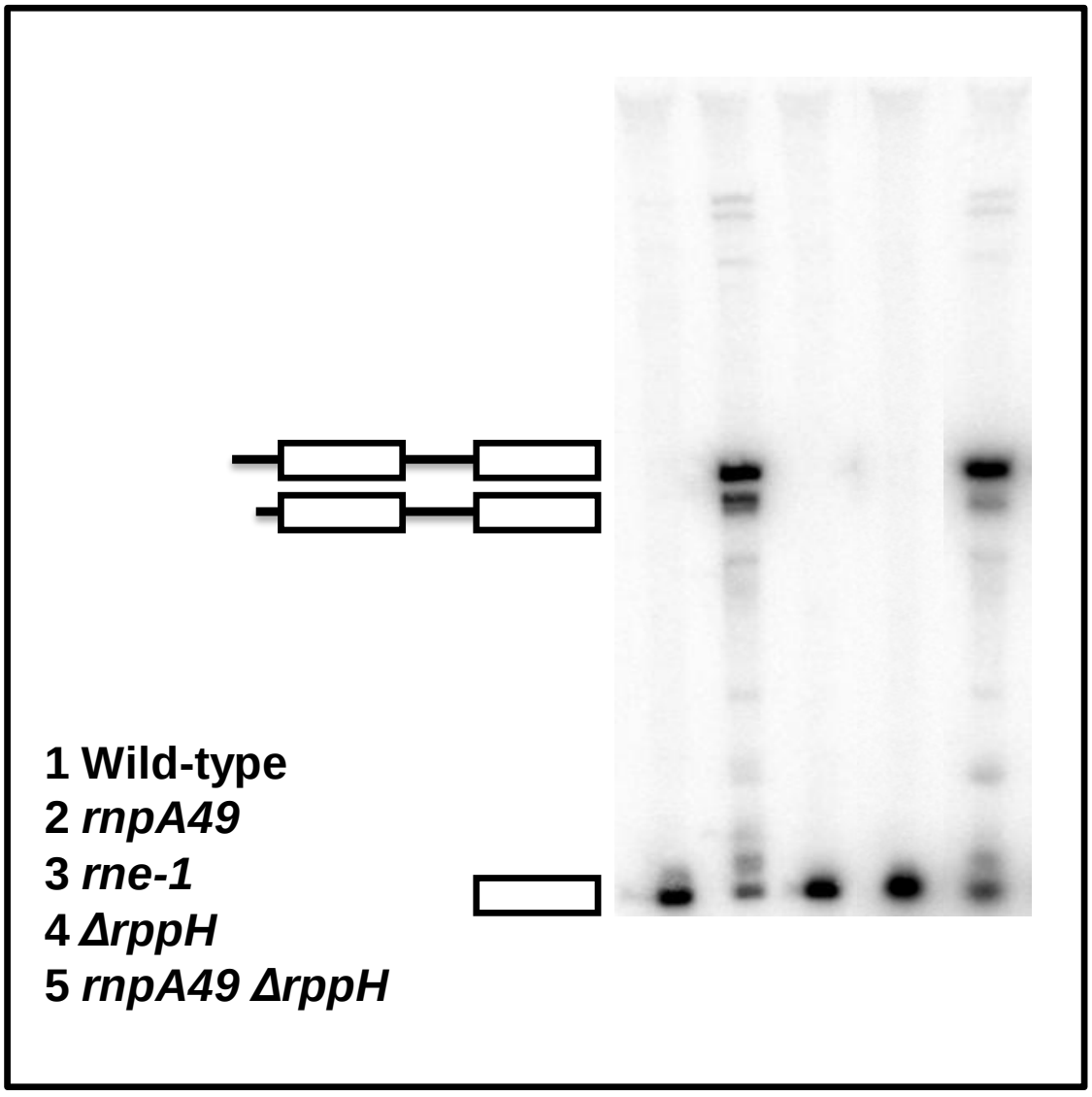
1 Wild-type
2 rnpA49
3 rne-1
4 ΔrppH
5 rnpA49 ΔrppH

Fig. 4. Processing of the *leuX* monocistronic operon in the *rppHΔ754*, *rne-1*, and *rnpA49* mutant backgrounds.

Northern analysis was conducted as described in Materials and Methods. (A) Schematic of the *leuX* transcript. Numbers (nt) indicate the size of the 5' leader of $tRNA^{Leu}$. Downward arrow labeled P indicates RNase P cleavage. Downward arrow labeled P* indicate Rho-independent terminator removal by RNase P and 3'→5' exoribonuclease activity, indicated by ¾ open circle. The diagram is not drawn to scale. (B) Northern analysis of the *leuX* transcript with the use of the *leuX* oligonucleotide probe that hybridizes to both mature sequences of *leuX*. Processing intermediates of the transcript are indicated on the left-hand side of the Northern blot.

A

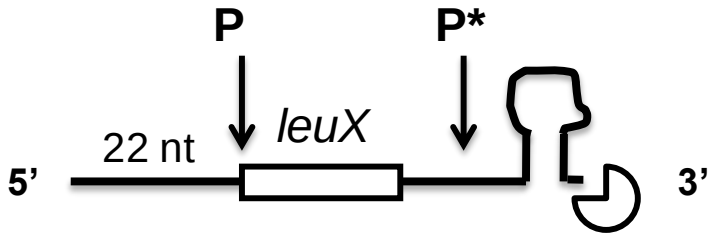
P
P*
22 nt
leuX
5'
3'

B

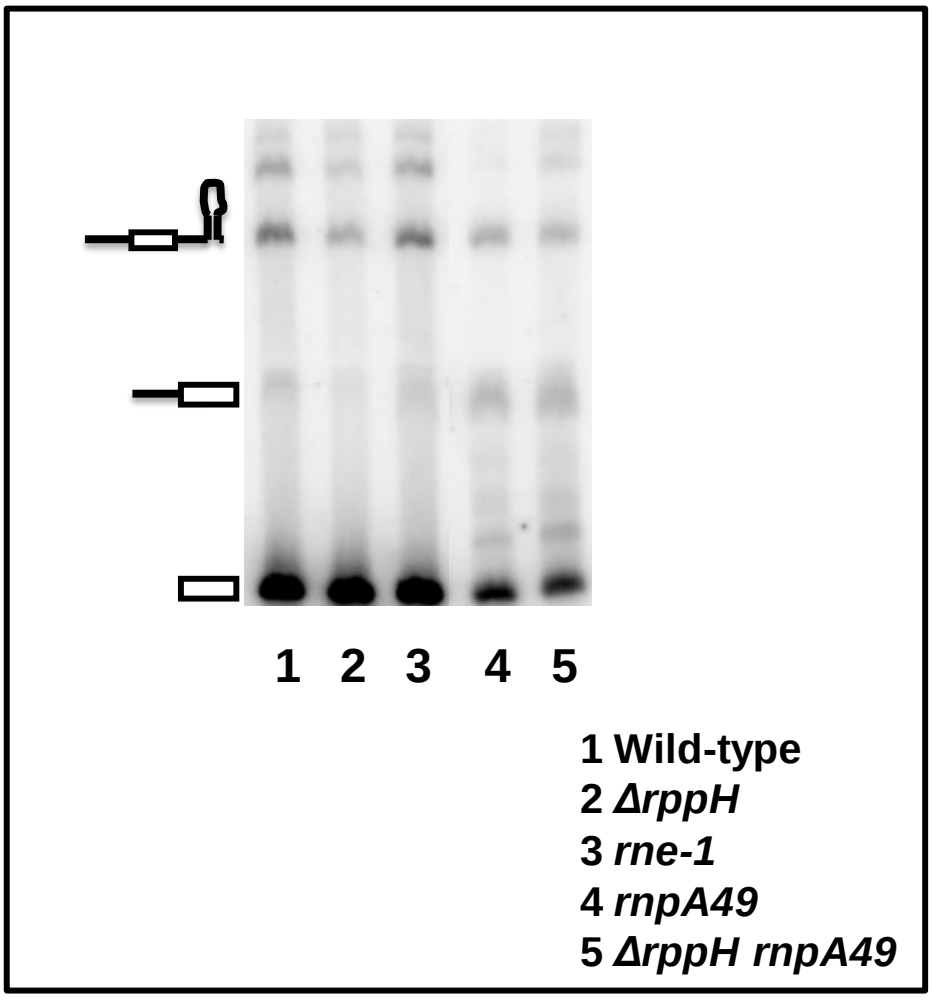
1 2 3 4 5
1 Wild-type
2 ΔrppH
3 rne-1
4 rnpA49
5 ΔrppH rnpA49

Fig. 5. Processing of the *asnT*, *asnU*, *asnV*, and *asnW* monocistronic operons in the *rppHΔ754*, *rne-1*, and *rnpA49* mutant backgrounds.

Northern analysis was conducted as described in Materials and Methods. (A) Schematic of the *asn* transcripts. Numbers (nt) indicate the size of the 5' leader of $tRNA^{Asn}$. Downward arrow labeled P indicates RNase P cleavage. Downward arrow labeled E indicate Rho-independent terminator removal by RNase E. The diagram is not drawn to scale. (B) Northern analysis of the *asn* transcripts with the use of the *asn* oligonucleotide probe that hybridizes to the mature sequences of all monocistronic *asn* precursors. Processing intermediates of the transcript are indicated on the left-hand side of the Northern blot.

A

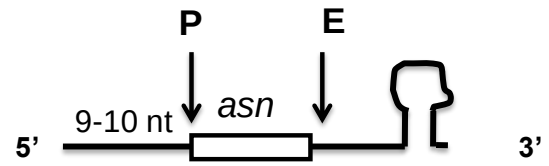
P
E
9-10 nt
asn
5'
3'

B

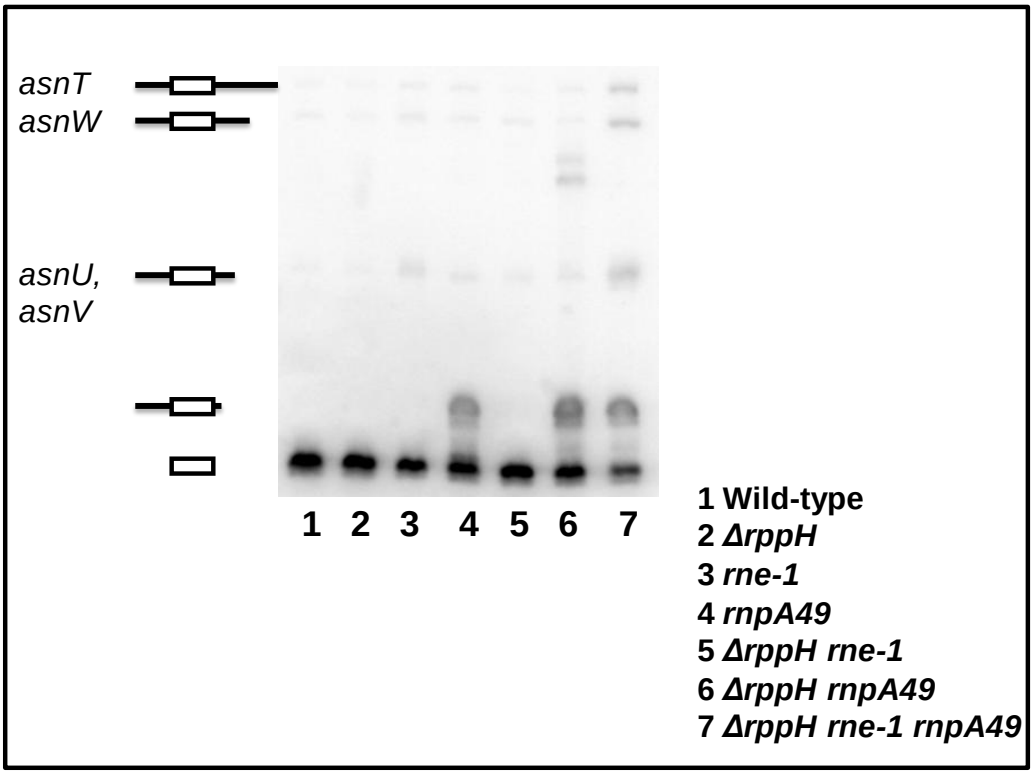
asnT
asnW
asnU,
asnV
1 2 3 4 5 6 7
1 Wild-type
2 ΔrppH
3 rne-1
4 rnpA49
5 ΔrppH rne-1
6 ΔrppH rnpA49
7 ΔrppH rne-1 rnpA49

Fig. 6. Processing of the *pheU* and *pheV* monocistronic operons in the *rppHΔ754*, *rne-1*, and *rnpA49* mutant backgrounds.

Northern analysis was conducted as described in Materials and Methods. (A) Schematic of the *phe* transcripts. Numbers (nt) indicate the size of the 5' leader of $tRNA^{Asn}$. Downward arrow labeled P indicates RNase P cleavage. Downward arrow labeled E indicate Rho-independent terminator removal by RNase E. The diagram is not drawn to scale. (B) Northern analysis of the *phe* transcripts with the use of the *phe* oligonucleotide probe, indicated by the black bar in (A), that hybridizes to the mature sequences of both *pheU* and *pheV* transcripts. Processing intermediates of the transcript are indicated on the left-hand side of the Northern blot.

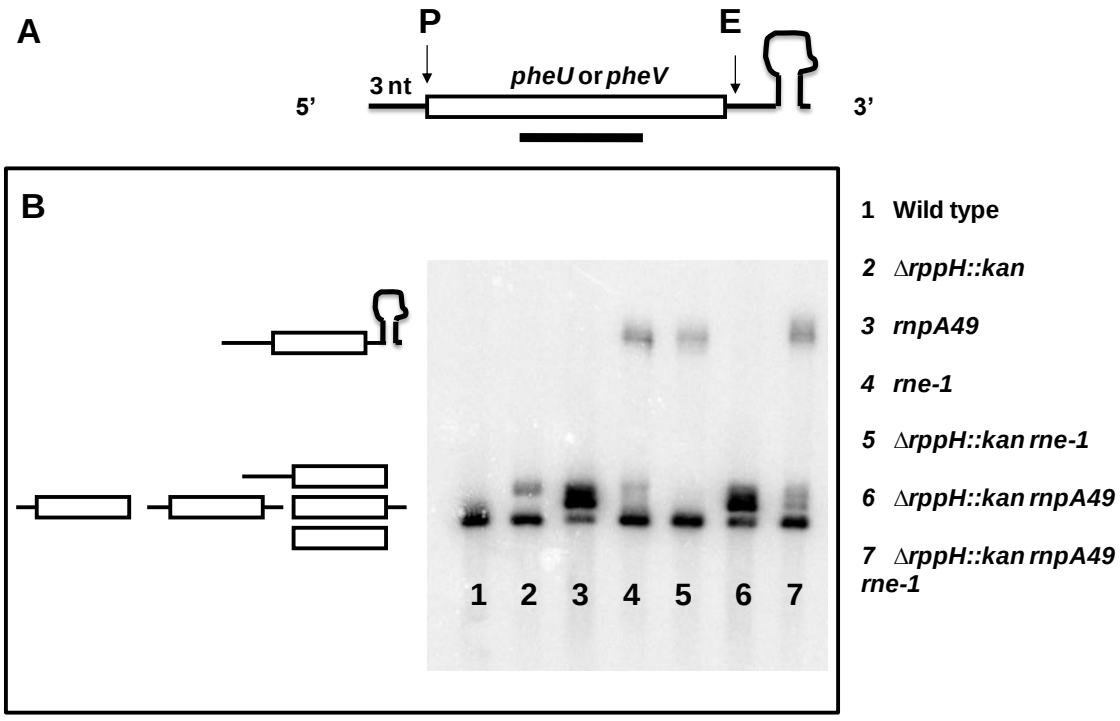
A
P
E
3 nt
pheU or pheV
5'
3'
B
1 2 3 4 5 6 7
1 Wild type
2 ΔrppH::kan
3 rnpA49
4 rne-1
5 ΔrppH::kan rne-1
6 ΔrppH::kan rnpA49
7 ΔrppH::kan rnpA49 rne-1

Fig. 7. Analysis of the 5’ termini of *pheU* and *pheV* in the *rppHΔ754* and *rnpA49* mutant backgrounds.

Primer extension analysis was conducted as described in Materials and Methods. The transcription start sites of *pheU* and *pheV* are indicated by a purple bracket. The mature 5’-termini of *pheU* and *pheV* are indicated by red arrows, the thicker indicating the major transcription start site and the thinner indicating the minor transcription start site. The expanded sequence is shown to the left and at bottom of the figure. The schematic below the figure indicates the mature sequence with a gray box.

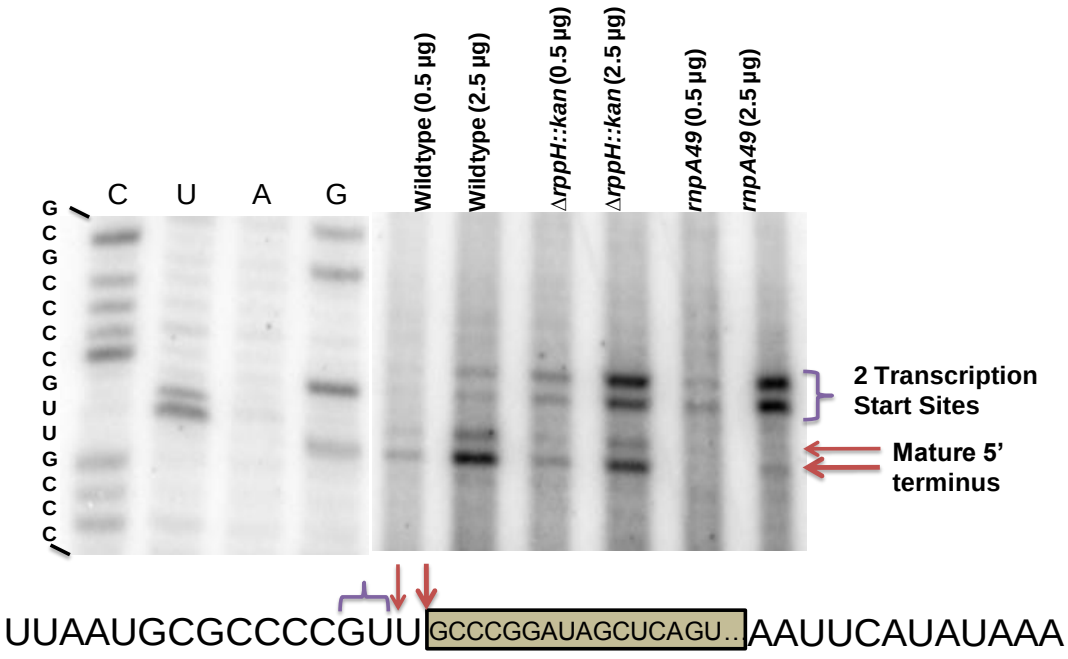
C
U
A
G
Wildtype (0.5 µg)
Wildtype (2.5 µg)
ΔrppH::kan (0.5 µg)
ΔrppH::kan (2.5 µg)
rnpA49 (0.5 µg)
rnpA49 (2.5 µg)
G
C
G
C
C
C
C
G
U
U
G
C
C
C
2 Transcription Start Sites
Mature 5' terminus
UUAAUGCGCCCCGUUGCCCGGAUAGCUCAGU..AAUUCAUAUAAA

Fig. 8. Analysis of 5’ and 3’ termini of *pheU* and *pheV* in the *rppHΔ754* and *rnpA49* mutant backgrounds.

RNA self-ligation and RT-PCR was conducted as described in Materials and Methods. (A) Ligation products of *pheU* and *pheV* in the MG1693 background in the absence of TAP. Thin downward arrows indicate 5’ termini, while thick downward arrows indicate 3’ termini. Numbers above the arrows indicate number of clones that ligated at that nucleotide. 5’-leader and mature sequence, indicated by gray bar, is identical for both *pheU* and *pheV*. The 3’ termini of *pheU* and *pheV* are highly variable, as indicated to the right of the mature sequence (gray bar). (B) Ligation products of *pheU* and *pheV* in the MG1693 background in the presence of TAP. Data is presented as described in Fig. 8A. (C) Ligation products of *pheU* and *pheV* in the *rnpA49* mutant background in the absence of TAP. Data is presented as described in Fig. 8A. (D) Ligation products of *pheU* and *pheV* in the *rppHΔ754* mutant background in the absence of TAP. Data is presented as described in Fig. 8A. (E) Ligation products of *pheU* and *pheV* in the *rppHΔ754* background in the presence of TAP. Data is presented as described in Fig. 8A.

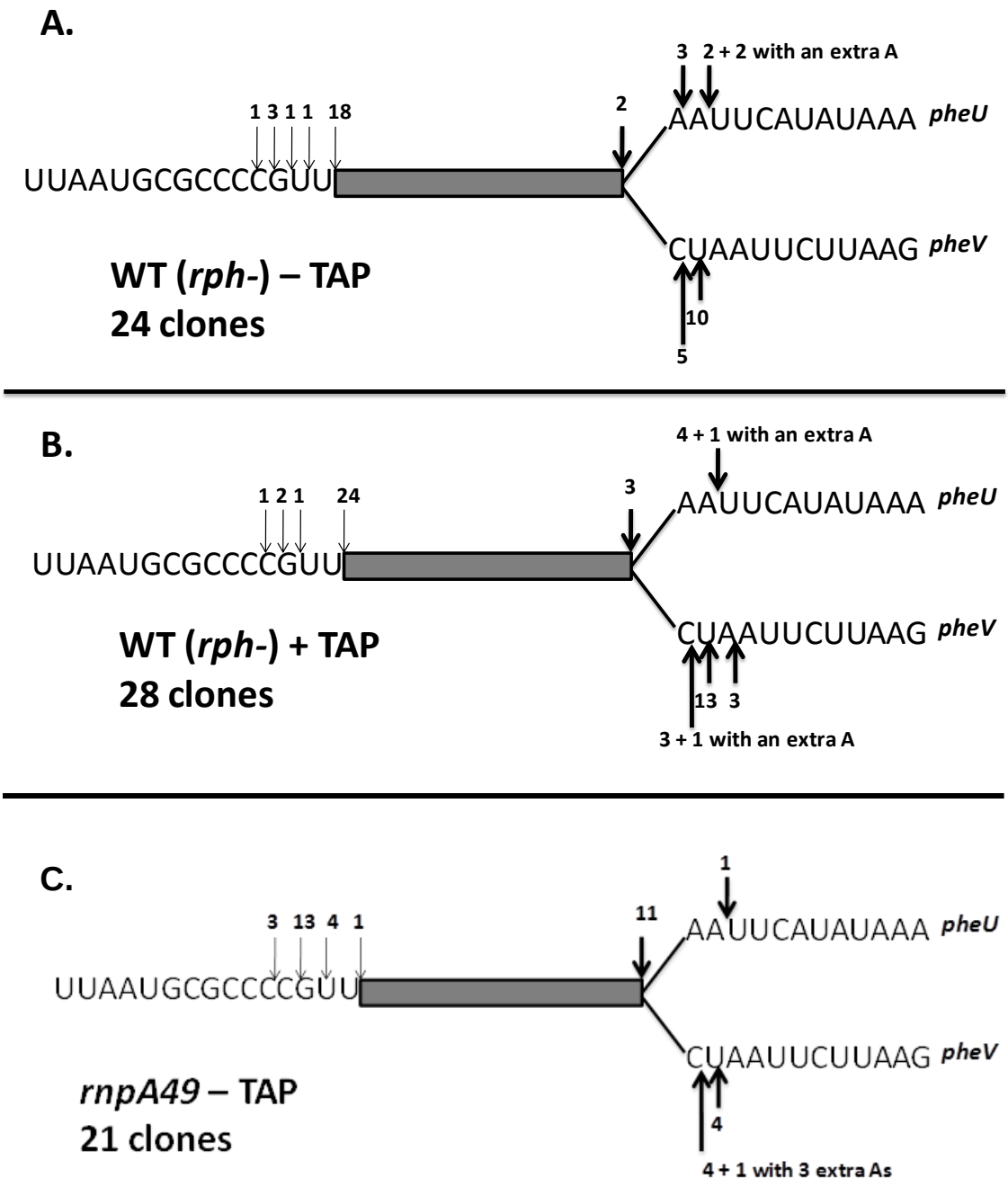
A.
3 2 + 2 with an extra A
1 3 1 1 18
2
AAUUCAUAUAAA pheU
UUAAUGCGCCCCGUU
CUAAUUCUUAAG pheV
WT (rph-) – TAP
24 clones
10
5
B.
4 + 1 with an extra A
1 2 1 24
3
AAUUCAUAUAAA pheU
UUAAUGCGCCCCGUU
CUAAUUCUUAAG pheV
WT (rph-) + TAP
28 clones
13 3
3 + 1 with an extra A
C.
1
3 13 4 1
11
AAUUCAUAUAAA pheU
UUAAUGCGCCCCGUU
CUAAUUCUUAAG pheV
rnpA49 – TAP
21 clones
4
4 + 1 with 3 extra As

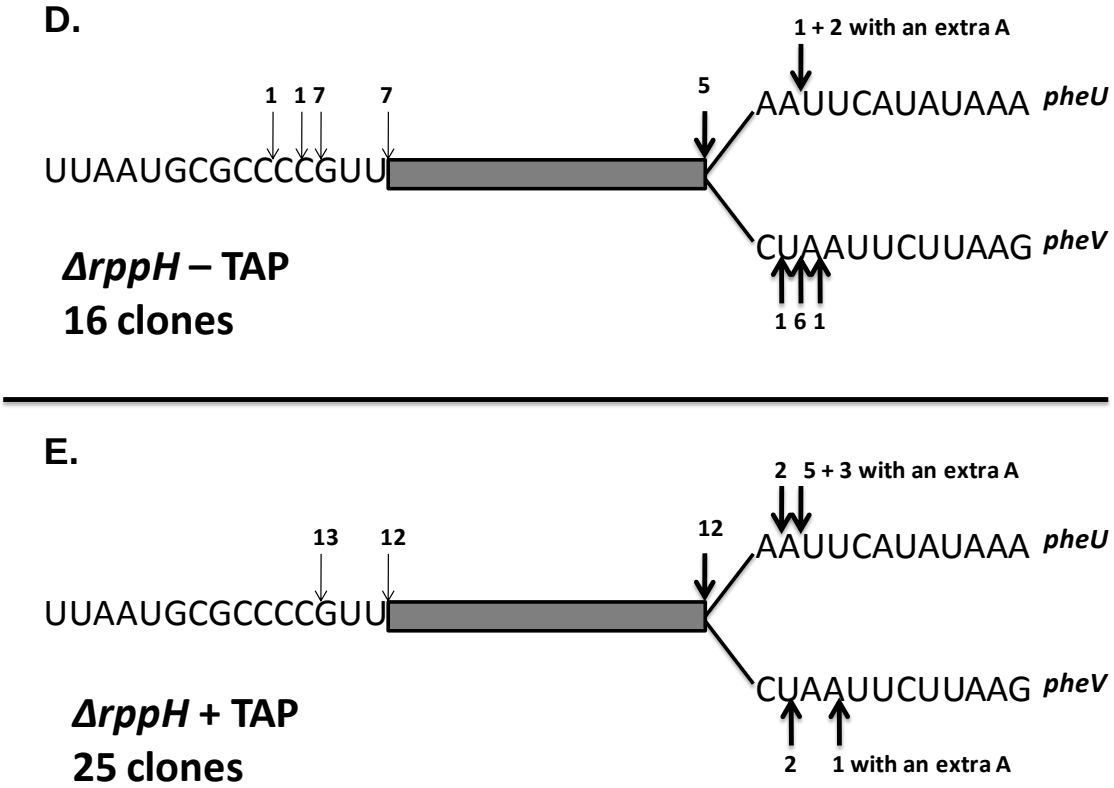
D.
1 + 2 with an extra A
1 1 7
7
5
AAUUCAUAUAAA pheU
UUAAUGCGCCCCGUU
CUAAUUCUUAAG pheV
ΔrppH – TAP
16 clones
1 6 1
E.
2 5 + 3 with an extra A
13
12
12
AAUUCAUAUAAA pheU
UUAAUGCGCCCCGUU
CUAAUUCUUAAG pheV
ΔrppH + TAP
25 clones
2
1 with an extra A

Fig. 9. Processing of the *ileX* monocistronic operons in the *rppHΔ754*, *rne-1*, and *rnpA49* mutant backgrounds.

Northern analysis was conducted as described in Materials and Methods. (A) Schematic of the *ileX* transcript. Numbers (nt) indicate the size of the 5' leader of $tRNA^{Asn}$. Downward arrow labeled P indicates RNase P cleavage. The diagram is not drawn to scale. (B) Northern analysis of the *ileX* transcripts with the use of the *ileX* oligonucleotide probe. Processing intermediates of the transcript are indicated on the left-hand side of the Northern blot.

A

B

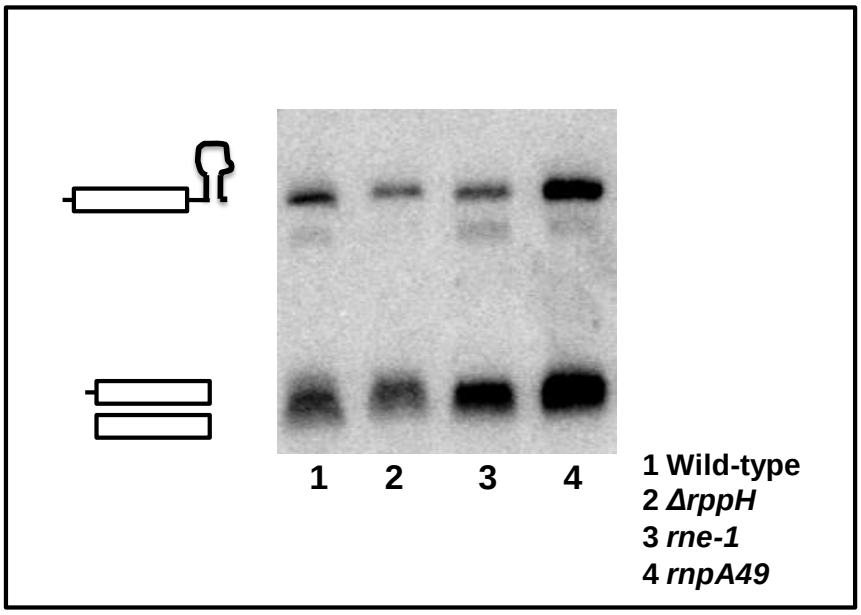

Fig. 10A. Analysis of 5’ and 3’ termini of *ileX* in the MG1693 background.

RNA self-ligation and RT-PCR was conducted as described in Materials and Methods. (A) Ligation products of *ileX* in the MG1693 background in the absence of TAP. Data is presented as described in Fig. 8A. (B) Ligation products of *ileX* in the MG1693 background in the presence of TAP. Data is presented as described in Fig. 8A.

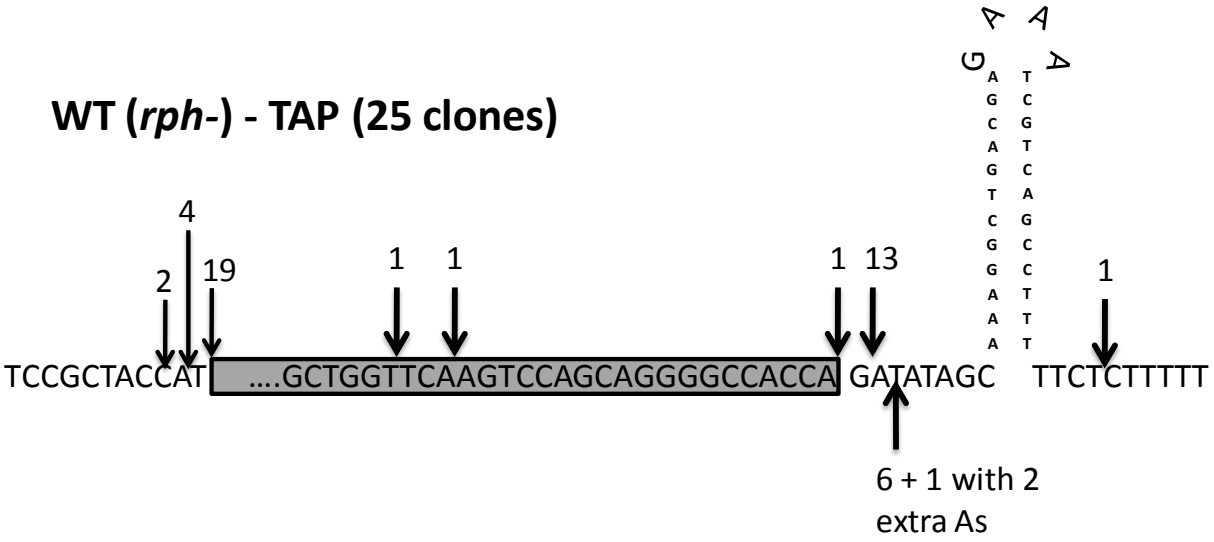
WT (rph-) - TAP (25 clones)
4
2
19
1
1
1
13
1
TCCGCTACCAT
....GCTGGTTCAAGTCCAGCAGGGGCCACCA
GATATAGC
TTCTCTTTTT
6 + 1 with 2 extra As

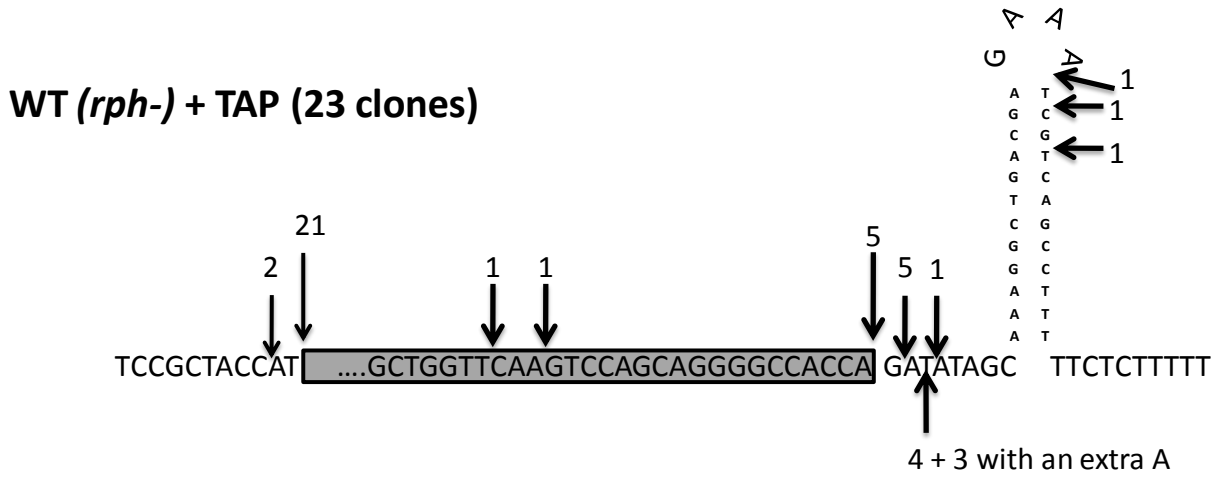
WT (rph-) + TAP (23 clones)
21
2
1
1
5
5
1
1
1
1
TCCGCTACCAT
....GCTGGTTCAAGTCCAGCAGGGGCCACCA
GATATAGC
TTCTCTTTTT
4 + 3 with an extra A

Fig. 10B. Analysis of 5’ and 3’ termini of *ileX* in the *rppHΔ754* mutant background.

RNA self-ligation and RT-PCR was conducted as described in Materials and Methods. (A) Ligation products of *ileX* in the *rppHΔ754* mutant background in the absence of TAP. Data is presented as described in Fig. 8A. (B) Ligation products of *ileX* in the *rppHΔ754* mutant background in the presence of TAP. Data is presented as described in Fig. 8A.

***ΔrppH* - TAP (24 clones)**

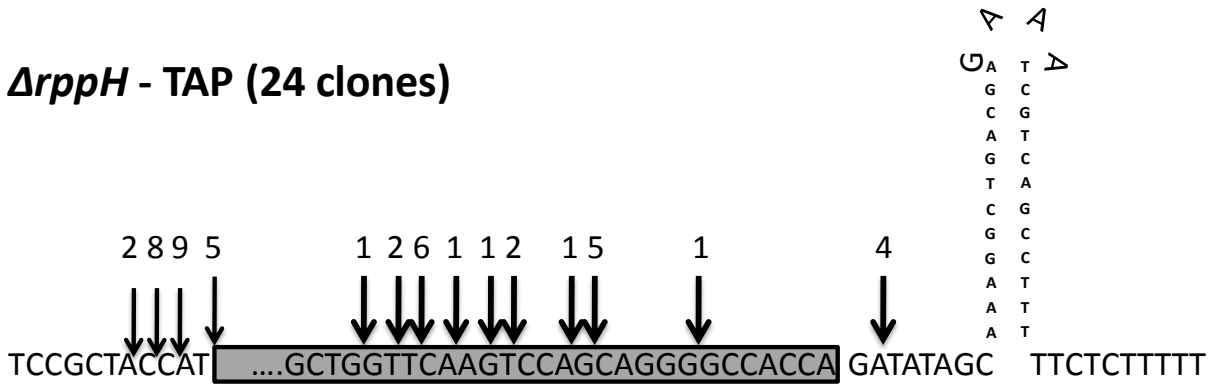

***ΔrppH* + TAP (21 clones)**

ileX

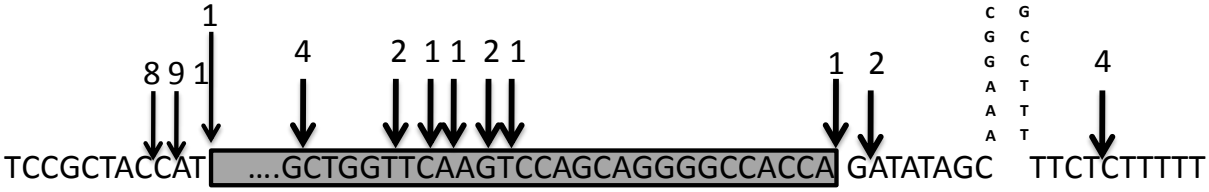

Fig. 10C Analysis of 5’ and 3’ termini of *ileX* in the *rnpA49* mutant background.

RNA self-ligation and RT-PCR was conducted as described in Materials and Methods. (A) Ligation products of *ileX* in the *rnpA49* mutant background in the absence of TAP. Data is presented as described in Fig. 8A. (B) Ligation products of *ileX* in the *rnpA49* mutant background in the presence of TAP. Data is presented as described in Fig. 8A.

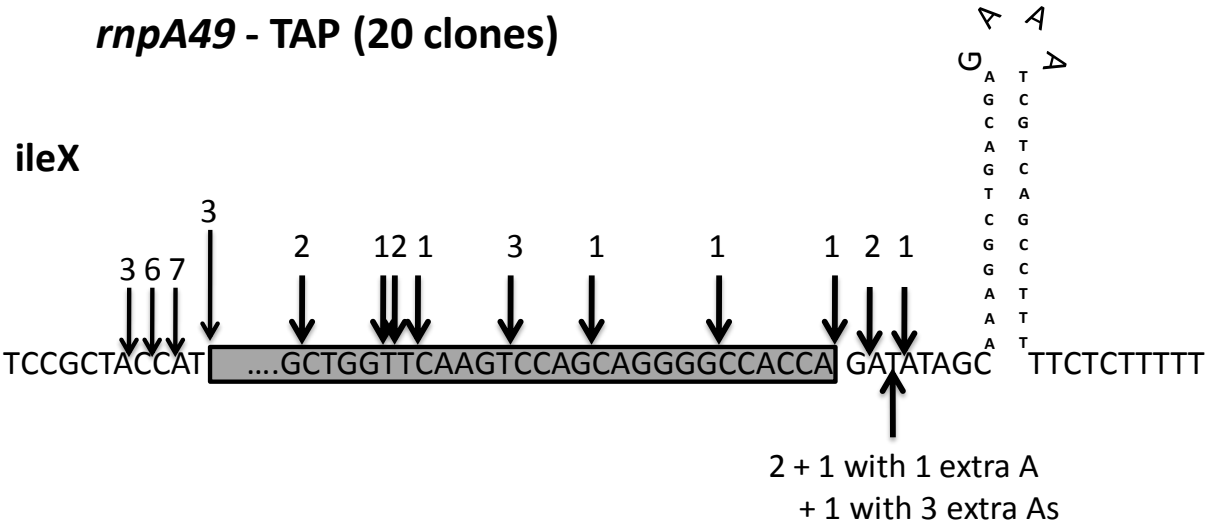
rnpA49 - TAP (20 clones)
ileX
3
3 6 7
2
12 1
3
1
1
1 2 1
TCCGCTACCAT
....GCTGGTTCAAGTCCAGCAGGGGCCACCA
GATATAGC
TTCTCTTTTT
2 + 1 with 1 extra A
+ 1 with 3 extra As

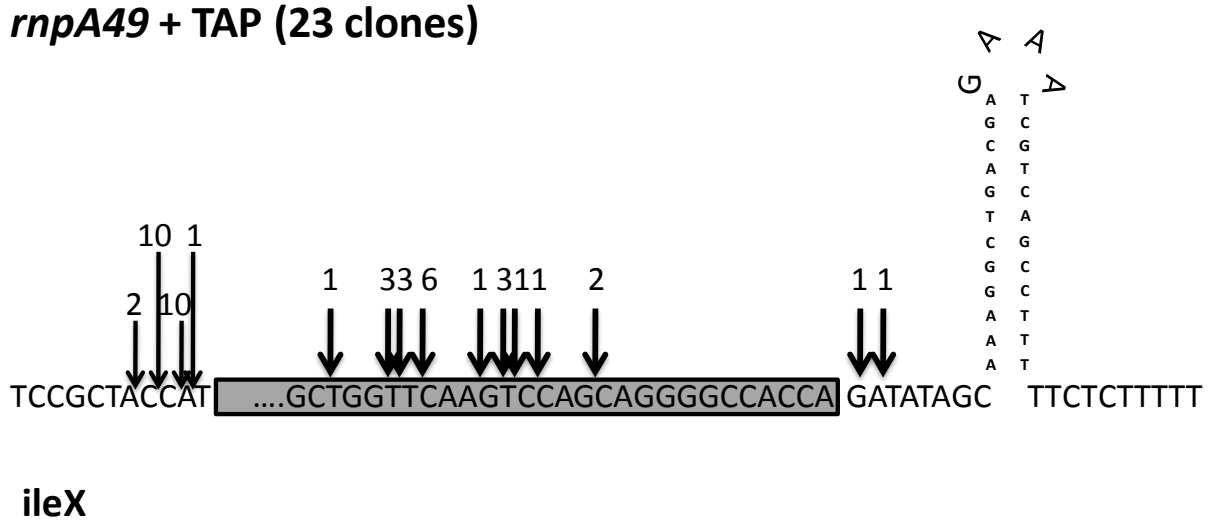
rnpA49 + TAP (23 clones)
10 1
2 10
1
33 6
1 311
2
1 1
TCCGCTACCAT
....GCTGGTTCAAGTCCAGCAGGGGCCACCA
GATATAGC
TTCTCTTTTT
ileX

Fig. 11. Processing of the *pheU* and *pheV* monocistronic operons in the presence and absence of RNase PH.

Northern analysis was conducted as described in Materials and Methods. (A) Schematic of the *phe* transcripts. Numbers (nt) indicate the size of the 5' leader of $tRNA^{Asn}$. Downward arrow labeled P indicates RNase P cleavage. Downward arrow labeled E indicate Rho-independent terminator removal by RNase E. The diagram is not drawn to scale. (B) Northern analysis of the *phe* transcripts with the use of the *phe* oligonucleotide probe that hybridizes to the mature sequences of both *pheU* and *pheV* transcripts. Processing intermediates of the transcript are indicated on the left-hand side of the Northern blot.

A

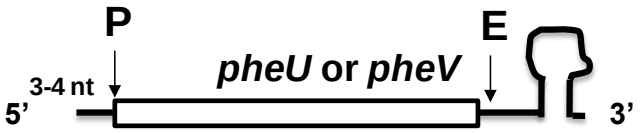
P
E
3-4 nt
pheU or pheV
5'
3'

B

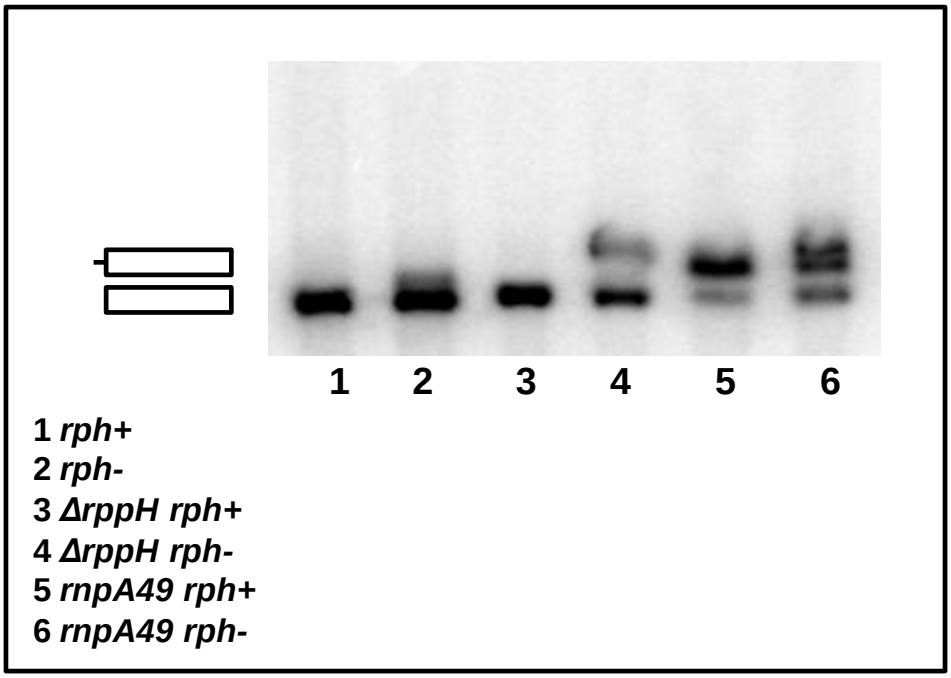
1 2 3 4 5 6
1 rph+
2 rph-
3 ΔrppH rph+
4 ΔrppH rph-
5 rnpA49 rph+
6 rnpA49 rph-

Fig. 12 Model of maturation of tRNA precursors.

This model is not drawn to scale. Scissors indicate endoribonuclease cleavages while ¾ yellow circles indicate 3'→5' endoribonucleases. The pathway on the left indicates maturation of polycistronic tRNA operons and monocistronic precursors with leaders longer than 5 nucleotides, which does not require RppH. The pathway on the right indicates maturation of monocistronic precursors with leaders shorter than 5 nucleotides. Without RppH present, RNase P is unable to remove the 5'-leader, as indicated by the STOP sign.

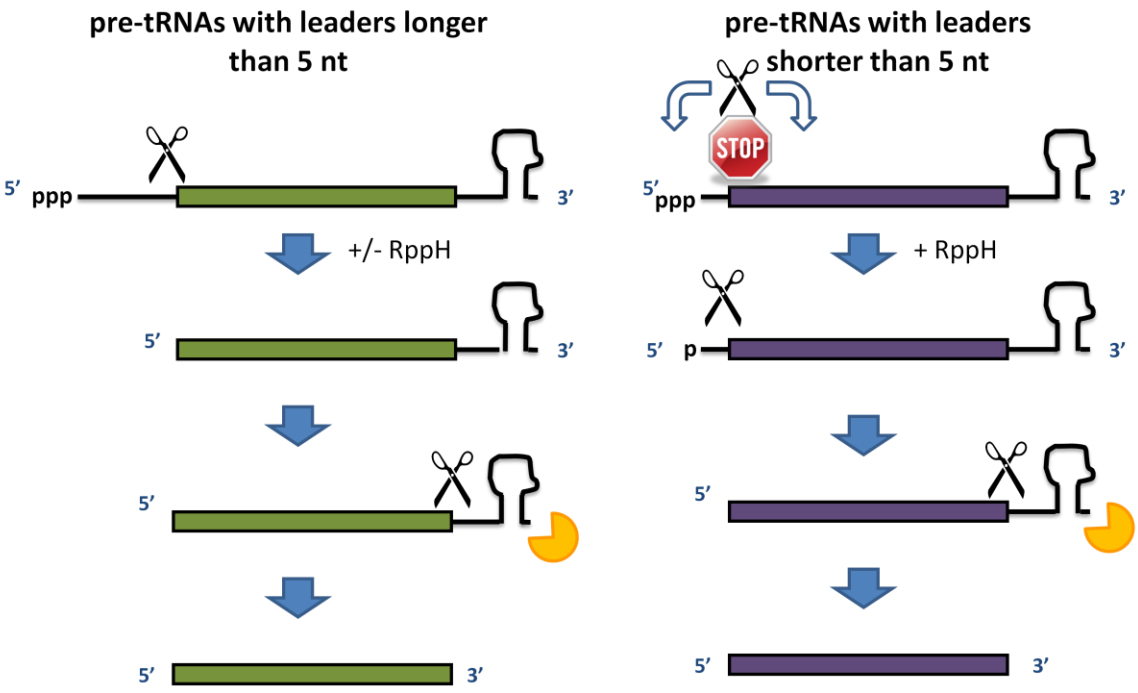
pre-tRNAs with leaders longer than 5 nt
5′ ppp
3′
+/- RppH
5′
3′
5′
5′
3′
pre-tRNAs with leaders shorter than 5 nt
STOP
5′ ppp
3′
+ RppH
5′ p
3′
5′
5′
3′

CHAPTER 3

ANALYSIS OF THE ROLE OF RPPH ON THE *ESCHERICHIA COLI* TRANSCRIPTOME[1]

---

[1]Bowden, Katherine E., and S.R. Kushner. To be submitted to Nucleic Acids Research.

ABSTRACT

RppH is known to be the “decapping” enzyme in *Escherichia coli* and its activity has been implicated in initiation of mRNA decay, tRNA maturation of certain tRNA precursors, hybrid jamming, and invasiveness of *E. coli* in brain tissue. To get a more clear understanding of its role in these complicated processes, microarray analysis has been previously conducted, but with limited scope. Here, through the use of tiling microarrays, we have implemented the use of a full RppH deletion and analyzed its effect on all genes across the entire genome of *E. coli* with a 20 nucleotide resolution. Through this analysis it is evident that RppH regulates the entire flagellar gene regulatory network. Further, the *rppHΔ745* exhibits hypermotility and rescues motility defects in a known nonmotile background. Interestingly, this effect on motility is abolished in the presence of the 3’→5’ exoribonulcease RNase PH, similar to previous data involving RNase P inhibition of 5’ processing of a subset of tRNA precursors.

INTRODUCTION

rppH, formerly *ygdP*, encodes RNA pyrophosphohydrolase in *Escherichia coli* and has been shown to initiate mRNA decay by removal of a 5'-pyrophosphate from 5' terminus of primary mRNA transcripts [1]. These findings have been bolstered by several studies showing the requirement of a 5'-monophosphated RNA substrate by RNase E, an essential endoribonuclease that is involved in mRNA decay and the 3'-terminal maturation of several tRNAs [1-4]. Along with helping to regulate the decay of various mRNAS, RppH has also been linked to the invasiveness of *E. coli* in human brain microvascular endothelial cells and the regulation of the *E. coli* general secretory (Sec) pathway [5-7]. Seeing that RppH has substrate specificities for molecules other than 5' triphosphate RNA caps, which include diadenosine *tetra*-, *penta*-, and *hexa*-phosphates, getting a clearer, more comprehensive picture of the role RppH plays in cellular RNA metabolism is of utmost importance [6].

With the identification that *rppH* encoded an RNA pyrophosphohydrolase activity, Deana *et al*. [1] carried out an analysis of all *E. coli* ORFs using JW2798 a strain deleted for *rppH* but containing the plasmid pPlacRppH-E53A, which had a mutant RppH protein under the control of the *lac* promoter. This mutant form of the RppH protein contains a substitution at an essential active-site residue and renders the protein nonfunctional, but it is unclear whether this altered protein is capable of RNA-binding, thereby protecting some transcripts from against endonucleolytic decay [1]. In their mutant they observed increased steady-state levels for a significant number of ORFs as well as decreased steady-state levels

for a more limited number of transcripts [1]. However, there analysis did not include non-translated RNAs [1].

Recently, our laboratory has developed a tiling microarray for *E. coli* that provides 20 nt resolution across the entire genome [8]. In addition, with current advances in RNA isolation, particularly the RNAsnap™ method, it is now possible to have a more accurate depiction of the intracellular RNA pool, unlike other isolation methods that enrich or deplete certain size classes of RNA [9]. Lastly, transcriptome analysis of a true chromosomal deletion of RppH has yet to be characterized.

Accordingly, we performed a tiling array analysis of MG1693 (*rph-1*) versus SK4390 (*rppHΔ754 rph-1*) grown into mid exponential phase growth. We show here that far fewer transcripts are affected by deletion of RppH than previously seen [1]. In comparing the tiling microarrays using two different RNA isolation methods, the RNAsnap™ RNA showed 98 transcripts were affected by the *rppHΔ754* chromosomal deletion. With Catrimide isolated RNA, 138 transcripts were affected by the *rppHΔ754* chromosomal deletion. This data contrast with earlier results using a RppH inactive protein in which 382 gene transcripts were reported to show increased steady-state levels [1].

More importantly, we provide evidence that RppH regulates flagellar operon transcription. We show that *flhDC*, the transcript encoding the master regulator of flagellar transcription in *E. coli*, is stabilized in the absence of RppH. Previous studies have shown that transcription of *flhDC* is regulated in a cell cycle-dependent manner, with an increase of its transcription observed

immediately following cell division [10]. So far only the RNA-binding protein CsrA has been shown to regulate the stability of the *flhDC* mRNA [11]. Once translated into protein, FlhDC activates transcription of class II genes in the flagellar gene regulatory network, which include genes that encode the flagellar protein apparatus, basal body, hook, and the alternative sigma factor σ^{28} [12-16]. σ^{28} will then activate transcription of class III genes in the flagellar gene regulatory network, specifically *fliC* which encodes flagellin, the protein that forms the filament of bacterial flagella, and the anti-sigma factor FlgM, which is exported out of the cell upon completion of the basal body-hook [17-19]. Our data indicate that hypermotility is a result of this stabilization of the *flhDC* transcript. This is the first evidence that RppH regulates motility and may provide more insight into the mechanism in which RppH regulates the secretory pathway and invasion of human cells [6, 7].

MATERIALS AND METHODS

Construction of the *E. coli* tiling microarray

The tiling microarray was constructed as previously described by Stead *et al.* [8].

Bacterial strains

The *E. coli* strains used in this study were all derived from MG1693 (*rph-1 thyA715*) (*E. coli* Genetic Stock Center, Yale University). This strain contains no RNase PH activity and shows reduced expression of *pyrE* due to the single nucleotide frameshift in the *rph* gene [20]. The true wild-type, SK10153

(*thyA715*), contains a functional RNase PH [21]. For this study, a P1 lysate grown on JW2798 (Keio Collection, Japan) was used to transduce MG1693 and SK10153 to construct SK4390 (*rppH∆754 rph-1*) and SK4426 (*rppH∆754*). A P1 lysate grown on JW0048 (Keio Collection, Japan) was used to transduce MG1693 to construct SK4417 (*∆apaH rph-1*). To construct SK4420 (*rppH∆754 ∆apaH*), the Kanamycin cassette in SK4390 was removed with the use of Flp recombinase, as previously described [22-24], with exceptions. The SK4390 cells were made electrocompetent and transformed with pCP20, the plasmid carrying the FLP recombinase. Once the Kanamycin cassette was confirmed to be absent, these cells were transduced with the P1 lysate grown on JW0048 to construct the *rppH∆754 ∆apaH rph-1* triple mutant strain.

Growth of bacterial strains and isolation of total RNA

Bacterial strains were grown with shaking in at 37°C in Luria broth supplemented with thymine (50 µg/mL) and kanamycin (25 µg/mL) (when *rppH∆754* was present) until a cell density of 50 Klett units above background (No. 42 green filter) was reached. RNA was extracted using one of two methods previously described by either O'Hara *et al.* [25], with the exception of 10% trimethyl(tetra-decyl)ammonium bromide (Sigma) was used in place of Catrimide [26] or the RNAsnap™ method as described by Stead *et al.* [9]. RNA was further treated with the DNA-free kit™ (Ambion) to remove contaminating DNA, and further quantified on a NanoDrop™ (Thermo Scientific) apparatus. 500 ng of each RNA sample were run on a 1% Agarose-Tris-acetate-EDTA gel and visualized with

ethidium bromide to ensure accurate quantities and satisfactory quality for further analysis.

Microarray analysis

Microarray analysis was conducted as previously described by Stead *et al.* [8].

Northern analysis

RNA isolation for Northern analysis was conducted as described by Stead *et al.* [9], while Northern analysis itself was performed as described by O'Hara *et al.* and Stead *et al.* [9, 25].

Determination of mRNA half-lives

Total RNA was extracted as previously described by Stead *et al.* [9]. Once cell density reached 50 Klett units above background (No. 42 green filter), transcription was inhibited with rifampcin (25mg/750µL DMSO) and DNA synthesis was inhibited with naladixic acid (2mg/mL). To allow for rifampcin and naladixic acid to enter the cells, time point 0 was taken 2 minutes after their addition to the culture medium. Subsequent time points were taken at 1, 2, 4, 8, and 16 minutes, respectively. Total RNA was purified using a standard sodium acetate precipitation and 500 ng of RNA was run on a 1% Agarose-Tris-acetate-EDTA gel and visualized with ethidium bromide to ensure accurate quantities and satisfactory quality for further analysis. Fifteen µg of RNA was then run on a 1x

BPTE gel using 6M Glyoxal reaction mix [27]. Northern analysis was performed as described by O'Hara *et al.* [25].

Motility assay

Motility was tested using motility plates as described by [28], with the following changes. Initially, 0.35% agar plates were supplemented with 1% Thymine and 25µg/mL kanamycin (when required). For time course motility assays, M9 agar plates were used, supplemented with 1% Thymine, 0.1% Glucose, 0.1% Thiamine, 1 mM $MgSO_4$, and 0.2 mM $CaCl_2$ to ensure that all strains grew with comparable generation times.

RESULTS

Analysis of the *E. coli* transcriptome in the absence of RppH

Through the use of tiling microarrays, we compared the transcriptome of MG1693 (*rph-1*) to an RppH deletion mutant (SK4390, *rppHΔ754 rph-1*), using two distinct RNA isolation methods. In one case we use the method described by O'Hara *et al.* [25], with the exception of 10% trimethyl(tetra-decyl)ammonium bromide (Sigma) was used in place of Catrimox-14 [26]. In the second case, the RNAsnap™ method as described by Stead *et al.* [9] was employed. In comparing the tiling microarrays from both RNA isolation methods, the Catrimide method showed 138 transcripts were affected by the *rppHΔ754* chromosomal deletion, with the up-regulation of 78 transcripts and the down-regulation of 60 transcripts (Table 1). The RNAsnap™ method RNA showed 98 transcripts affected by the

rppH∆754 chromosomal deletion, 82 showing up-regulation and 16 showed down-regulation (Table 1). In comparing both RNA isolation methods, 66 transcripts had equivalent ratios of change for both methods (Table 1).

Analysis of transcripts involved in the flagellar gene regulatory network

We then analyzed specific transcripts in order to determine if RppH had an effect on any major cell process. Through this analysis we discovered that 59% (39/66) of genes upregulated in the absence of RppH belonged to the flagellar gene regulatory network, when comparing both RNA isolation methods (Table 1). Interestingly all of these transcripts showed an increase in abundance in the absence of RppH (Table 1, Fig. 1). It should be noted that all ratios were calculated from the averages of both RNA isolation method arrays (Table 1), unless otherwise noted. The transcript of *flhDC,* the flagellar gene regulatory pathway master regulator in *E. coli*, showed a 1.5 fold increase (s.d. 1.1) in the *rppH∆754* mutant compared to wild-type, when averaging both arrays (Table 1, Fig. 1A). The transcripts of the class II genes in the regulatory pathway were stabilized similarly.

Class II genes are known to form the basal body, the flagellar protein export apparatus, the hook and hook associated proteins, along with σ^{28} and the anti-σ^{28} factor (for review see [29-31]). The transcript *flgBCDEFGHIJKL* encodes the proteins that make up the flagellar rod (FlgB, FlgC, FlgF, FlgG), the hook-capping protein (FlgD), the hook protein (FlgE), 2 class III hook-associated proteins (FlgK, FlgL), the rod cap (FlgJ), the P-ring (FlgI), and the L-ring (FlgH)

[29-31]. This entire transcript showed a 1.52 fold increase (s.d. 0.02) in the *rppHΔ754* mutant when compared to the wild type control (Table 1, Fig. 1B). The transcript *flhBAE* encodes 3 of the 6 integral membrane components of the flagellar export apparatus [29-31].

This transcript exhibited a 1.5 fold increase (s.d. 0.9) in the *ΔrppH* mutant when compared to wild-type (Figure 3, 4A). The transcript *fliAZY* encodes σ^{28} and two novel genes thought to regulate σ^{28} activity [29-32]. *fliA* and *fliZ* showed a 1.745 fold increase (s.d. 0.05) in the *rppHΔ754* mutant when compared to wild-type, while the increase of *fliY* was not significant enough to be calculated using the parameters set for our analysis (Table 1, Fig. 1C). The transcript *fliE* encodes the last of the five proteins, FliE, that make up the flagellar rod, and exhibited a 1.6 fold increase in abundance (s.d. 0.01) in the *rppHΔ754* mutant when compared to wild-type (Table 1, Fig. 1C).

The transcript *fliFGHIJK* encodes FliF, the MS ring of the flagellar basal body, FliG, one of the three components of the flagellar motor's "switch complex", and soluble components of the flagellar export system (FliH, FliI, FliJ, and FliK) [33-37]. This transcript showed a 1.40 fold increase in abundance (s.d. 0.03) in the *rppHΔ754* mutant when compared to wild-type (Table 1, Fig. 1C). The transcript *fliLMNOPQR* encodes motor/switch proteins and proteins associated with the flagellar export apparatus and shows a 1.42 fold increase (s.d. 0) in the *ΔrppH* mutant when compared to wild-type (Table 1, Fig. 1C) [31]. The transcript *flgAMN* encodes the FlgA, the chaperone of FlgI, while FlgM and FlgN are class III proteins, where FlgM binds to σ^{28} to help in its regulation while FlgN acts as a

chaperone of hook-binding proteins [38-41]. *flgA* showed a 1.55 fold increase (s.d. 0.04) in the *rppH∆754* mutant when compared to wild-type (Table 1, Fig. 1B), while *flgM* and *flgN* only showd a 1.51 fold increase in abundance (s.d. 0) in the *rppH∆754* mutant when compared to wild-type in the RNAsnap™ array (Table 1, Fig. 1B).

Class III genes in the flagellar gene regulatory pathway were also analyzed. These genes encode proteins that make up the filament, the cap, flagellins and hook associated proteins [29-31]. *fliC* encodes flagellin, the protein subunit that forms the flagellar filament, and shows a 1.52 fold increase in abundance (s.d. 0.01) in the *ΔrppH* mutant when compared to wild-type (Table 1, Fig. 1C) [29-31]. The transcript *motABcheAW* encodes the proteins that form the flagellar stator (MotA and MotB), the non-rotating part of the motor, and proteins involved in chemotaxis (CheA and CheW) [31]. This transcript showed a 1.5 increase in abundance (s.d. 0.12) in the *rppH∆754* mutant when compared to wild-type (Table 1, Fig. 1A). Lastly, the transcript that encodes Tar, Tap, CheR, CheB, CheY, and CheZ, all involved in chemotaxis, had varying abundance patterns [29-31]. The *tap* and *tar* RNA levels showed a 1.52 fold increase (s.d. 0.22) in the *rppH∆754* mutant when compared to wild-type (Table 1, Fig. 1A), while *cheRBYZ* was only within statistical parameters in the Catrimide array, exhibiting a 1.51 fold increase (s.d. 0.06) in the *rppH∆754* mutant when compared to wild-type (Table 1, Fig. 1A).

RppH affects the abundance of *flhDC*, the major regulator of the flagellar gene regulatory pathway

To validate the array results and confirm that the *flhDC* transcript was stabilized in the absence of RppH, Northern analysis was conducted to observe steady-state levels of *flhDC*. It should be noted that due to the fact that *flhDC* is the master regulator of the flagellar gene regulatory pathway, changes in the stability of its mRNA could in turn upregulate all downstream genes in the pathway if the change in mRNA stability result in increased levels of the master regulator protein. Thus, our focus here was to understand the effect RppH specifically had on the *flhDC* transcript. Northern analysis results showed *flhDC* was 31.0 times more abundant in the *rppHΔ754* mutant background as compared to wild-type (Figure 2, lanes 1 and 2). It is important to note that in the wild-type background, this transcript was barely present (Figure 2, lane 1).

In order to determine if the presence of the 5'-triphosphate on the *flhDC* transcript, due to the absence of RppH, was directly involved in the abundance of *flhDC* and that this transcript's abundance was not an effect of regulation of its transcription or downstream protein stability, we are currently determining the half-life of the *flhDC* transcript in the MG1693 and SK4390 genetic backgrounds.

The *ΔrppH* mutation restores motility to the nonmotile *ΔapaH* mutant strain

With microarray and Northern data supporting the idea that inactivation of RppH stabilizes the master regulator and downstream classes of genes in the flagellar gene regulatory network, we determined if the changes in mRNA levels resulted in altered cellular motility. To test this, the *rppHΔ754* chromosomal deletion was transduced into an *ΔapaH* mutant background. ApaH is a known

tetraphosphate pyrophosphohydrolase that has substrate specificity for similar diadenosine polyphosphates as RppH in the cell, but cleaves them symmetrically unlike asymmetrical cleavages by RppH [42-44]. The *ΔapaH* mutant background causes an accumulation of AppppA and leads to decreased transcription of genes in the flagellar regulatory network, thereby rendering the cells nonmotile [28]. We were interested in determining if the *rppHΔ754* mutation restored motility to the nonmotile *ΔapaH* mutant. Through the use of motility assays that measure the circumference of a migration halo on 0.35% agar plates, we observed that the *rppHΔ754 rph-1* strain had the highest motility, with an average halo circumference of 2.44 cm (s.d. 0.09) (Figure 3). The *ΔapaH* mutant background was much less motile than the wild-type strain, migrating an average of 0.3 cm (s.d. 0.07) and 0.74 cm (s.d. 0.19) over 24 hours, respectively (Figure 3). As hypothesized, the *rppHΔ754* mutation restored motility to the *ΔapaH* mutant to levels far above wild-type, with migration averaging 1.72 cm (s.d. 0.19) over 24 hours (Figure 3).

The effect RppH has on motility is dependent on RNase PH

When we observed that the effect of RppH on RNase P activity was dependent on the presence or absence of RNase PH (see Chapter 2), we were interested in determining if the mutation of this 3'→5' exoribonuclease had an impact on motility in the *rppHΔ754 rph*$^{+}$ genetic background. Surprisingly, in comparing the *rph*$^{+}$ strain to the *rph*$^{-}$ strain, no significant changes in motility were evident over a 48 hour period (Figure 4). However, when motility was compared

for these backgrounds that contained the *ΔrppH* mutation, the results were drastically different. The *rppHΔ754 rph-1* double mutant was the most motile, showing increased motility after each time period tested (Figure 4). Surprisingly, *rppHΔ754 rph*$^{+}$ genetic background showed motility comparable to both the *rph*$^{+}$ and *rph*$^{-}$ strains (Figure 4). An array comparing the transcriptomes of wild type and *rppHΔ754* strains showed no changes in the steady-state levels of any of the genes involved in motility (data not shown).

DISCUSSION

Our study set out to get a more precise picture as to the effects of RppH on the *E. coli* transcriptome through the analysis of a chromosomal deletion of RppH by high density tiling microarrays. Our data indicate that, when compared to the previous array data which analyzed a non-functional RppH derivative, only 21% of the reported transcripts were seen to increase in abundance with a chromosomal deletion of RppH (80/382) (Table 1). These results suggest that completely eliminating the protein from the cell of RppH has very different effects on the transcriptome than having a non-functional form present in high abundance. Even though decapping activity is abolished in the RppH derivative used in the previous array [1], this form of RppH may still be functional on other substrates it has specificity for, such as the polyphosphates which do not structurally resemble 5'-mRNA caps [6, 44]. This in itself can change the profile of the transcriptome, either directly or indirectly. Further, this derivative could also still exhibit RNA binding, resulting in non-functional RppH proteins bound to RNA

substrates, which could stabilize a substrate by protecting against ribonucleolytic degradation. It is for these reasons our data reflect a more accurate depiction of how RppH affects the entire transcriptome.

It is also important to point out that even though the Catrimide and RNAsnap™ methods of RNA isolation differ in the enrichment of certain classes of RNAs, 98% (78/82) of the transcripts that showed increased abundance in the *rppHΔ754* mutant when compared to wild-type using the RNAsnap™ showed the same trend in the Catrimide method (Table 1). However, more transcripts showed a decrease in abundance in the *ΔrppH* mutant when compared to wild-type using the Catrimide isolation method (60 versus 16). This is most likely due to the ability of Catrimide to enrich for larger RNA species, seeing that many of these RNA species were within larger transcripts [9].

Our data are the first to implicate RppH in the regulation of the flagellar gene regulatory network. We have shown that in the absence of RppH, all transcripts in this pathway increase in abundance by an average of 1.5 fold (Table 1, Fig. 1). Previous data have only implicated various environmental factors on transcription regulation of *flhDC*, such as pH levels, cAMP-CAP (carbon sources), quorum sensing, cell cycle, and the surface of adhesion [29]. To date, only CsrA has been identified in regulating the message stability of *flhDC* [45]. As for protein stability, the protease ClpXP is known to negatively regulate FlhDC [46, 47]. FliZ has been shown to positively regulate FlhDC, either by down regulating ClpXP expression, or by inducing transcription of the factor that directly stabilizes FlhDC [29, 48-50]. Lastly, FliT can also affect FlhDC

activity by sequestering the protein and preventing it from activating transcription of class II genes in the regulatory network [48, 51]. Though extremely complicated, understanding regulation of the *flhDC* transcript is paramount for fully understanding the entire bacterial flagellar regulatory network. This study has provided new insights into understanding this exact regulation.

Through Northern analysis, we have shown that *flhDC* is up-regulated to the extent of a 31-fold increase, which would indicate higher levels than determined through tiling microarray analysis (Figure 2). This in itself can provide insight into the limitations of the tiling microarrays and support the need for validation for Northern analysis. Seeing that the *rppH∆754* mutant showed hypermotility and provided complementation of the nonmotile *∆apaH*, it would make sense that a 1.5 fold increase, as seen in the array data, would not be enough to cause this drastic change in motility (Table 1, Fig. 2, 3). Therefore our Northern data allow for a more exact validation of both the array data and the results seen in the motility assays.

As for motility, it is still unclear the mechanism that allows for hypermotility in the *rppH∆754* mutant background. Seeing that the *rppH∆754* mutant that was tested was not in a true wild-type background, we wanted to see if the addition of a functional RNase PH would influence the effect RppH had on motility. Surprisingly, we were able to show that in the presence of RNase PH, the *rppH∆754* mutation does not have the same effect on motility (Figure 4). It is possible that the activity of RNase PH, a 3→5 exoribonuclease, is influencing how the 5'-triphosphate is recognized by ribonucleases, thereby allowing the

flhDC transcript to be degraded and restoring motility to wild-type levels. It is still unclear if and how this is occurring. More experimentation is needed to determine if *flhDC* is actually a substrate of RNase PH or if this is an indirect effect involving another aspect of *flhDC* regulation.

It is also unclear how hypermotility is occurring in the *rppHΔ754 rph-1* mutant background. Hypermotility can result from a number of factors: more flagella, longer flagella, faster rotation, increased cell division that results in more cells being flagellated. To date, the regulation of increased motility is not well understood. Filament growth is known to be independent of cell cycle while filament length is controlled in a more localized fashion at the base of each flagellum [52]. Further, the number of filaments or flagellar basal bodies is dependent on cell cycle and can be increased by either increasing levels of FlhDC or σ^{28} [30, 53, 54]. A mutation in *flgM*, the anti-σ^{28}, showed a two- to three-fold increase in the number of flagellum in *S. enteric* serovar Typhimurium, while increasing the transcription of *flhDC* resulted in a transition from swimmers to swarmers and a two-fold increase in flagellum number in both *S. enteric* serovar Typhimurium and *E. coli* [30, 55, 56]. These studies would indicate a feedback loop for class I and class II genes, allowing σ^{28} to regulate *flhDC* transcription. This would further increase the already abundant *flhDC*, therefore resulting in hypermotility. To determine what is actually occurring in the *rppHΔ754 rph-1* mutant background, it is important to determine which of these scenarios is actually occurring. Through the use of fluorescent microscopy, one can determine the number and length of flagella or the number of cells that are

flagellated in the *rppHΔ754 rph-1* mutant background. Thus far, we hypothesize that it is a combination of all these scenarios.

Although this is an extremely complicated pathway, it is important to understand how it is being regulated. Seeing that the flagellar protein export apparatus is a type III secretion system, this study can provide answers to how *rppH* is involved in suppressing hybrid jamming in the general secretory (Sec) pathway, which may result in the presence of more export apparatus' to overcome the jamming [7, 36]. Further studies need to be conducted to determine how the polyphosphates that RppH has specificity for are involved in the hypermotility effect seen in our study, whether directly or indirectly. Levels of Ap_4A, Ap_5A, and Ap_6A need to be measured to see how much RppH actually influences these levels, especially in the presence and absence of ApaH. One could determine how these polyphosphates regulate motility by manipulating the intracellular populations and seeing their effects on motility. Only time will tell how this intricate pathway of motility regulation is working in the cell. Our study paves the way for narrowing the search and better understanding all the key players in the flagellar gene regulatory network.

REFERENCES

1. Deana, A., H. Celesnik, and J.G. Belasco, *The bacterial enzyme RppH triggers messenger RNA degradation by 5' pyrophosphate removal.* Nature Biotechnology, 2008. **451**(7176): p. 355-8.
2. Celesnik, H., A. Deana, and J.G. Belasco, *Initiation of RNA decay in Escherichia coli by 5' pyrophosphate removal.* Molecular Cell, 2007. **27**: p. 79-90.
3. Jiang, X. and J.G. Belasco, *Catalytic activation of multimeric RNase E and RNase G by 5'-monophosphorylated RNA.* Proceedings of the National Academy of Sciences of the United States of America, 2004. **101**: p. 9211-9216.
4. Mackie, G.A., *Ribonuclease E is a 5'-end-dependent endonuclease.* NAture, 1998. **395**: p. 720-723.
5. Badger, J.L., C.A. Wass, and K.S. Kim, *Identification of Escherichia coli K1 genes contributing to human brain microvascular endothelial cell invasion by differential fluorescence induction.* Mol Microbiol, 2000. **36**(1): p. 174-82.
6. Bessman, M.J., et al., *The gene ygdP, associated with the invasiveness of Escherichia coli K1, designates a Nudix hydrolase, Orf176, active on adenosine (5')-pentaphospho-(5')-adenosine (Ap5A).* J Biol Chem, 2001. **276**(41): p. 37834-8.

7. Hand, N.J. and T.J. Silhavy, *Null mutations in a Nudix gene, ygdP, implicate an alarmone response in a novel suppression of hybrid jamming.* J Bacteriol, 2003. **185**(22): p. 6530-9.

8. Stead, M.B., et al., *Analysis of Escherichia coli RNase E and RNase III activity in vivo using tiling microarrays.* Nucleic Acids Res, 2011. **39**(8): p. 3188-203.

9. Stead, M.B., et al., *RNAsnap: a rapid, quantitative and inexpensive, method for isolating total RNA from bacteria.* Nucleic Acids Res, 2012.

10. Pruss, B.M. and P. Matsumura, *Cell cycle regulation of flagellar genes.* J Bacteriol, 1997. **179**(17): p. 5602-4.

11. Wei, B.L., et al., *Positive regulation of motility and flhDC expression by the RNA-binding protein CsrA of Escherichia coli.* Mol Microbiol, 2001. **40**(1): p. 245-56.

12. Claret, L. and C. Hughes, *Interaction of the atypical prokaryotic transcription activator FlhD2C2 with early promoters of the flagellar gene hierarchy.* J Mol Biol, 2002. **321**(2): p. 185-99.

13. Frye, J., et al., *Identification of new flagellar genes of Salmonella enterica serovar Typhimurium.* J Bacteriol, 2006. **188**(6): p. 2233-43.

14. Gillen, K.L. and K.T. Hughes, *Transcription from two promoters and autoregulation contribute to the control of expression of the Salmonella typhimurium flagellar regulatory gene flgM.* J Bacteriol, 1993. **175**(21): p. 7006-15.

15. Liu, X. and P. Matsumura, *The FlhD/FlhC complex, a transcriptional activator of the Escherichia coli flagellar class II operons.* J Bacteriol, 1994. **176**(23): p. 7345-51.

16. Pruss, B.M., et al., *FlhD/FlhC-regulated promoters analyzed by gene array and lacZ gene fusions.* FEMS Microbiol Lett, 2001. **197**(1): p. 91-7.

17. Ohnishi, K., et al., *Gene fliA encodes an alternative sigma factor specific for flagellar operons in Salmonella typhimurium.* Mol Gen Genet, 1990. **221**(2): p. 139-47.

18. Kutsukake, K., Y. Ohya, and T. Iino, *Transcriptional analysis of the flagellar regulon of Salmonella typhimurium.* J Bacteriol, 1990. **172**(2): p. 741-7.

19. Hughes, K.T., et al., *Sensing structural intermediates in bacterial flagellar assembly by export of a negative regulator.* Science, 1993. **262**(5137): p. 1277-80.

20. Jensen, K.G., *The Escherichia coli K-12 "wild types" W3110 and MG1655 have an rph frameshift mutation that leads to pyrimidine starvation due to low pyrE expression levels.* J. Bacteriol., 1993. **175**: p. 3401-3407.

21. Mohanty, B.K., V.F. Maples, and S.R. Kushner, *Polyadenylation helps regulate functional tRNA levels in Escherichia coli.* Nucleic Acids Res, 2012.

22. Baba, T., et al., *Construction of Escherichia coli K-12 in-frame, single-gene knockout mutants: the Keio collection.* Mol Syst Biol, 2006. **2**: p. 2006 0008.

23. Cherepanov, P.P. and W. Wackernagel, *Gene disruption in Escherichia coli: TcR and KmR cassettes with the option of Flp-catalyzed excision of the antibiotic-resistance determinant.* Gene, 1995. **158**(1): p. 9-14.

24. Datsenko, K.A. and B.L. Wanner, *One-step inactivation of chromosomal genes in Escherichia coli K-12 using PCR products.* Proc Natl Acad Sci U S A, 2000. **97**(12): p. 6640-5.

25. O'Hara, E.B., et al., *Polyadenylylation helps regulate mRNA decay in Escherichia coli.* Proc. Natl. Acad. Sci. USA, 1995. **92**: p. 1807-1811.

26. Mohanty, B.K., et al., *Analysis of RNA decay, processing, and polyadenylation in Escherichia coli and other prokaryotes.* Methods Enzymol, 2008. **447**: p. 3-29.

27. Burnett, W.V., *Northern blotting of RNA denatured in glyoxal without buffer recirculation.* BioTechniques, 1997. **22**: p. 668-671.

28. Farr, S.B., et al., *An apaH mutation causes AppppA to accumulate and affects motility and catabolite repression in Escherichia coli.* Proc Natl Acad Sci U S A, 1989. **86**(13): p. 5010-4.

29. Smith, T.G. and T.R. Hoover, *Deciphering bacterial flagellar gene regulatory networks in the genomic era.* Adv Appl Microbiol, 2009. **67**: p. 257-95.

30. Chilcott, G.S. and K.T. Hughes, *Coupling of flagellar gene expression to flagellar assembly in Salmonella enterica serovar typhimurium and Escherichia coli.* Microbiol Mol Biol Rev, 2000. **64**(4): p. 694-708.

31. Apel, D. and M.G. Surette, *Bringing order to a complex molecular machine: the assembly of the bacterial flagella.* Biochim Biophys Acta, 2008. **1778**(9): p. 1851-8.

32. Mytelka, D.S. and M.J. Chamberlin, *Escherichia coli fliAZY operon.* J Bacteriol, 1996. **178**(1): p. 24-34.

33. Ueno, T., K. Oosawa, and S. Aizawa, *M ring, S ring and proximal rod of the flagellar basal body of Salmonella typhimurium are composed of subunits of a single protein, FliF.* J Mol Biol, 1992. **227**(3): p. 672-7.

34. Minamino, T., et al., *FliK, the protein responsible for flagellar hook length control in Salmonella, is exported during hook assembly.* Mol Microbiol, 1999. **34**(2): p. 295-304.

35. Minamino, T. and R.M. MacNab, *FliH, a soluble component of the type III flagellar export apparatus of Salmonella, forms a complex with FliI and inhibits its ATPase activity.* Mol Microbiol, 2000. **37**(6): p. 1494-503.

36. Minamino, T. and R.M. Macnab, *Components of the Salmonella flagellar export apparatus and classification of export substrates.* J Bacteriol, 1999. **181**(5): p. 1388-94.

37. Kubori, T., et al., *Molecular characterization and assembly of the needle complex of the Salmonella typhimurium type III protein secretion system.* Proc Natl Acad Sci U S A, 2000. **97**(18): p. 10225-30.

38. Macnab, R.M., *How bacteria assemble flagella.* Annu Rev Microbiol, 2003. **57**: p. 77-100.

39. Nambu, T. and K. Kutsukake, *The Salmonella FlgA protein, a putativeve periplasmic chaperone essential for flagellar P ring formation.* Microbiology, 2000. **146 (Pt 5)**: p. 1171-8.

40. Fraser, G.M., J.C. Bennett, and C. Hughes, *Substrate-specific binding of hook-associated proteins by FlgN and FliT, putative chaperones for flagellum assembly.* Mol Microbiol, 1999. **32**(3): p. 569-80.

41. Daughdrill, G.W., et al., *The C-terminal half of the anti-sigma factor, FlgM, becomes structured when bound to its target, sigma 28.* Nat Struct Biol, 1997. **4**(4): p. 285-91.

42. Mechulam, Y., et al., *Molecular cloning of the Escherichia coli gene for diadenosine 5',5'''-P1,P4-tetraphosphate pyrophosphohydrolase.* J Bacteriol, 1985. **164**(1): p. 63-9.

43. Plateau, P., M. Fromant, and S. Blanquet, *Heat shock and hydrogen peroxide responses of Escherichia coli are not changed by dinucleoside tetraphosphate hydrolase overproduction.* J Bacteriol, 1987. **169**(8): p. 3817-20.

44. Guranowski, A., *Specific and nonspecific enzymes involved in the catabolism of mononucleoside and dinucleoside polyphosphates.* Pharmacol Ther, 2000. **87**(2-3): p. 117-39.

45. Wei, B.L., et al., *Positive regulation of motility and flhDC expression by the RNA-binding protein CsrA of Escherichia coli.* Molecular Microbiol., 2001. **40**: p. 245-256.

46. Claret, L. and C. Hughes, *Functions of the subunits in the FlhD(2)C(2) transcriptional master regulator of bacterial flagellum biogenesis and swarming.* J Mol Biol, 2000. **303**(4): p. 467-78.

47. Tomoyasu, T., et al., *Turnover of FlhD and FlhC, master regulator proteins for Salmonella flagellum biogenesis, by the ATP-dependent ClpXP protease.* Mol Microbiol, 2003. **48**(2): p. 443-52.

48. Kutsukake, K., T. Ikebe, and S. Yamamoto, *Two novel regulatory genes, fliT and fliZ, in the flagellar regulon of Salmonella.* Genes Genet Syst, 1999. **74**(6): p. 287-92.

49. Lanois, A., G. Jubelin, and A. Givaudan, *FliZ, a flagellar regulator, is at the crossroads between motility, haemolysin expression and virulence in the insect pathogenic bacterium Xenorhabdus.* Mol Microbiol, 2008. **68**(2): p. 516-33.

50. Saini, S., et al., *FliZ Is a posttranslational activator of FlhD4C2-dependent flagellar gene expression.* J Bacteriol, 2008. **190**(14): p. 4979-88.

51. Yamamoto, S. and K. Kutsukake, *FliT acts as an anti-FlhD2C2 factor in the transcriptional control of the flagellar regulon in Salmonella enterica serovar typhimurium.* J Bacteriol, 2006. **188**(18): p. 6703-8.

52. Aizawa, S.I. and T. Kubori, *Bacterial flagellation and cell division.* Genes Cells, 1998. **3**(10): p. 625-34.

53. Kutsukake, K., *Autogenous and global control of the flagellar master operon, flhD, in Salmonella typhimurium.* Mol Gen Genet, 1997. **254**(4): p. 440-8.

54. Yanagihara, S., et al., *Structure and transcriptional control of the flagellar master operon of Salmonella typhimurium.* Genes Genet Syst, 1999. **74**(3): p. 105-11.

55. Harshey, R.M. and T. Matsuyama, *Dimorphic transition in Escherichia coli and Salmonella typhimurium: surface-induced differentiation into hyperflagellate swarmer cells.* Proc Natl Acad Sci U S A, 1994. **91**(18): p. 8631-5.

56. Kutsukake, K. and T. Iino, *Role of the FliA-FlgM regulatory system on the transcriptional control of the flagellar regulon and flagellar formation in Salmonella typhimurium.* J Bacteriol, 1994. **176**(12): p. 3598-605.

57. Nicol, J.W., et al., *The Integrated Genome Browser: free software for distribution and exploration of genome-scale datasets.* Bioinformatics, 2009. **25**(20): p. 2730-1.

Table 1. Comparison of RNAsnap™ and Catrimide RNA isolation methods to previously reported microarray data.

Fold increases calculated as described in Stead et *al*. [8][1] and Deana et *al*. [1][2]. Values below 1.0 indicate a decrease in abundance in the *ΔrppH* mutant compared to wild-type, while values higher than 1.0 indicate an increase in abundance in the *ΔrppH* mutant compared to wild-type. Average indicates the average fold change between the RNAsnap™ and Catrimide array data. S.D. indicates standard deviation. No value indicates no fold change reported.

Gene	RNAsnap™[1] Fold change	Catrimide[1] Fold change	Average	S.D.	Deana et *al.*[2] Fold change	S.D.[2]
aceE		0.74			1.09	0.03
aceF		0.74				
aer		1.59				
alaE	1.47	1.57	1.52	0.07		
alsA		0.67				
alsB		0.67				
amyA		1.46				
aspA		0.67				
bsmA	0.64	0.60	0.62	0.03		
carA	0.65					
carB	0.65					
cdd		0.70				
cheA	1.41	1.58	1.495	0.12		
cheB	1.41	1.58	1.495	0.12		
cheR		1.59				
cheW	1.41	1.58	1.495	0.12		
cheY		1.46				
cheZ		1.46				
clpB	1.63				1.30	0.09
csiE		0.77				
cspD		0.67				

Gene	RNAsnap™[1] Fold change	Catrimide[1] Fold change	Average	S.D.	Deana et *al.*[2] Fold change	S.D.[2]
cspH		1.41				
deoA	0.72	0.68	0.7	0.03	1.52	0.27
deoB		0.68			2.78	0.20
deoC	0.72	0.68	0.7	0.03	2.22	0.45
deoD		0.68			1.51	0.04
dgoK		0.66				
dnaJ	1.56					
dnaK	1.56				1.80	0.04
dsdA	1.28					
dsdX	1.47					
emrE	1.41	1.55	1.48	0.10		
fabA		1.32				
fadA		0.62				
fadB		0.66				
feaR		0.77				
fimA	1.46	1.66	1.56	0.14	1.67	0.11
fimB	1.38					
fimC	1.46	1.66	1.56	0.14		
fimD	1.62	1.56	1.59	0.04		
fimI	1.46	1.66	1.56	0.14	1.55	0.27
flgA	1.58	1.52	1.55	0.04		
flgB	1.52	1.51	1.515	0.01		
flgC	1.52	1.51	1.515	0.01		
flgD	1.52	1.51	1.515	0.01		
flgE	1.52	1.51	1.515	0.01		
flgF	1.52	1.51	1.515	0.01		
flgG	1.52	1.51	1.515	0.01		
flgH	1.52	1.51	1.515	0.01		
flgI	1.52	1.51	1.515	0.01		
flgJ	1.52	1.51	1.515	0.01		
flgK	1.52	1.51	1.515	0.01		
flgL	1.52	1.51	1.515	0.01		
flgM	1.51					
flgN	1.51					
flhA	1.48	1.45	1.465	0.02		
flhB	1.48	1.45	1.465	0.02		
flhC	1.42	1.58	1.5	0.11		
flhD	1.42	1.58	1.5	0.11		

Gene	RNAsnap™[1] Fold change	Catrimide[1] Fold change	Average	S.D.	Deana et *al.*[2] Fold change	S.D.[2]
flhE	1.72	1.49	1.605	0.16		
fliA	1.71	1.78	1.745	0.05		
fliC	1.73	1.78	1.755	0.04		
fliD		1.46				
fliE	1.59	1.61	1.60	0.01		
fliF	1.48	1.36	1.42	0.08		
fliG	1.48	1.36	1.42	0.08		
fliH	1.48	1.36	1.42	0.08		
fliI	1.48	1.36	1.42	0.08		
fliJ	1.37	1.36	1.365	0.01		
fliK	1.37	1.36	1.365	0.01		
fliL	1.48	1.36	1.42	0.08		
fliM	1.48	1.36	1.42	0.08		
fliN	1.48	1.36	1.42	0.08		
fliO	1.48	1.36	1.42	0.08		
fliP	1.48	1.36	1.42	0.08		
fliQ	1.48	1.36	1.42	0.08		
fliR	1.48	1.36	1.42	0.08		
fliS		1.46				
fliT		1.46				
fliZ	1.71	1.78	1.745	0.05		
glcC		0.72				
gntK		0.73				
gntT		0.68				
groL	1.58					
groS	1.58					
gtrS		0.60				
hcaR		0.71				
hsdR	0.74	0.64	0.69	0.07		
hslU	1.43					
hslV	1.43					
htpG	1.61				2.00	0.06
ibpA	1.35					
ibpB	1.35					
insL	1.56					
ilvC		0.58				
intR		1.50				
lpd		0.74				

Gene	RNAsnap™[1] Fold change	Catrimide[1] Fold change	Average	S.D.	Deana et *al.*[2] Fold change	S.D.[2]
lrhA	0.74	0.69	0.715	0.04		
malS		0.71				
mdtK		1.58				
mdtL	0.68	0.67	0.675	0.01		
mhpC	1.56					
mhpD	1.43	1.83	1.63	0.28		
mhpE	1.49					
mhpF	1.39	1.47	1.43	0.06		
motA	1.42	1.58	1.50	0.11		
motB		1.58				
nemR		1.38				
nupG		0.60			2.93	0.34
ompF	1.40					
phoH		0.73				
prfC		1.57			3.00	0.19
raiA		0.64				
rbn		1.43				
rbsA		0.59				
rbsB		0.59				
rbsC		0.59				
rbsD		0.59				
rbsK		0.59				
rbsR		0.59				
rcsA		1.83				
rmuC		0.74				
rpiB		0.68				
rpiR		0.70				
rplU	1.47	1.42	1.445	0.04		
rpmA		1.42			2.37	0.16
rppH	0.63	0.56	0.595	0.05		
ryfD	1.63					
sanA		0.70				
tabA	1.68	1.49	1.585	0.13		
tap	1.37	1.78	1.575	0.29		
tar	1.37	1.57	1.47	0.14		
tdcA	0.59	0.54	0.565	0.04		
tdcB	0.70	0.69	0.695	0.01		
tdcC	0.70	0.69	0.695	0.01		

Gene	RNAsnap™[1] Fold change	Catrimide[1] Fold change	Average	S.D.	Deana et *al.*[2] Fold change	S.D.[2]
tdcD	0.60					
thyA		1.54				
tnaA	0.68				1.74	0.40
tnaB	0.68	0.67	0.675	0.01		
tnaC	0.68					
trg		1.44				
trxB	1.38				3.09	0.19
tsr	1.51	1.60	1.555	0.06		
tsx		0.80			1.35	0.07
ubiE		0.74				
udp		0.74				
ugpB		0.69				
yagU	1.38					
yciU	1.42				2.54	0.15
ydhO		0.75				
ydiY		1.51				
yecR	1.49	1.56	1.525	0.05		
yedN		1.61				
yeiP	1.56	1.67	1.615	0.08	5.93	0.45
yfiQ		0.72				
ygeV		0.63				
yhjC		0.79				
yhjD		0.73				
yhjH		1.59				
yhjX		0.63				
yifE	1.53					
yihM		0.72				
yjbQ		0.76				
yjcZ	1.28	1.60	1.44	0.23		
yjdA	1.28	1.60	1.44	0.23		
yjdP		0.68				
yjfN		0.60				
yjgL	1.70	1.49	1.595	0.15		
yjhB	1.65				1.84	0.29
yjhC	1.39					

Fig. 1. Microarray data for the the flagellar gene regulatory network operons.

Changes in the steady-state levels of the genes that are involved in the flagellar gene regulatory network. The image presented was obtained from a screen shot of the Integrated Genome Browser program [57]. Gene names appear above or below the operons that encode them, which indicate their location in the genome relative to nucleotide coordinates, as displayed in the center of the graph. Black arrows indicate the direction of transcription. The array data is displayed as vertical lines representing the $\log_2$ ratio of fluorescence between the mutant and wild-type strains. The horizontal line in the array data is equal to the $\log_2$ ratio of 0, with vertical lines above or below the baseline representing changes in the $\log_2$ ratio of greater or less than 0 for each probe. Vertical lines above the baseline indicate higher RNA abundance in the mutant compared to wild-type, while lines below the baseline indicate lower RNA abundance in the mutant compared to wild-type. (A) Master regulator *flhDC*; Class II genes: *flhEAB*; Class III genes: cheWAmotBA, tar, tap, cheZYBR; (B) Class II genes; (C) Class II genes: *fliAZY* sigma 28; Class III gene: *fliC* flagellin

1A.

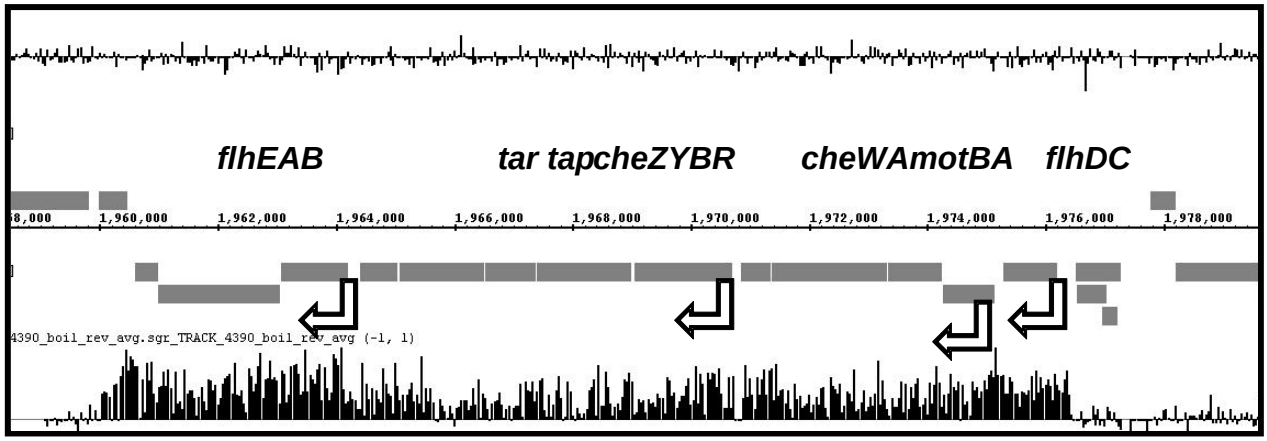
flhEAB
tar tapcheZYBR
cheWAmotBA
flhDC
1,960,000
1,962,000
1,964,000
1,966,000
1,968,000
1,970,000
1,972,000
1,974,000
1,976,000
1,978,000

1B.

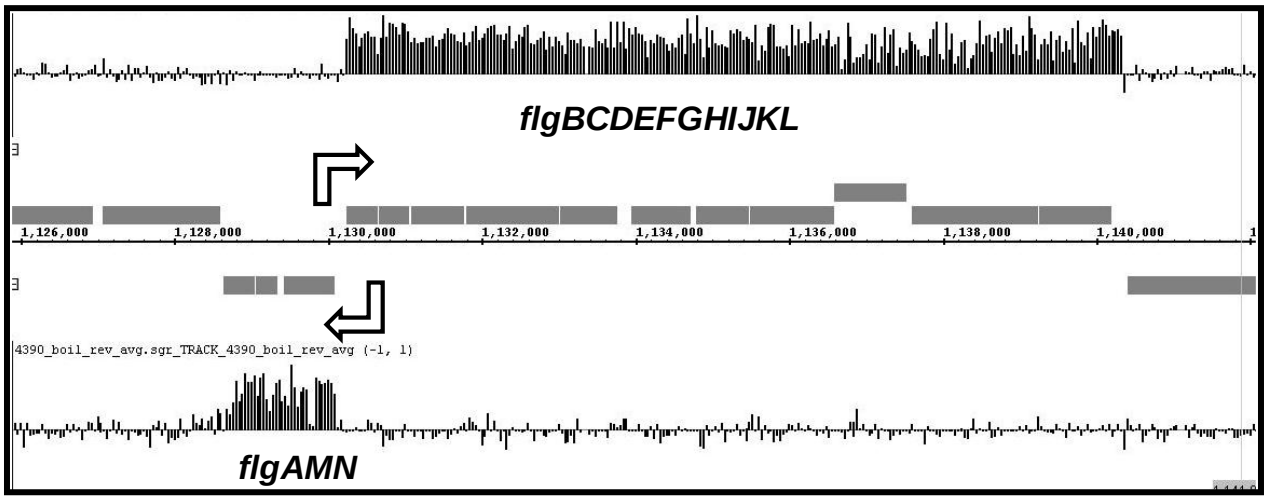
flgBCDEFGHIJKL
1,126,000
1,128,000
1,130,000
1,132,000
1,134,000
1,136,000
1,138,000
1,140,000
flgAMN

1C.

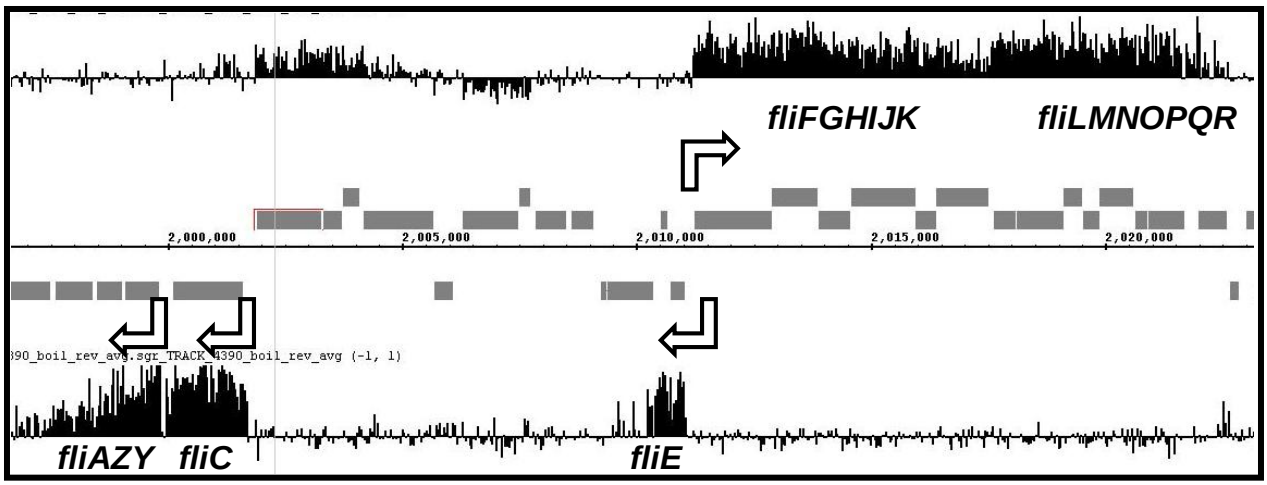
fliFGHIJK
fliLMNOPQR
2,000,000
2,005,000
2,010,000
2,015,000
2,020,000
fliAZY
fliC
fliE

Fig. 2. Northern analysis of *flhDC*, the master regulator of the flagellar gene regulatory network, in the *rppHΔ745* mutant background

Northern analysis was conducted as described in Materials and Methods. Relative quantities of total signal as compared to wild-type are indicated below the image. Ribonucleotide size estimates are indicated to the left of the image.

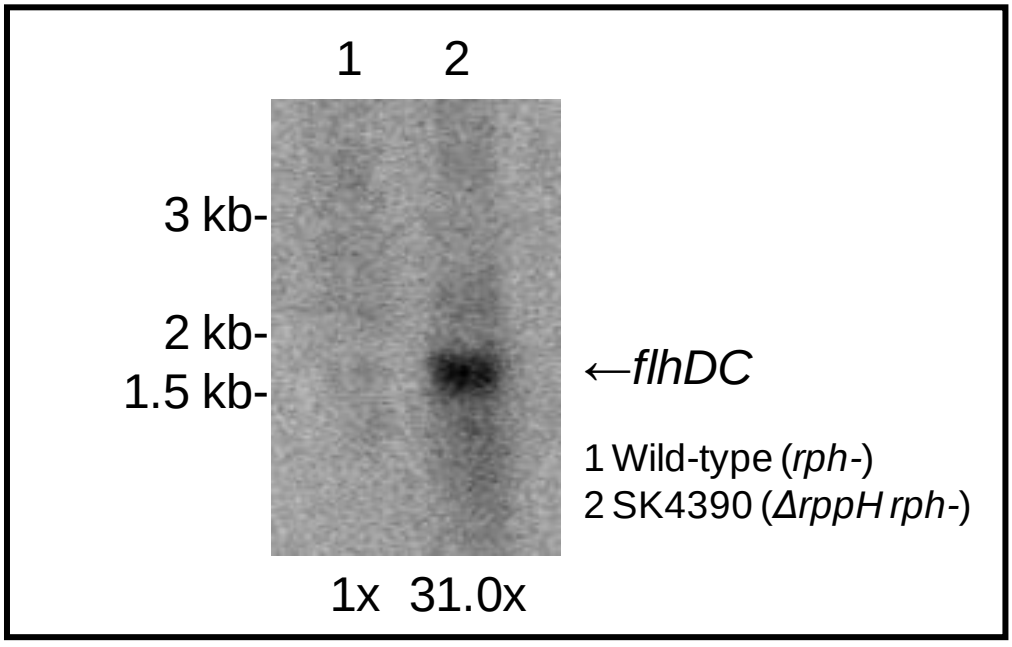
1
2
3 kb-
2 kb-
1.5 kb-
←flhDC
1 Wild-type (rph-)
2 SK4390 (ΔrppH rph-)
1x
31.0x

Fig. 3. Motility analysis of *rppHΔ745* and *ΔapaH* mutant strains after 24 hours

Motility analysis was conducted as described in Materials and Methods. Each strain examined is indicated in a different color. Halo circumference was calculated by measuring the halo that was seen around the original stab site after plates were left to grow for 24 hours. Bars indicate average halo circumference, brackets indicate values of standard deviation.

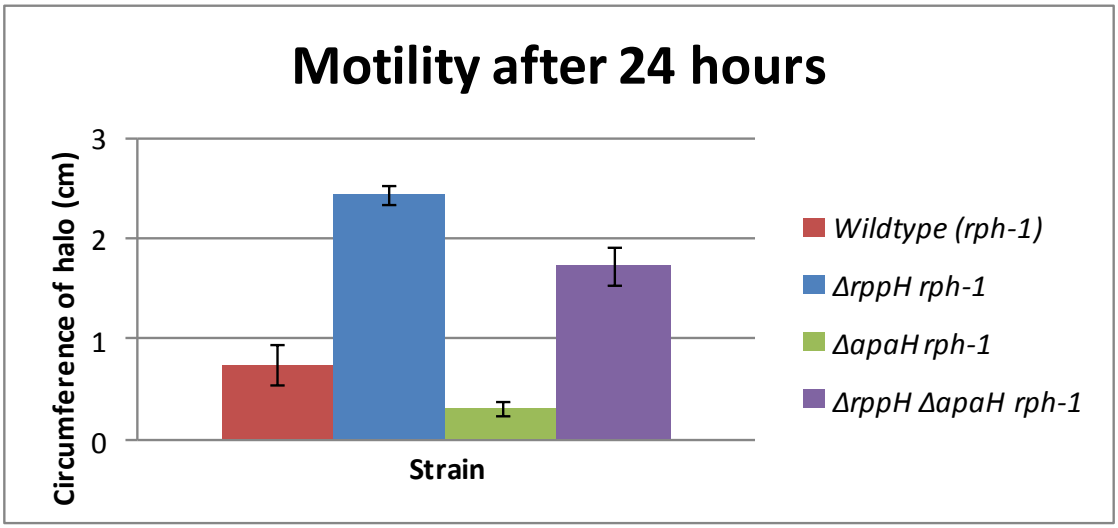
Motility after 24 hours
Circumference of halo (cm)
3
2
1
0
Strain
Wildtype (rph-1)
ΔrppH rph-1
ΔapaH rph-1
ΔrppH ΔapaH rph-1

Fig. 4. Motility analysis of *rppHΔ745* and *rph*- mutant strains over 2 days Motility analysis was conducted as described in Materials and Methods. Each strain examined is indicated below the graph. Time points are indicated in different colors. Halo circumference was calculated by measuring the halo that was seen around the original stab site after plates were left to grow for 24 hours, 36 hours, and 48 hours. Bars indicate average halo circumference, brackets indicate values of standard deviation.

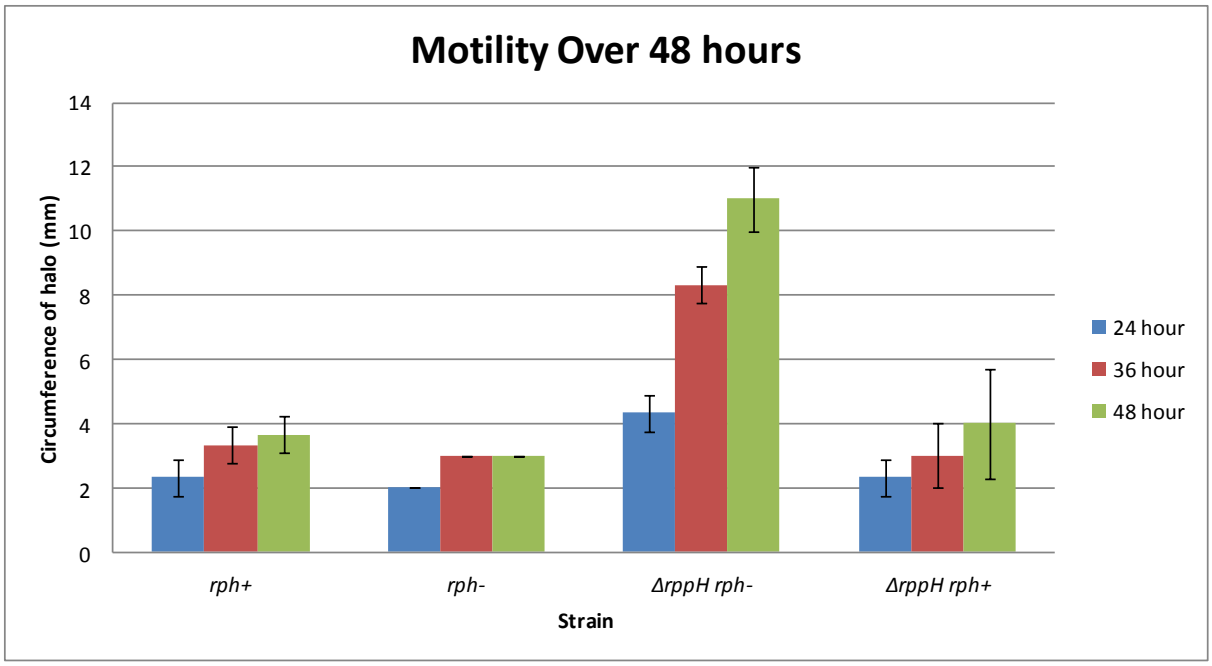
Motility Over 48 hours
Circumference of halo (mm)
14
12
10
8
6
4
2
0
rph+
rph-
ΔrppH rph-
ΔrppH rph+
Strain
24 hour
36 hour
48 hour

CHAPTER 4

CONCLUSIONS

Since the discovery of RppH as the *E.coli* decapping enzyme in 2008 by Deana *et al.* [1], it has become of interest to scientists to ascertain what this enzyme regulates in the cell. Deana *et al.* [1] provided evidence to support a model in which RppH action on a 5' triphosphate initiates mRNA degradation by removal of the 5'-pyrophosphate thereby stimulating decay by the action of RNase E. Prior to understanding this aspect of catalysis by RppH, researchers were limited to understanding its activity through mutational analysis, which identified suppression of hybrid jamming and invasiveness into brain microvascular endothelial cells as processes associated with RppH [2, 3]. Here, we have attempted to develop a better understanding of the role of RppH in *E. coli* based on its ability to convert 5' triphosphates into 5' monophosphates.

Specifically, this dissertation set out to understand aspects of RppH function that have not been previously studied. Chapter 2 describes a role for RppH in tRNA maturation. Here, we showed evidence that RppH activity is required for the maturation of certain tRNA precursors, but not all. We also demonstrated that the removal of the 5'-pyrophosphate by RppH from both *pheU* and *pheV*, along with *ileX*, was required for RNase P to properly cleave the 5'-

terminus in order to generate a mature 5'-terminus. This was the first evidence that RppH was required to stimulate the catalytic activity of a ribonuclease other than RNase E. We also provided evidence that in many cases involving tRNA processing, RNase E did not require decapping to endonucleolytically cleave its RNA substrates. These results supported the claim that RNase E can bypass the 5'-terminus and undergo internal entry in the processing and degradation of certain RNA substrates [4].

We were also interested in finding additional cell processes in which RppH was involved. Through the use of tiling microarrays, we were able to identify a role of RppH in regulating motility in *E. coli* as described in Chapter 3. These experiments were prompted by the fact that previous array data on RppH did not utilize a deletion of the *rppH* gene, but rather used a strain in which a catalytically inactive RppH protein was overproduced [1]. Upon deletion of *rppH*, all classes of genes in the flagellar gene regulatory network showed significant increases in their steady-state levels. This observation was further supported by motility assays that confirmed the hypothesis that cells showing increased motility due to a stabilization of the mRNAs for the genes in this network. Chapter 3 also demonstrated the ability of the *ΔrppH* mutation to restore motility to the nonmotile *ΔapaH* mutant. This was the first evidence that RppH is involved in regulation of motility in *E. coli*.

An interesting aspect of both Chapter 2 and Chapter 3 was the role RNase PH played in the activity of RppH. Seeing that all “wild-type” backgrounds used in our study and the previous survey of RppH function actually contained a

mutation in *rph*, it was important to determine if this mutation influenced the way the cell behaved in the absence of RppH. Therefore in both Chapter 2 and Chapter 3, we analyzed *rppHΔ754* allele in the presence of RNase PH. Interestingly in both cases, the presence of RNase PH eliminated many of the phenotypes observed in the *rppHΔ754 rph-1* double mutant. The inhibition of RNase P removal of 5'-leader from the *pheU* and *pheV* tRNA precursors and the increase in cell motility disappeared. In addition, a tiling array of the *rppHΔ754* single mutant showed that many fewer transcripts were affected, either positively or negatively, by the loss of RppH. This evidence indicates that the activity of a 3'→5' exoribonuclease, RNase PH, influences the ability of a 5'-decapping enzyme, a phenomenon that has not been previously observed in any prokaryote.

The fact that RNase PH can suppress many of the phenotypes associated with inactivation of RppH can be explained in several possible ways. In one case, there may be a physical interaction between the two proteins that possibly alters the catalytic activity of RppH. Antibody studies will be required to address this question. Alternatively, it is possible that RNase PH has a previous undetected catalytic activity associated with removal of a 5' triphosphate.

Our results open the possibility that prokaryotic decapping is more similar to eukaryotic decapping then originally thought. In eukaryotic decapping, the 3'-poly(A) tail on mRNA transcripts actually inhibits decapping and must be removed in order for decapping to occur [5-11]. Although this is most likely not true for prokaryotes, it is interesting that there appears to be a connection

between 3'-processing (RNase PH) and 5'-decapping (RppH). In this dissertation, we have shown that in the presence of only RNase PH, the *ΔrppH* mutation has no effect on the maturation of tRNAs or motility. That would indicate that the activity of RNase PH at the 3'-termini of a substrate can compensate for the presence of the 5'-triphosphate that arises in the absence of RppH. When a few extra nucleotides are present on the 3'-termini in *rph*$^{-}$ mutant backgrounds, the presence of the 5' triphosphate cannot be overcome, therefore leaving the specific tRNAs immature and the cell with significantly increased motility resulting from stabilization of the master regulatory switch mRNA.

To answer these questions, sequencing analysis of tRNA intermediates seen in both *rph*$^{+}$ and *rph*$^{-}$ backgrounds in the presence of the *rppHΔ754* mutation need to be conducted to determine how many additional nucleotides are present at the 3'-terminus. Further, tiling microarray analysis of the *rppHΔ754* mutation in the presence of RNase PH can be compared to the analysis conducted in Chapter 3 to determine candidate transcripts that can be used for further analysis of this phenomenon. Although complicated, this analysis is necessary in understanding if this is a transcriptome-wide issue or transcript-specific.

REFERENCES

1. Deana, A., H. Celesnik, and J.G. Belasco, *The bacterial enzyme RppH triggers messenger RNA degradation by 5' pyrophosphate removal.* Nature Biotechnology, 2008. **451**(7176): p. 355-8.
2. Hand, N.J. and T.J. Silhavy, *Null mutations in a Nudix gene, ygdP, implicate an alarmone response in a novel suppression of hybrid jamming.* J Bacteriol, 2003. **185**(22): p. 6530-9.
3. Bessman, M.J., et al., *The gene ygdP, associated with the invasiveness of Escherichia coli K1, designates a Nudix hydrolase, Orf176, active on adenosine (5')-pentaphospho-(5')-adenosine (Ap5A).* J Biol Chem, 2001. **276**(41): p. 37834-8.
4. Baker, K.E. and G.A. Mackie, *Ectopic RNase E sites promote bypass of 5'-end-dependent mRNA decay in Escherichia coli.* Molecular Microbiol., 2003. **47**: p. 75-88.
5. Decker, C.J. and R. Parker, *A turnover pathway for both stable and unstable mRNAs in yeast: Evidence for a requirement for deadenylation.* Genes and Development, 1993. **7**: p. 1632-1643.
6. LaGrandeur, T. and R. Parker, *The cis acting sequences responsible for the differential decay of the unstable MFA2 and stable PGK1 transcripts in yeast include the context of the translational start codon.* RNA, 1999. **5**(3): p. 420-33.

7. Muhlrad, D., C.J. Decker, and R. Parker, *Deadenylation of the unstable mRNA encoded by the yeast MFA2 gene leads to decapping followed by 5' to 3' digestion of the transcript.* Genes and Development, 1994. **8**(7): p. 855-866.

8. Muhlrad, D., C.J. Decker, and R. Parker, *Turnover mechanisms of the stable yeast PGK1 mRNA.* Mol Cell Biol, 1995. **15**(4): p. 2145-56.

9. Muhlrad, D. and R. Parker, *Mutations affecting stability and deadenylation of the yeast MFA2 transcript.* Genes Dev, 1992. **6**(11): p. 2100-11.

10. Shyu, A.-B., J.G. Belasco, and M.E. Greenberg, *Two distinct destabilizing elements in the cfos message trigger deadenylation as a first step in rapid mRNA decay.* Genes and Development, 1991. **5**: p. 221-231.

11. Wilusz, C.J., et al., *Poly(A)-binding proteins regulate both mRNA deadenylation and decapping in yeast cytoplasmic extracts.* RNA, 2001. **7**: p. 1416-1424.